



Cairo University

# **USE OF MODEL CALIBRATION TECHNIQUE TO DERIVE ACCURATE FRAGILITY CURVES**

By

**Omar Khaled Wahba Metwally Omar**

A Thesis Submitted to the  
Faculty of Engineering at Cairo University  
in Partial Fulfillment of the  
Requirements for the Degree of  
**MASTER OF SCIENCE**  
in  
**Structural Engineering**

FACULTY OF ENGINEERING, CAIRO UNIVERSITY  
GIZA, EGYPT  
2022

# **USE OF MODEL CALIBRATION TECHNIQUE TO DERIVE ACCURATE FRAGILITY CURVES**

By  
**Omar Khaled Wahba Metwally Omar**

A Thesis Submitted to the  
Faculty of Engineering at Cairo University  
in Partial Fulfillment of the  
Requirements for the Degree of  
**MASTER OF SCIENCE**  
in  
**Structural Engineering**

Under the Supervision of

**Prof. Dr. Shrief A. Mourad**

**Dr. Hazem H. El-Anwar**

Professor of Steel Structures and Bridges  
Structural Engineering Department  
Faculty of Engineering, Cairo University

Assistant Professor  
Structural Engineering Department  
Faculty of Engineering, Cairo University

**Dr. Hussam N. Mahmoud**

Associate Professor  
Department of Civil and Environmental  
Engineering  
Colorado State University

FACULTY OF ENGINEERING, CAIRO UNIVERSITY  
GIZA, EGYPT  
2022

# **USE OF MODEL CALIBRATION TECHNIQUE TO DERIVE ACCURATE FRAGILITY CURVES**

By  
**Omar Khaled Wahba Metwally Omar**

A Thesis Submitted to the  
Faculty of Engineering at Cairo University  
in Partial Fulfillment of the  
Requirements for the Degree of  
**MASTER OF SCIENCE**  
in  
**Structural Engineering**

Approved by the  
Examining Committee

---

Prof. Dr. Shrief A. Mourad, Thesis Main Advisor

---

Dr. Hussam N. Mahmoud, Advisor

Associate Professor, Department of Civil and Environmental Engineering, Colorado  
State University

---

Prof. Dr. Ashraf Mahmoud Osman, Internal Examiner

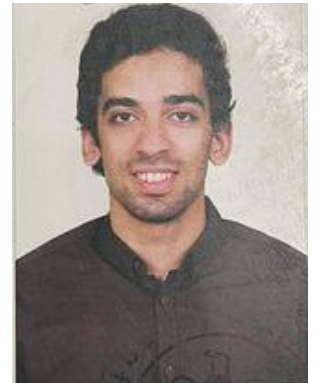
---

Prof. Dr. Sherif Mohamed Ibrahim, External Examiner

Professor of Structural Engineering, Ain shams University

**FACULTY OF ENGINEERING, CAIRO UNIVERSITY  
GIZA, EGYPT  
2022**

**Engineer's Name:** Omar Khaled Wahba Metwally Wahba Omar  
**Date of Birth:** 19/02/1996  
**Nationality:** Egyptian  
**E-mail:** omar\_kwm@yahoo.com  
**Phone:** 00201140038877  
**Address:** Rostom st. Cairo, Egypt  
**Registration Date:** 1/10/2018  
**Awarding Date:** / /2022  
**Degree:** Master of Science  
**Department:** Structural Engineering



**Supervisors:**  
Prof. Dr. Shrief A. Mourad  
Dr. Hazem H. El-Anwar  
Dr. Hussam N. Mahmoud

**Examiners:**  
Prof. Dr. Shrief A. Mourad (Thesis main advisor)  
Dr. Hussam N. Mahmoud (advisor),  
Colorado State University  
Prof. Dr. Ashraf Mahmoud Osman (Internal examiner)  
Prof. Dr. Sherif Ibrahim (External examiner)  
Ain shams University

**Title of Thesis:**

Use of Model Calibration Technique to Drive Accurate Fragility Curves

**Key Words:**

Fragility analysis, Multiple Stripes Analysis, Model Updating, Finite Element Modeling, Buckling Restrained Bracing

**Summary:**

Finite Element Analysis (FEA) has been used extensively for modeling of structures. However, the details and accuracy of FE models may be limited due to computational demand particularly, for problems requiring extensive iterations such as fragility analysis. Fragility analysis, defined as the conditional probability of reaching a performance limit state as a function of intensity measure, is an essential component in seismic risk analysis of building and infrastructure. Therefore, developing accurate fragility functions is critical for proper seismic risk assessment. In this research we propose a two stage framework to evaluate accurate fragility curves using nonlinear dynamic analysis without the expensive computational cost. First, we reduce the discrepancies between a detailed model and simplified model in order to reduce the computational expenses as much as possible while approximating the results of the simplified model to the detailed model. Then we calculate the fragility curves utilizing a nonlinear dynamic analysis without cumbersome run time. The framework is then applied to a four-story buckling restrained frame building to assess its feasibility.

## **Disclaimer**

I hereby declare that this thesis is my own original work and that no part of it has been submitted for a degree qualification at any other university or institute.

I further declare that I have appropriately acknowledged all sources used and have cited them in the references section.

Name:

Date: ../../...(it's the date that you handover the thesis)

Signature:

# **Dedication**

I wish to dedicate this thesis to my passed mother who always believed in me. I would have never achieved anything in my life without her support.

## Acknowledgments

I would to thank all the people around me who provided support and guidance throughout the journey and had the patience and belief in me.

I want to thank my advisors **Prof. Shrief Ahmed Mourad, Dr. Hazem AL-Anwar and Dr. Hussam N. Mahmoud** for their invaluable guidance and support with their extensive knowledge and experience as they provided the necessary feedback which sharpened my mind throughout my research.

I want to thank **Dr Emad Shafik** for his generous support and advice throughout my work

I want to thank **Eng M. Hisham Ismail** for his tremendous guidance to me throughout the learning of the necessary software for my research.

I want to thank my family and friends for all the efforts they provided me with.

# Table of Contents

<b>ACKNOWLEDGMENTS .....</b>	<b>I</b>
<b>DEDICATION.....</b>	<b>ERROR! BOOKMARK NOT DEFINED.</b>
<b>TABLE OF CONTENTS.....</b>	<b>IV</b>
<b>LIST OF FIGURES .....</b>	<b>VII</b>
<b>ABSTRACT .....</b>	<b>IX</b>
<b>CHAPTER 1 : INTRODUCTION .....</b>	<b>1</b>
1.1.            FRAGILITY ANALYSIS .....	1
1.2.            FINITE ELEMENT MODEL CALIBRATION (FEMC) .....	3
1.3.            ORGANIZATION OF THE THESIS .....	3
<b>CHAPTER 2 : LITERATURE REVIEW .....</b>	<b>5</b>
2.1.            FEMC.....	5
2.1.1.            Comparison and Correlation .....	7
2.1.1.1.            Comparison of FRFs .....	7
2.1.1.2.            Comparison of Natural Frequencies .....	8
2.1.1.3.            Comparison of Mode Shapes .....	9
2.1.2.            Compatibility techniques .....	10
2.1.2.1.            Coordinate Expansion .....	10
2.1.2.2.            Model Reduction.....	11
2.1.3.            Techniques of FEMC.....	11
2.1.3.1.            Direct Techniques .....	11
2.1.3.2.            Iterative Techniques.....	13
2.1.4.            Application of FEMC.....	15
2.1.4.1.            Neural Network based FEMC to Calibrate Steel Frame FE Model.....	16
2.1.4.2.            Application in SHM field.....	16
2.1.4.3.            Incorporating Hybrid Simulation in Model Updating .....	16
2.2.            FRAGILITY ANALYSIS .....	17
2.2.1.            Fragility Curves.....	17
2.2.2.            Types of Fragility Curves .....	18
2.2.2.1.            Expert Opinion.....	18
2.2.2.2.            Empirical Fragility .....	18
2.2.2.3.            Experimental Fragility .....	19
2.2.2.4.            Analytical Fragility .....	20
2.2.2.4.1.            Analytical modeling .....	20
2.2.2.4.2.            Attainment of limit states.....	21
2.2.2.4.3.            Ground Motion Records selection and scaling .....	25
2.2.3.            Nonlinear Dynamic Analysis .....	26
2.2.3.1.            Incremental Dynamic Analysis (IDA) .....	26
2.2.3.2.            Multiple Stripes analysis.....	29
2.2.4.            Nonlinear Static Based Approach for Fragility.....	31
<b>CHAPTER 3 METHODOLOGY .....</b>	<b>33</b>
3.1.            MODEL UPDATING STAGE.....	33
3.1.1.            Detailed versus Simplified models .....	33



3.1.2.	Updating Parameters .....	34
3.1.3.	FEMC Technique.....	34
3.1.4.	Objective function.....	35
3.1.5.	Implementation of the Framework.....	35
3.2.	DERIVATION OF FRAGILITY CURVES.....	37
<b>CHAPTER 4 NUMERICAL MODELING.....</b>		<b>39</b>
4.1.	INTRODUCTION .....	39
4.2.	CASE STUDY DESCRIPTION .....	39
4.3.	DETAILED SIMULATION MODEL.....	42
4.3.1.	Model General Description.....	42
4.3.2.	Material Modeling.....	44
4.3.3.	Type of Elements .....	45
4.3.4.	Meshing of Elements .....	45
4.3.5.	Contact Between Elements .....	47
4.3.5.1.	Bonded contact .....	48
4.3.5.2.	Frictional Contact.....	49
4.3.6.	Modeling of Bolts .....	51
4.3.6.1.	Use bonded regions.....	51
4.3.6.2.	Beam Bolts.....	51
4.3.6.3.	3D Solid Bolts.....	51
4.3.6.4.	Used Method in Study.....	53
4.3.7.	Modeling of Buckling restrained bracing .....	54
4.4.	SIMPLIFIED MODEL .....	55
4.4.1.	Model General Description.....	55
4.4.2.	Type of elements .....	56
4.4.2.1.	BEAM188 Element.....	56
4.4.2.2.	LINK180 element .....	56
4.4.3.	Meshing of elements .....	57
4.4.4.	Connections.....	57
<b>CHAPTER 5 FEMC PROCESS .....</b>		<b>59</b>
5.1.	COMPARISON AND CORRELATION RESULTS .....	59
5.1.1.	Comparison of Natural Frequencies.....	59
5.1.2.	Visual Comparison of Mode Shapes.....	59
5.1.3.	MAC Correlation .....	59
5.2.	STEP SIZE COMPATIBILITY .....	62
5.3.	UPDATING PARAMETERS.....	63
5.4.	FEMC METHOD.....	65
5.5.	RESULTS OF FEMC.....	68
<b>CHAPTER 6 FRAGILITY ANALYSIS .....</b>		<b>71</b>
6.1.	SELECTION OF GROUND MOTIONS .....	71
6.2.	SCALING RECORDS OF GROUND MOTION .....	72
6.3.	LIMIT STATES FOR DERIVING FRAGILITIES.....	73
6.4.	FRAGILITY CURVES.....	73
<b>CHAPTER 7 DISCUSSION AND CONCLUSIONS.....</b>		<b>76</b>

<b>REFERENCES.....</b>	<b>78</b>
------------------------	-----------

# List of Figures

Figure 1-1 Example of fragility curves and corresponding DPM. ....	2
Figure 1-2 Flowchart depicting the process of FEMC .....	3
Figure 1-3 Flowchart of the Proposed Two-Stage Framework .....	4
Figure 2-1 Sources of errors existing in FE Models.....	6
Figure 2-2 Cross-Functional flowchart illustrating the steps of FEMC .....	7
Figure 2-3 Example of visual inspection of correlation (a) show good correlation while (b) Show No Correlation [Sehgal et al. 2016] .....	8
Figure 2-4 Example of MAC plot the left plot represent good correlation while the right represent poor correlation [Sehgal et al. 2016]. ....	10
Figure 2-5 Steps of the direct method by Baruch and Bar-Itzhack 1978 .....	12
Figure 2-6 Steps of the Direct Method by Berman and Nagy 1983 .....	12
Figure 2-7 Flowchart of the procedure along with the equations Used by Collins et al. 1974. ....	13
Figure 2-8 Procedure of Using Neural Networks as introduced by Atalla et al. 1998...	14
Figure 2-9 Example of Fragility Curves at Different Limit States.....	18
Figure 2-10 The general framework for constructing empirical fragilities .....	19
Figure 2-11 Framework for deriving analytical fragility curves .....	20
Figure 2-12 Different detail levels of the analytical model of the same structure .....	21
Figure 2-13 Definition of the Considered Four Damage States [D'Ayala, D., et al. 2015]. ....	22
Figure 2-14 Example of Spectral Matching (Scaling Techniques) [D'Ayala, D., et al. 2015]. ....	25
Figure 2-15 The Procedure of Generating One IDA Curve [D'Ayala, D., et al. 2015] .	27
Figure 2-16 Example of IDA curve with three step response [D'Ayala, D., et al. 2015] .....	28
Figure 2-17 a) Example of IDAs and b) The associated empirical and fitted fragility [Baker 2015] .....	28
Figure 2-18 a) the output of multiple stripes analysis and b) the conversion to fragility curves [Baker 2015]. ....	30
Figure 3-1 Flowchart of the implemented framework .....	33
Figure 3-2 Examples of simplifications applied to the detailed model .....	34
Figure 3-3 Flowchart of the FEMC process .....	36
Figure 3-4 Input of the FFG [Gandage, S. et al. 2019] .....	37
Figure 4-1 Typical Plan of the Hospital [NIST GCR, 14-917-2].....	40
Figure 4-2 Typical Elevation of the Braced Bay [NIST GCR, 14-917-2]. ....	41
Figure 4-3 Elevation of the Full Structure in Study .....	42
Figure 4-4 Elevation of the First Floor .....	43
Figure 4-5 Connection of BRB to Column Beam Joint .....	43
Figure 4-6 Inverted-V Connection of BRB to Beam.....	44
Figure 4-7 Idealized Stress-Strain Curve With 3% Isotropic Hardening .....	44
Figure 4-8 SOLID186 Structural Element Geometry [ANSYS Element Reference Manual].....	45
Figure 4-9 Meshing of the First Floor .....	46
Figure 4-10 Meshing of the Inverted-V BRB Connection to Beam.....	46
Figure 4-11 Meshing of the Beam to Column Connection .....	47
Figure 4-12 Bonded Contact between Column and Base Plate.....	48

Figure 4-13 Bonded Contact between Column and Base Plate (Continued) .....	49
Figure 4-14 Example of Contact between Two Bolted Plates .....	50
Figure 4-15 Example of Bolted Connection Using Bonded Regions [ENDEAVOS Innovations Inc.] .....	51
Figure 4-16 Example of Beam Bolts [ENDEAVOS Innovations Inc.] .....	52
Figure 4-17 Contact in 3D Solid Bolted Connection [ENDEAVOS Innovations Inc.] ..	52
Figure 4-18 Verification Study on the Use of Beam Bolts Instead of 3D Solid Bolts ...	53
Figure 4-19 Extruded View of the Simplified Model .....	55
Figure 4-20 BEAM188 Structural Element Geometry [ANSYS Element Reference Manual] .....	56
Figure 4-21 Link180 Structural Element Geometry [ANSYS Element Reference Manual] .....	56
Figure 4-22 Meshed View of Portion of the Model .....	57
Figure 5-1 Comparison of Mode 1 .....	60
Figure 5-2 Comparison of Mode 2 .....	60
Figure 5-3 Comparison of Mode 3 .....	61
Figure 5-4 Comparison of Mode 4 .....	61
Figure 5-5 Calculation of MAC Values .....	62
Figure 5-6 Four Vertical DOF Located at 1/4 Distance of the Beam Length .....	63
Figure 5-7 Four Vertical DOF Located at 1/8 Distance of the Beam Length .....	63
Figure 5-8 Model with the BRB Members and the Error in Natural Frequencies .....	64
Figure 5-9 The Four Updating Parameters .....	64
Figure 5-10 The Pushover Curves of the Initial and Detailed Models .....	65
Figure 5-11 Final Updated Parameters and the Value of the Fitness Function at each Generation .....	68
Figure 5-12 Pushover Curves of the Detailed, Initial and Updated Models .....	69
Figure 6-1 Fragility curves of initial model at different damage limit states .....	73
Figure 6-2 Fragility curves of updated model at different damage limit states .....	74
Figure 6-3 Fragility curves of initial and updated model at slight damage limit state ...	74
Figure 6-4 Fragility curves of initial and updated model at moderate damage limit state .....	75
Figure 6-5 Fragility curves of initial and updated model at extensive damage limit state .....	75

# Abstract

Finite Element Analysis (FEA) has emerged as a reliable analysis approach as a result of the advancement of computational methods and power. Nevertheless, accurate representation of large-scale problems using FEA might be hindered by the impractical computational demand, particularly for problems requiring extensive iterations or multiple run times. One of these cases is when deriving fragility curves where often nonlinear dynamic analysis is needed, requiring extensive number of simulations. Previous studies have addressed the issue of requiring significant number of analysis for developing fragility functions by reducing the number of nodes or conducting static analysis, instead of dynamic analysis which could negatively impact the accuracy of the results. In this study, a two-stage computationally efficient procedure is proposed to develop fragility curves without compromising on accuracy. Specifically, two models are developed one of them is fully detailed and the other is simplified with some parameters that can be adjusted if needed. The two models are analyzed and integrated where the simplified model parameters are calibrated to that of the detailed model so that both models' results are as close as possible to each other. Once the simplified model is calibrated to the detailed model, fragility curves can be derived using the simplified model in a much more efficient manner.

To calibrate the simplified model, a genetic algorithm-based optimization technique is used as the calibration tool to update the simplified model based on the difference between the pushover curves between the detailed and simplified models. Then the updated model is used to derive accurate fragility curves.

In order to evaluate the proposed procedure, non-linear dynamic analysis is used to derive fragility curves for a four-story buckling restrained braced frame building. The detailed model is developed using ANSYS WORKBENCH, which is a general-purpose finite element software, utilizing 3D solid meshes. The simplified model, on the other hand, is developed using ANSYS APDL utilizing 1D beam elements. The calibration procedure is applied to the simplified model using the genetic algorithm to find the most optimal parameters for the model. Finally, the updated model is used to develop fragility curves aiming to capture the behavior of the detailed model as close as possible. The results showed the proposed framework was able to increase the accuracy of the fragility function by more than 20% at some values of the spectral acceleration.

# Chapter 1 : Introduction

In the last few decades, there have been an increasing interest in the field of seismic assessment of building. The advancement in computers enhanced the capability of performing different types of complicated analysis methods. Due to the inherent uncertainties in earthquakes' properties, probabilistic assessment approach is more realistic than a deterministic approach [Sadraddin 2015]. One of these probabilistic approaches is the fragility analysis which establishes a relation between the excitation intensity and the resistance of the structure. In the following section the concept of fragility analysis is introduced briefly

## 1.1. Fragility analysis

Fragility function is a relationship that indicates the likelihood of an event to occur given a defined demand level. In contrast to traditional design methods, with their focus on structural members and connections, fragility analysis addresses the performance of structures and component, as appropriate to the needs of the performance assessment [Kennedy and Ravindara 1984]. Fragilities were first implemented in civilian engineering practice in the nuclear industry. With advances in computational power and modeling techniques, the past decade has seen numerous papers on fragility development of common buildings and infrastructure. Fragility functions are usually plotted on a curve with the horizontal axis indicating an increase in the intensity of the demand parameter whereas the vertical axis indicates the probability of exceeding a predefined performance limit state. Fragility function can be developed for any type of hazards. In this research only seismic fragility analysis is considered. In Seismic fragility analysis the limit state considered is usually the inter-story drift and the excitation level is usually measured in terms of spectral acceleration or peak ground acceleration. The fragilities of a structure can be depicted with Damage Probability Matrix (DPM). A DPM is a matrix including values of probabilities of exceedance at a predefined set of excitation levels. Fig 1-1 shows example of fragility curves and corresponding DPM, where LS is the considered limit state, DS is the damage state, and IL is the intensity level.

There are several methods for developing seismic fragilities [Erberik, Murat Altug 2014; Sadraddin 2015] such as:

- 1- The opinion of experts in earthquake engineering, which is called judgmental fragility curves.
- 2- Fragility curves obtained from field observation of damage data, which is called empirical fragility curves.
- 3- Experimental fragility curves, developed using laboratory tests.
- 4- Analytical simulation of building, which is called analytical fragility curves.

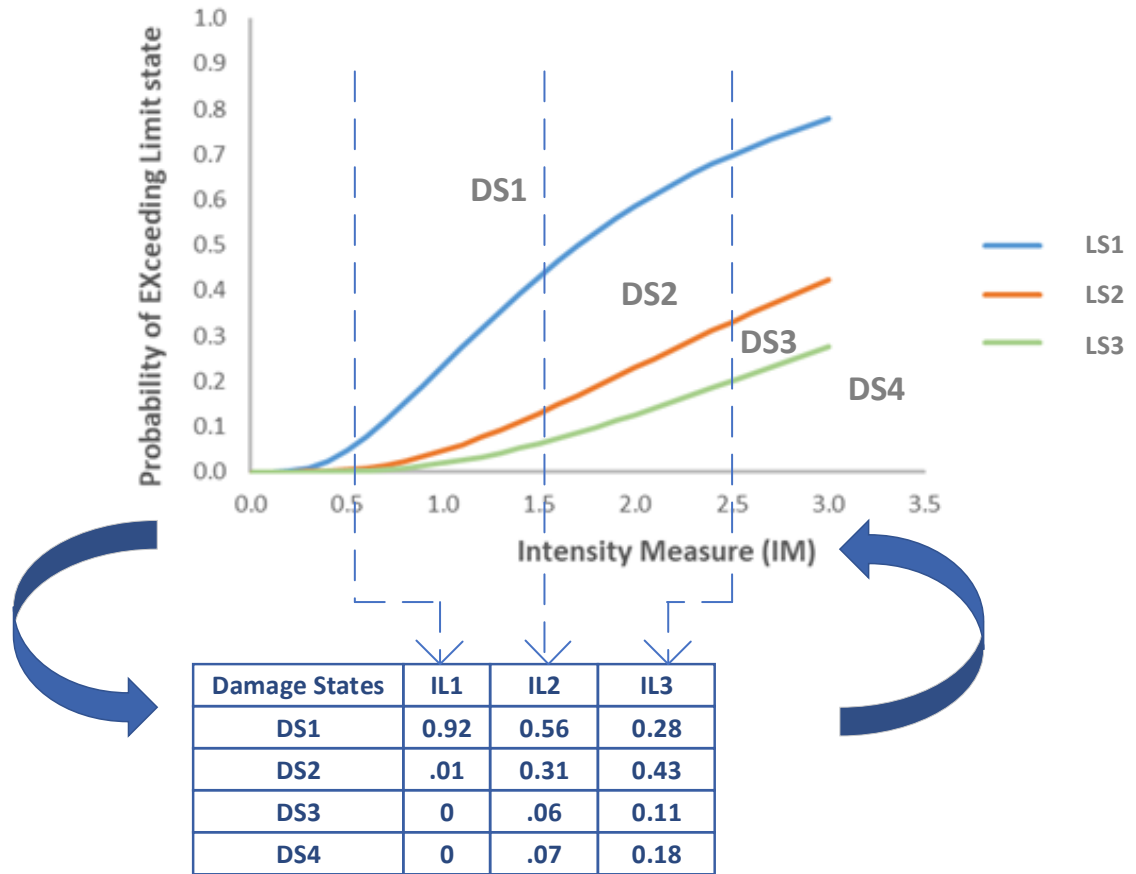


**Figure 1-1 Example of fragility curves and corresponding DPM.**

The most common method used for developing fragility curves is the numerical simulations. The computational demand associated with numerical simulations, particularly for detailed models, hinder their use in the development of fragilities. Accordingly, researchers have relied on lowering the resolution of models used to derive the functions. However, such simplifications might cause the response to deviate from the actual response.

In this research we propose a two-stage framework to evaluate accurate fragility curves using nonlinear dynamic analysis without the expensive computational cost associated with the analysis of detailed method. First, we reduce the discrepancies between a detailed model and simplified model in order to reduce the computational expenses as much as possible while approximating the results of the simplified model to the detailed model. The calibration technique in the first is called Finite Element Model Calibration (FEMC). An overview of the technique is presented in the next section.

In the second stage, we calculate fragility curves using nonlinear dynamic analysis of the updated model without cumbersome run time. The simplified model, once calibrated, is then used to derive fragility functions for a four-story buckling restrained braced frame building.

## 1.2. Finite Element Model Calibration (FEMC)

In most cases of FEMC, parameters that are most susceptible to be the source of the discrepancies between the simplified and more complex FEMs, or between an FEM and its experimental counterpart, are identified and then calibrated to match the response of the reference model. this process may be performed manually by using trial and error. However, this may require significant effort and time and sometimes it becomes impossible. For this reason, several methods were introduced such as the direct methods or matrix methods where the solution is found in one step [Baruch et al. 1978, Chen et al 1983, Jiang et al. 2013] or iterative methods which require several iterations to converge on the solution. From these methods are the neural network-based method [Atalla et al. 1998, Zapico et al. 2008] and optimization methods such as genetic algorithm [Levin RI et al. 1998, Marwala 2010], particle swarm optimization [Tran-Ngoc et al. 2018] and simulated annealing [Levin RI et al. 1998]. These different methods all follow a generic flow chart shown in Fig 1-2

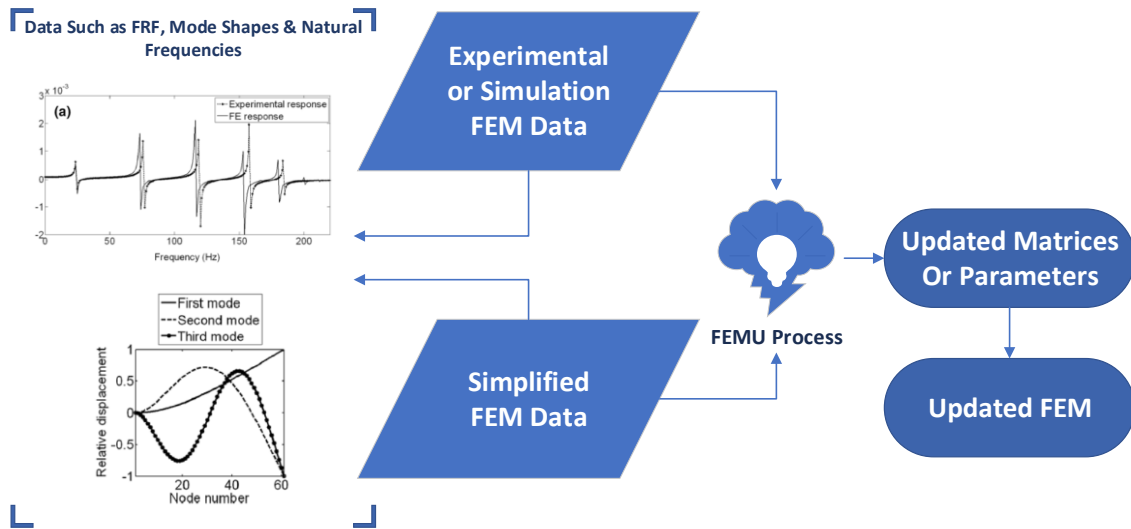
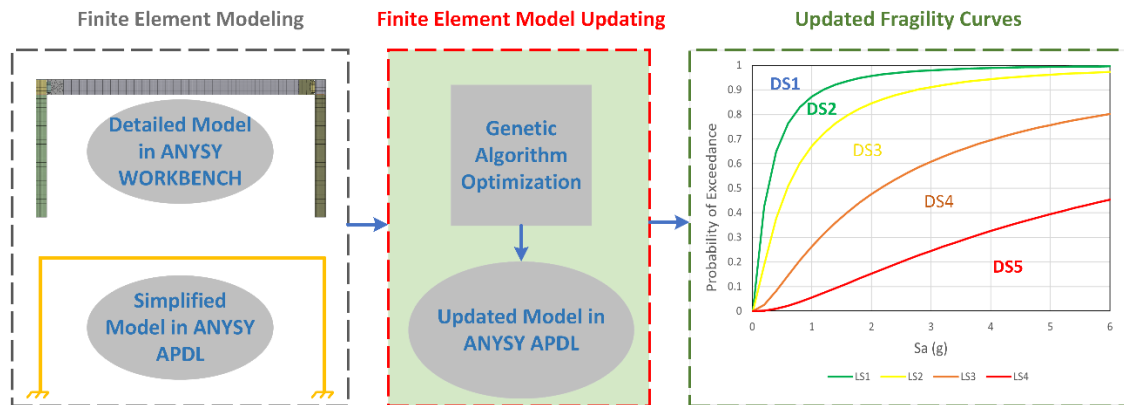


Figure 1-2 Flowchart depicting the process of FEMC

## 1.3. Organization of the thesis

This thesis is organized such as: 0 provides a detailed literature review on both the subjects of fragility analysis and FEMC. Chapter 3 describe the adopted methodology. Chapter 4 provides description and modeling aspects of the case study building. Chapter 5 describes the steps of the FEMC implemented on the case study building. Chapter 6 provides the derivation of fragilities for both initial and updated models and comparison of results. Finally, discussions and conclusions are presented in chapter 7. Figure 1-3 shows the flow chart of the proposed framework implemented throughout the thesis.





**Figure 1-3 Flowchart of the Proposed Two-Stage Framework**

## Chapter 2 : Literature Review

The FEMC approach is used to approximate the response of a simplified model to either experimental results or a detailed model whose results are considered correct and are regarded as the targets of the FEMC process. To implement this process, different methods have been introduced in the literature. Each method can be more suitable for specific problem depending on its size and nature. The methods can be broadly classified into direct and iterative methods. These methods will be introduced with some detail in the literature review to allow for correct selection of the suitable method for the problem presented herein.

After conducting the FEMC process, the fragility curves will be derived using the calibrated model. Deriving fragility curves can be done through several approaches such as the experts' opinion approach, the experimental approach, the empirical approach and the analytical approach. By conducting a literature review on these different methods, it can be concluded that the analytical approach is the most common. The literature review introduced herein provides an introduction to the field of fragility analysis and its different approaches, requirements and limitation of each one. Also, the different codes and guidelines covering the topic are introduced.

The first section of this chapter will provide the literature review on the process of FEMC while the second section will present fragility analysis.

### 2.1. FEMC

Finite Element Models (FEMs) has emerged as one of the most convenient analysis tools. However, several assumptions and simplifications are typically induced in the developed model, which eventually leads to inaccurate representation of the actual behavior. To overcome some of the inaccuracies a more detailed model can be adopted. Nevertheless, there is always a tradeoff between accuracy and computational time since accurate FEM representation might be computationally expensive and model simplifications could result in some inherent errors highlighted in Fig. 2-1 [Sehgal et al. 2016].

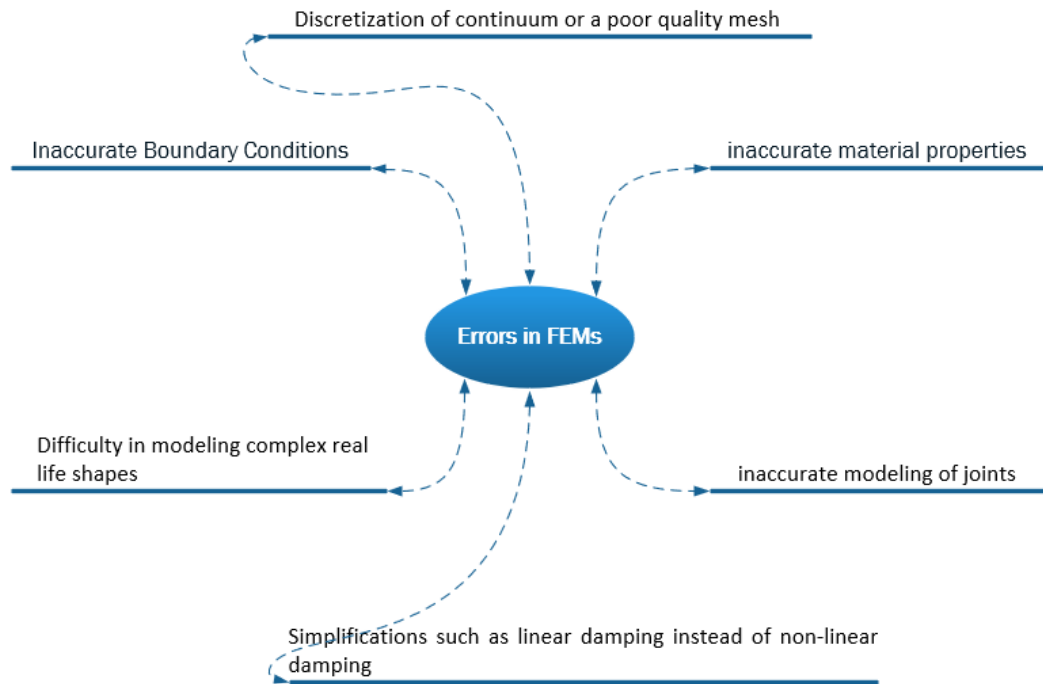


**Figure 2-1 Sources of errors existing in FE Models**

Due to the aforementioned errors, it becomes essential to calibrate a FE model so that its behavior match the real structure behavior as much as possible. The procedure utilized to calibrate the model is called finite element model calibration (FEMC). In FEMC the target results can be either experimental results or simulation detailed model whose results are regarded as the correct response. The output of FEMC can be in the form of updated stiffness, mass or damping matrices of the structure or in the form of updated parameters of analysis.

The cross-functional flow chart shown in Fig 2-2 illustrates the necessary steps for performing FEMC

- 1- Comparison and correlation between FE and experimental results.
- 2- Size compatibility.
- 3- Apply the appropriate FEMC technique.

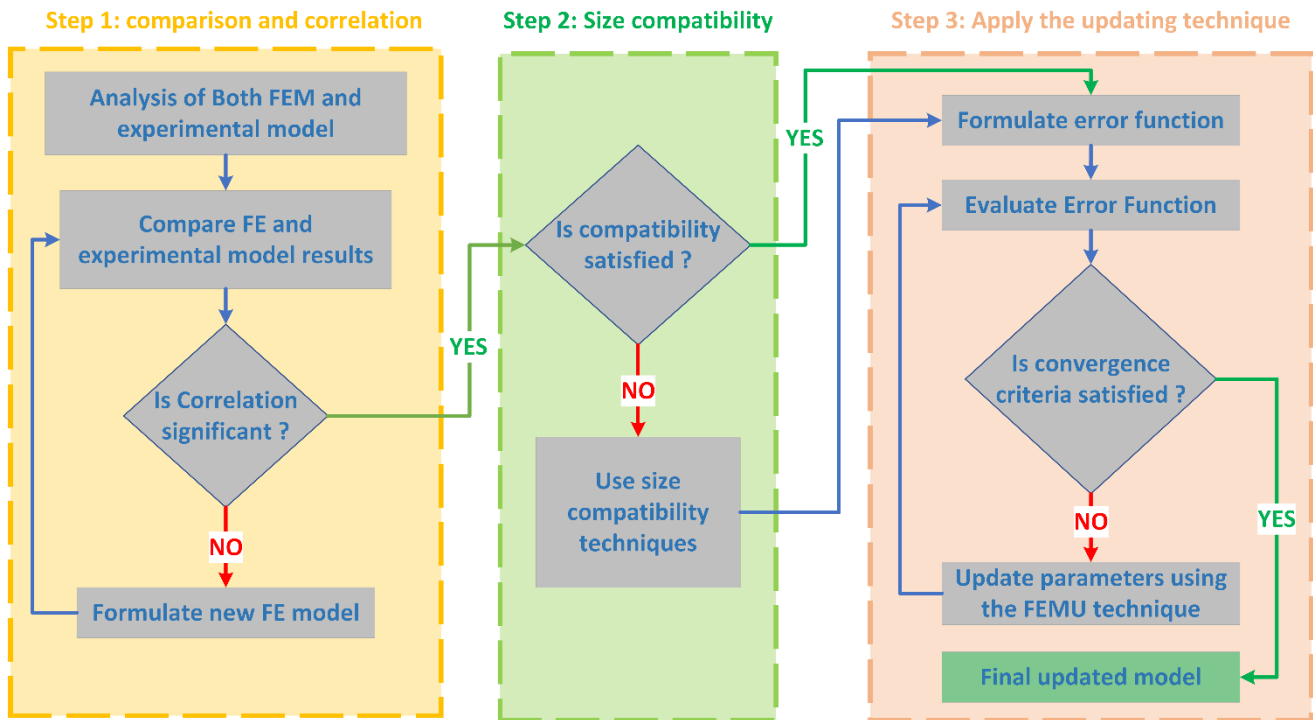


**Figure 2-2 Cross-Functional flowchart illustrating the steps of FEMC**

In the following section steps of FEMC will be presented in detail with the major contributions in the techniques used in the art of FEMC. Finally, some application of FEMC will be provided.

### 2.1.1. Comparison and Correlation

Accurate representation of either the experimental or detailed FEM requires that the simplified FE response to be compared to that of the detailed experimental or numerical response to assess whether or not the simplified FE is ready for updating. Comparison techniques ranging from graphical to numerical approaches can be used. Graphical approach cannot be automated and hence the numerical methods are most common. In this section some methods are introduced such as comparison of frequency response function (FRF), comparison of mode shapes, and comparison of natural frequencies. Introduction to this topic is given in Ewins Book (1984).

#### 2.1.1.1. Comparison of FRFs

This method utilizes a plot of FRF of FE model along with Experimental results on the same curve, then visual inspection is made to find out if any relation between the two FRFs can be detected. Fig. 2-3a shows a high correlation between the results indicating that the FE model is ready of updating. Fig. 2-3b shows that no correlation can be made

between both results and therefore a conceptually new FE model is required prior to proceeding in the updating [Sehgal et al. 2016].

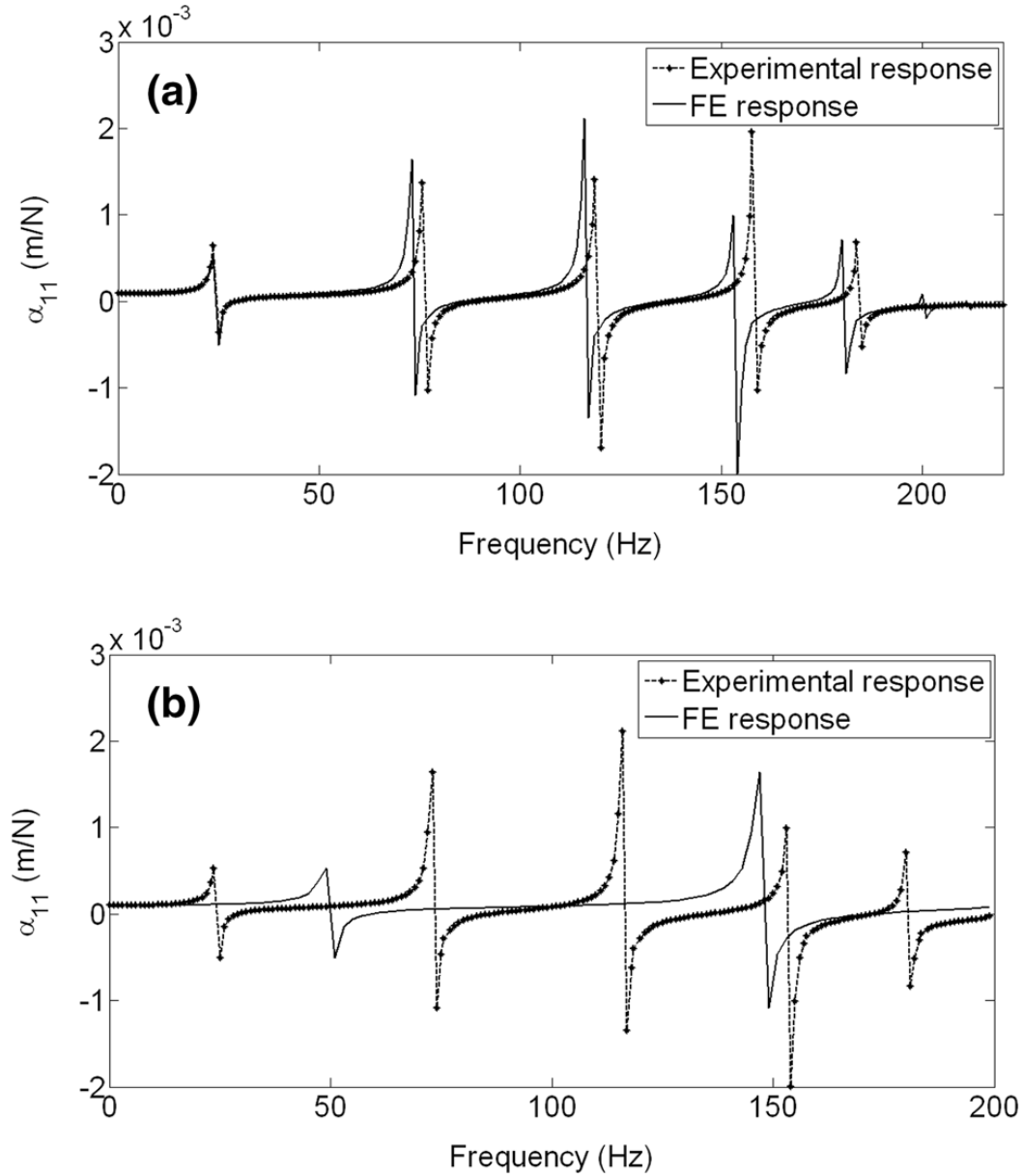


**Figure 2-3 Example of visual inspection of correlation (a) show good correlation while (b) Show No Correlation [Sehgal et al. 2016]**

#### 2.1.1.2. Comparison of Natural Frequencies

One of the comparison techniques is the comparison of natural frequencies. In case of simulation model, the natural frequencies are obtained by modal analysis of the analytical modal while in the case of experimental model, the natural frequencies are obtained through modal testing [Ewins 2009]. If large discrepancies are found between natural frequencies, then new FE model should be formulated. Table 2-1 shows a comparison between natural frequencies where the detailed model represents the

simulation model. In this example the errors indicate a good correlation between the results.

**Table 2-1 Comparison between natural frequencies**

Mode Number	Detailed Model	Simplified Model	Percentage error
1	1.3549	1.1186	17 %
2	4.1993	3.3780	20%
3	4.4803	3.9465	12%
4	5.4603	4.5701	16%

### 2.1.1.3. Comparison of Mode Shapes

The simplest method is by drawing the two sets of mode shapes of experimental and FE model on the same graph and make visual inspection. The main drawback is that this method cannot be measured with a scalar number and depends on the judgment of the engineer. Therefore, there is a need to a quantitative measure to assess the relation between mode shapes to be able to automate the process. Several quantitative coefficients are available. Modal Assurance Criteria (MAC) is among the most common techniques. This method was first introduced by Allemang and Brown (1982). MAC value of 1 represent good correlation whereas a value of zero represent no correlation. MAC is calculated according to the following equation.

$$MAC(\{\phi_X\}_i, \{\phi_A\}_j) = \frac{|\{\phi_X\}_i^T \{\phi_A\}_j|^2}{(\{\phi_X\}_i^T \{\phi_X\}_i)(\{\phi_A\}_j^T \{\phi_A\}_j)} \quad (2-1)$$

Where:

$\{\phi_X\}_i$ : the experimental  $i$ th mode shape

$\{\phi_A\}_j$ : the analytical  $j$ th mode shape

$\{\phi_X\}_i^T$ : the transpose of the experimental  $i$ th mode shape

$\{\phi_A\}_j^T$ : the transpose of the analytical  $j$ th mode shape

The previous equation is calculated between all mode shapes of the experimental and FE model which yield a matrix with diagonals equal to one and zero in off-diagonals in case of perfect correlation. Fig. 2-4 shows an example of MAC plot showing one case of good correlation and another of poor correlation [Sehgal et al. 2016].

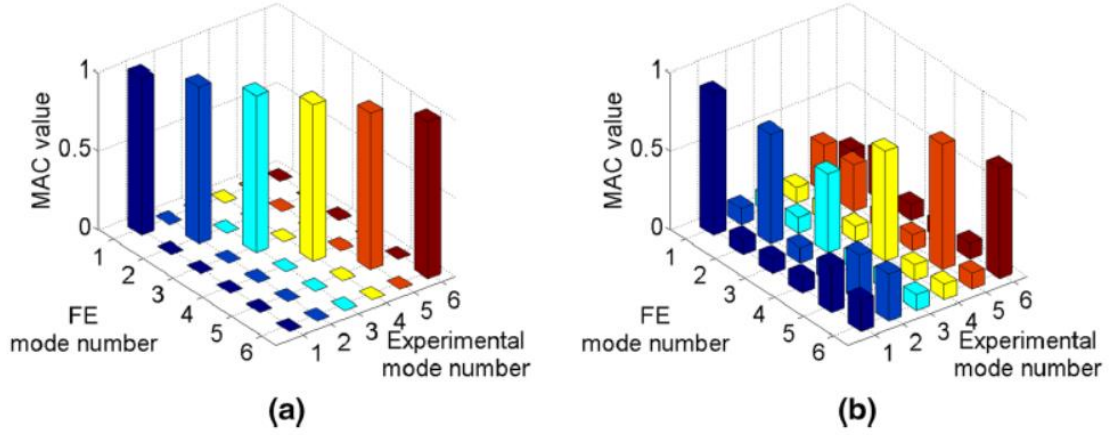


**Figure 2-4 Example of MAC plot the left plot represent good correlation while the right represent poor correlation [Sehgal et al. 2016].**

After comparing the results of the experimental and FE model and formulating a FE model that has a good correlation with the experimental results, compatibility techniques are applied to make the data of the FE model and Experimental model compatible with each other. In the following section these techniques are illustrated.

## 2.1.2. Compatibility techniques

Number of Degrees of freedom measured in the experimental model is very small compared to the number of degrees of freedom in FE model. This can be attributed to the few number of sensors that can be used, also some degrees of freedom are sometimes hard to measure such as torsional degree of freedom. Since FEMC techniques require data correspondence, the two sets must be similar in size this can be achieved by either reducing number of DOFs in the FE model or increasing the number in experimental results.

The following two sections illustrate the two methods

### 2.1.2.1. Coordinate Expansion

In this method measured data are expanded to reach the size of data in FE model. A simple technique is to substitute the missing degrees of freedom by their FE counterparts. From a computational cost perspective this method is efficient. But this method can yield errors in updating process. Other methods use transformation matrix technique as shown in the equation where the transformation matrix can be calculated by using Kidder's method [Kidder 1973].

$$\{\Phi_{expanded}\}_{Nx1} = [T]_{NxN}\{\Phi_{measured}\}_{Nx1} \quad (2-2)$$

#### **2.1.2.2. Model Reduction**

This method is the conjugate of the coordinate expansion method where reduction technique is applied to the FE model in order to make size of model matrices similar to the size of the experimental counterpart. A simple method is to eliminate the unmeasured degrees of freedom from the FE model.

#### **2.1.3. Techniques of FEMC**

FEMC can be classified into direct and iterative techniques. Direct techniques can find the solution in one step. Therefore, it is very efficient from a computational point of view and no convergence problems exist. High quality modal testing is required to avoid propagation of noise in the results of modal analysis since the direct techniques produce the measured data exactly. Direct techniques provide the solution in the form of updated system matrices therefore they are called matrix techniques. The main disadvantage of this type of FEMC techniques is that system matrices may not be symmetric and hence can't be understood physically.

Response of FE model is based on structural parameters. In iterative techniques selection of parameters is made to determine the parameters that are considered to be the major source of discrepancies between the experimental and the FE model. In this type of techniques, the solution is in the form of updated parameters through iterations that minimize an objective function representing the difference between the experimental and the FE model results. The main disadvantage of this method is that it requires high computational cost and convergence problems may exist. The direct and iterative techniques will be presented with major contributions to both types of techniques.

##### **2.1.3.1. Direct Techniques**

In this section major contribution to direct techniques are discussed. In 1978 Baruch and Bar-Itzhack proposed a direct technique where mass matrix is considered to be correct and then the eigenvector matrix is updated with the orthogonality constrain in consideration then the stiffness matrix is updated with the of objective of minimizing the difference between initial and updated matrix. This method uses Lagrange multiplier technique in minimizing process. Fig. 2-5 shows a flowchart depicting the steps of this method.

There was some doubt about considering the mass matrix to be true since static analysis produce more accurate results than modal analysis. Also, there is a concern about updating measured data. Berman and Nagy (1983) used a similar procedure of that used by Baruch but the measured eigenvector matrix is considered to be correct then the mass and stiffness matrix are updated. Fig. 2-6 illustrate the procedure of this method.

Caesar (1986) also made a modification of this method to start with updating the stiffness matrix and then update the mass matrix.



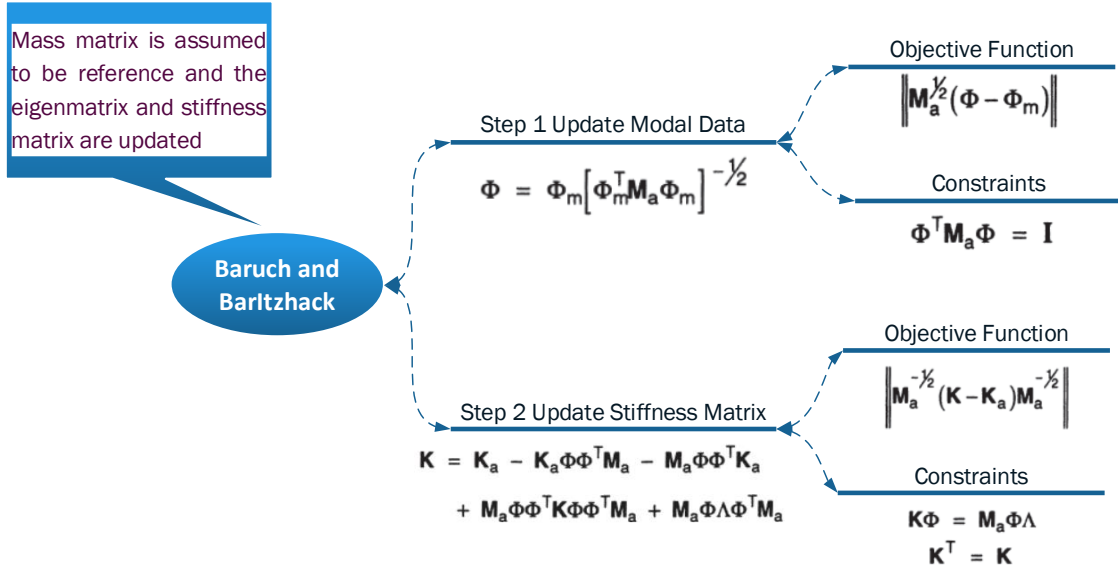


**Figure 2-5 Steps of the direct method by Baruch and Bar-Itzhack 1978**

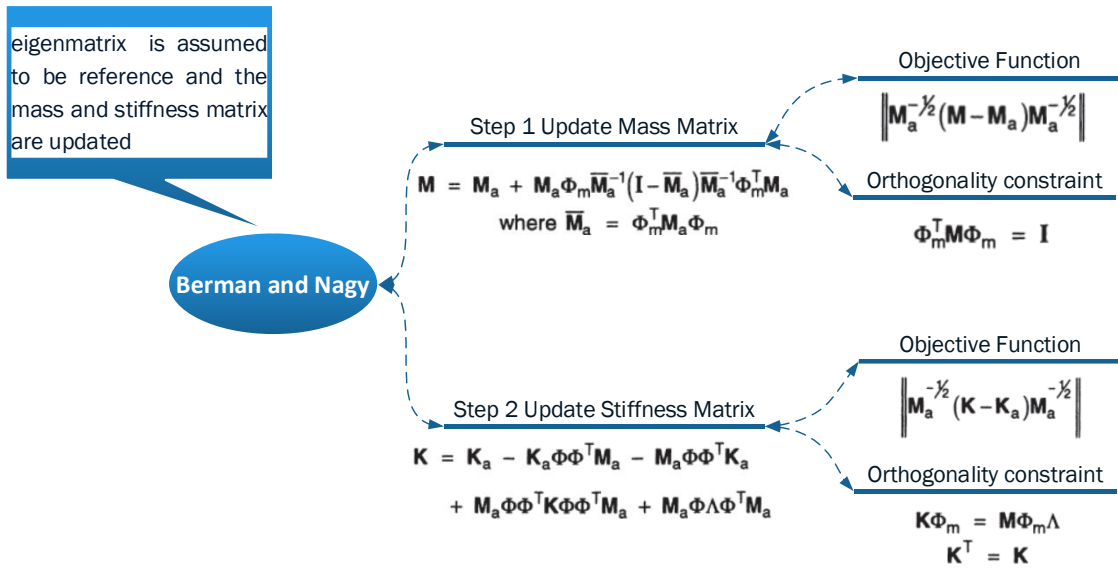


**Figure 2-6 Steps of the Direct Method by Berman and Nagy 1983**

Hu et al. (2007) proposed the cross-model-cross-mode method (CMCM)] in which calibration of physical properties is done to update mass and stiffness matrices. Forcing the symmetry of the mass and stiffness matrices Hu et al. developed a set of linear equations in a matrix form with vector of unknowns representing the correction factors of mass and stiffness properties. Moreover, in 2011 Fang et al. developed a new direct method called substructure energy approach. The main advantage of this method over CMCM method is that it can deal with incomplete measured data. In this method the structure is divided into several substructures and critical substructures are identified and updated using linear equations derived from energy functional of sub models [Fang et al. 2011].

In 2012, Jacquelin et al. incorporated uncertainty in measured natural frequency and mode shapes where they developed closed-form solution for mean and covariance of updated stiffness matrix based on random matrix approach [Jacquelin et al. 2012].

In 2013, Jiang et al. proposed a new method where they reduced the problem of model calibration to a best approximation problem where they updated the mass and stiffness matrices using constrained optimization. Main drawback is that this method needs to be verified in case of damped systems [Jiang et al. 2013].

Qiuping Wang et al 2021 proposed a new direct method where parameters are directly determined through kriging model, where they generate population of updating parameters using Latin hypercube Design (LHD) and then evaluate the response for these parameters. Then they derive function between updating parameters and response using kriging theory where they can find the updated parameters using the response from experimental measurements.

### 2.1.3.2. Iterative Techniques

In this section the major contribution to iterative techniques are introduced. In 1974 Collins et al. introduced inverse Eigen sensitivity method (IESM). The method starts with expressing the relationship between modal characteristics in Taylor series expansion as shown in the following equation [Collins et al. 1974].

$$\begin{pmatrix} \{\lambda\} \\ \{x\} \end{pmatrix} = \begin{pmatrix} \{\lambda(r_p)\} \\ \{x(r_p)\} \end{pmatrix} + [T](\{r\} - \{r_p\}) \quad (2-3)$$

Modal data was used to form the fitness function then based on statistical approach the best linear estimator of the error between the correct parameters and the initial parameters is determined. Fig. 2-7 shows the flowchart of the procedure along with the [Collins et al. 1974].

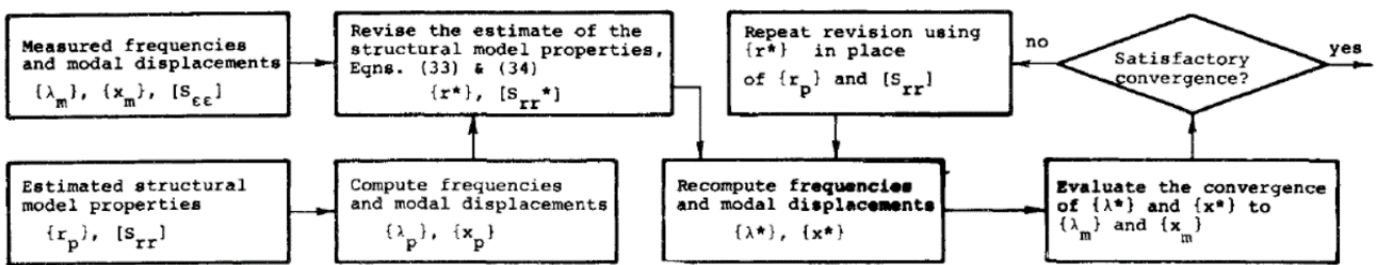


**Figure 2-7 Flowchart of the procedure along with the equations Used by Collins et al. 1974.**

IESM used modal data extracted from analysis of measured FRFs hence any error in analysis of measured data will be propagated to the modal data used in forming the fitness function. To avoid this issue, in 1990 Lin and Ewins introduced Response Function Method (RFM) where they used the measured FRFs to form the fitness function [Lin et al. 1990]. Modak et al. 2002 compared the IESM to RFM and concluded that RFM yields better results in case of incomplete measurements. However, in case of noise. IESM

performs better [Modak et al. 2002]. One of the drawbacks of the RFM developed by Lin and Ewins is that they didn't consider damping. This issue was addressed by Arora et al. where they proposed two approach to engage damping in the traditional RFM [Arora et al. 2009]. Petersen et al. applied sensitivity-based model calibration to Bergsøysund Bridge where they demonstrated how sensitivity matrix can be derived for floating bridges [Petersen et al. 2017]. Conde, B. et al. applied sensitivity-based technique to calibrate the young's modulus of the FE model of Vilanova Bridge to be utilized in structural evaluation of the bridge [Conde, B. et al. 2017].

Wei Tian et al (2021) used dynamic condensation to reduce the computational cost of model calibration of large-scale structures. where master DOFs are selected and transformation matrix is formulated to relate to total DOFs. Therefore, the global system matrices are reduced substantially. The method accuracy and efficiency were tested in two case studies and proved to achieve accurate results in only 5% of the computational time of traditional global approach.

The iterative methods mentioned so far are called sensitivity-based methods where it's required to calculate derivatives of the modal data or FRF data which impose high computational cost. Also, experimental data must be close to FE data in order for these methods to perform satisfactorily [Alkayem et al. 2018]. Other categories of methods exist such as neural networks, response surface-based method, optimization algorithm methods.

Neural networks have been employed for FEMC. In 1998 Atalla and Inman introduced neural network for FEMC [Atalla et al. 1998]. The procedure was to run the analysis of the FE model several times to obtain training data then train the neural network with FRFs as input and updating parameters as output. After training the neural network the updated parameters can be found by using the measured FRFs as input. Fig 2-8 shows the FEMC process using neural network. Application of this method will be presented later in this chapter. Major disadvantage of the neural network is that solution may converge to local minimum instead of global minimum. Tran-Ngoc et al. (2019) addressed this issue by proposing to combine artificial neural network with global optimization technique called cuckoo search and they concluded that results are accurate and computationally more efficient than using neural network. Zhang et al. (2021) Combined neural network damage detection technique based on measured data with finite element model calibration where they engage the output of the finite element model calibration into the neural network learning.

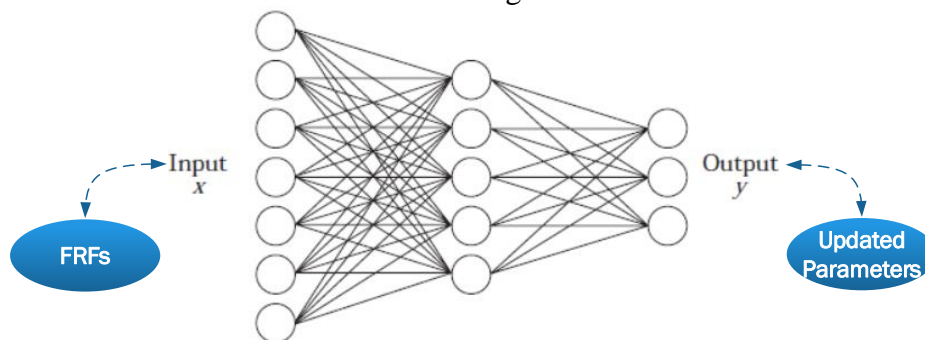


**Figure 2-8 Procedure of Using Neural Networks as introduced by Atalla et al. 1998**

The iterative FEMC process requires a high number of iterations imposing a high computational cost. One method to reduce the numerous numbers of iterations and hence

the corresponding cost is using the response surface methodology. Guo and Zhang (2004) introduced the response surface concept where a relationship between the parameters and the response of the FE model is developed using statistical approach. This method proved to be accurate as sensitivity-based methods but is more computationally efficient. Ren et al. (2010) Successfully applied response surface method to concrete bridge and compared the results with those from sensitivity-based method and concluded that response-based method is more efficient. Further in 2014, Chakraborty et al. increased the efficiency by using the moving least-squares method instead of ordinary least-squares method. The method showed better results than the ordinary method in the test. Emre et al. (2021) used response surface-based model updating in damage identification where, a reduced scale masonry bridge was built in laboratory and modal parameters were measured and compared to those from the analytical model developed in ANSYS then they used response surface method to calibrate the analytical model. Then regional damage was made to the laboratory model and the difference in modal properties was used to evaluate the damage locations. The results showed that RS can be effectively utilized in damage identification and utilization.

Traditional FEMC techniques may find difficulty in solving Complex updating problems and may introduce convergence problems or get stuck in local minimum. In such case it's advised to use optimization techniques that are capable of reaching global minimum such as Simulated Annealing (SA), Genetic Algorithms (GA) and Particle Swarm Optimization (PSO). PSO is more suitable when huge number of parameters exist. Levin and Lieven compared GA and PSA and concluded that PSA performs better [Levin RI et al. 1998]. Marwala applied GA in model calibration of H-shaped structure. Results were compared to the Nelder–Mead simplex method and it proved that GA produced more accurate results [Marwala 2010]. He et al introduced a technique that combined GA and SA to be used in damage identification [He et al 2006]. Marwala applied PSO in model calibration and showed that it yields more accurate results than GA [Marwala 2010]. Tran-Ngoc et al. compared GA and PSO where they applied model calibration to the stiffness of truss joints of the Nam O Railway bridge and concluded that PSO has higher accuracy with less computational cost [Tran-Ngoc et al. 2018]. Kang et al. introduced immunity enhanced particle swarm optimization method which include modification to the ordinary PSO. The method showed more accurate results than GA and PSO [Kang et al. 2012]. Yu Otsuki et al. Investigated the use of the branch-and-bound (B&B) algorithm in solving FEMC problems. where they used an objective function based on modal properties difference but was reformulated to suit the application of B&B method. The proposed model calibration was validated by shaking table test of 18 story building and it proved to produce accurate results [Yu Otsuki et al. 2021].

#### **2.1.4. Application of FEMC**

FEMC has been extensively applied in many fields such as damage detection, health monitoring, characterization of properties with high uncertainty and dynamic design [Sehgal et al. 2016]. Two of these applications are introduced briefly here.

#### **2.1.4.1. Neural Network based FEMC to Calibrate Steel Frame FE Model**

In this study J L Zapico et al, used a Neural Network Based FEMC technique to calibrate a FE model of a small scale steel frame structure based on the first three natural frequencies of the experimental model and then used different configuration derived from the original by changing masses and achieve cutting to some elements to simulate seismic damage. Then the initial model was compared to the updated model where the RMS error of all frequencies of supplementary configuration dropped from 4 to 2.1% [Zapico et al. 2008].

#### **2.1.4.2. Application in SHM field**

FEMC can be utilized in structure health monitoring (SHM). The procedure is to identify modal parameters using measured data and compare them to results of FE model. Then FEMC is applied to calibrate the stiffness matrix which will be compared to the undamaged case to identify the location and magnitude of damage.

In this study Jaishi et al, proposed a damage detection procedure using an optimization based FEMC technique namely the Trust Region Newton method [Jaishi et al, 2006]. The procedure was applied to both simulation beam and experimental beam. The results showed excellent prediction of location and intensity of damage.

#### **2.1.4.3. Incorporating Hybrid Simulation in Model Updating**

Hybrid simulation established itself as an efficient tool for seismic response evaluation where the structure is divided into two components: the analytical component and the experimental component. The experimental component represents the part which cannot be reliably modeled analytically. The response of the two components are then combined by an integration technique.

Elanwar and Elnashai 2016 proposed a framework for online model updating in hybrid simulation where the structure is divided into three component: the first component represents sample of the critical components and will be tested experimentally, the second component which represents the parts of the structure that share similar characteristics with the critical component will be numerically modeled and this part is the one that will be updated, the third is rest of the structure that can be reliably modeled without updating. For the experimental component a finite element model was developed to assess the response error between the experimental and FE model. Then if the error exceeds a certain limit, an updating procedure is applied. For updating they used neural network approach and optimization approach. The updated parameters are then applied to second component modeled numerically and share similar characteristics with the critical component.

After Conducting the FEMC process, an updated model is now available for deriving fragility curves which will be very approximate to those of the detailed model but without having to perform nonlinear analysis on the detailed model.

## 2.2. Fragility Analysis

Multiple analysis methods exist for performance evaluation. The complexity of these methods ranges from linear to nonlinear and from static to dynamic analysis. It was proved that nonlinear dynamic analysis is the most accurate to predict the response of the building (Shah and Tande 2014). In assessing the seismic performance of a building, it's not enough to use a limited number of earthquakes and use the results as deterministic values due to the inherent uncertainty in the characteristics of an earthquake therefore a probabilistic assessment must be utilized (Sadraddin 2015). One of these probabilistic assessments is the fragility curves. As mentioned before fragility curves may be derived for many hazards but the focus of this study is on seismic fragility analysis.

The output of fragility analysis can take the form of damage probability matrix (DPM) or fragility curve (Erberik, M. A 2015). While DPM provide discrete values of probability of collapse at certain levels of ground motion intensities, fragility curves provide a continuous representation.

### 2.2.1. Fragility Curves

Seismic fragility curves describe the probability of exceeding a predefined limit state at certain ground motion excitation level often called intensity measure (IM). Fig. 2-9 shows an example of fragility curve. The intensity measure (IM) of the earthquake can be peak ground acceleration (PGA) or spectral acceleration at the fundamental period ( $S_a$ ). The predefined limit state can be the building collapse or any other limit state of interest as will be described in latter section of this chapter.

Fragility curves can be expressed by a lognormal cumulative distribution function (CDF):

$$F(x) = P[DS / IM = x] \quad (2-4)$$

Where:

DS: the damage state or any other define limit state

x: particular value of intensity

F(x): the fragility function of the damage state (DS) evaluated at intensity x

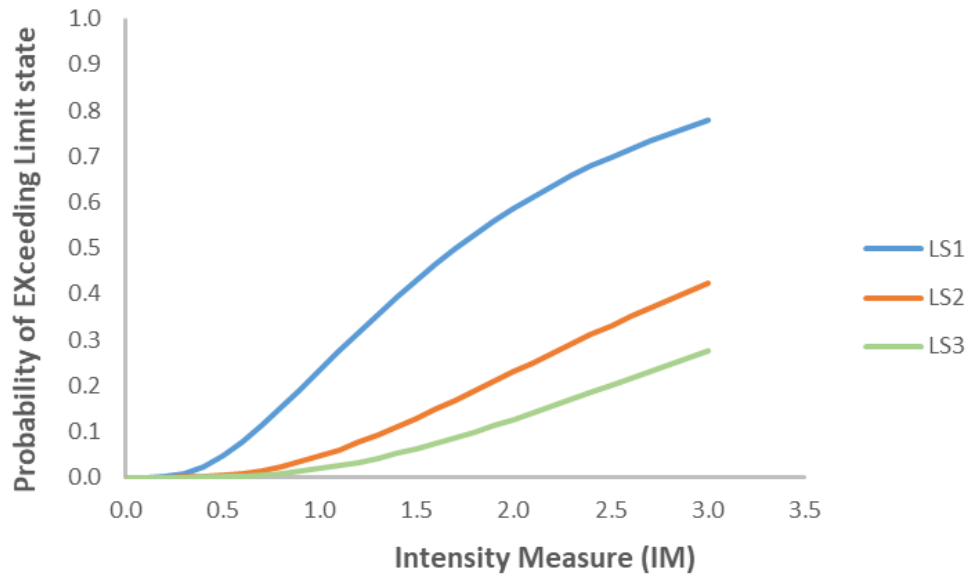


**Figure 2-9 Example of Fragility Curves at Different Limit States**

## 2.2.2. Types of Fragility Curves

Fragility curves based on 1) expert opinion 2)field data, 3)experimental data, and 4)analytical simulations (Erberik, M. A 2015 ; Sadraddin 2015). These four different methods are described in the sequel below.

### 2.2.2.1. Expert Opinion

Fragility curves can be constructed based on experts' opinion where the probable damage level, for the structure of interest, can be predicted for a specific level of seismic excitation. The fragility curves in this case are called judgmental fragility curves. This type was introduced in ATC-13 document [Applied Technology Council 1985] and HAZUS earthquake loss estimation methodology [National Institute of Building Sciences 1999]. Some of experts' opinion are listed in a paper by AmiriHormozak, 2013. The main drawback of this type of fragility curves is that it is subjective.

### 2.2.2.2. Empirical Fragility

Empirical fragilities are based on damage data collected from field observation after earthquake events. Whitman et al. (1973) introduced the concept of empirical fragility analysis where they constructed damage probability matrices after the 1971 San Fernando earthquake. Fig. 2-10 shows the general framework for developing fragility curves [Ioannou I. et al. 2015]. According to these procedures three types of data have to be collected:

- 1- **Damage State:** different types of surveys are conducted to collect observations on damage of structures to identify the damage scale of structures in the study area. Seismic damage of structure is expressed in a scale of damage that typically

varies from 3 to 6 damage levels. HAZUS documentation provides description of the expected damage in each level for each category of structures.

- 2- **Characteristics of structures:** different types of structures will suffer different damage states when subjected to the same level of intensity. This can be attributed to different structural characteristics. Therefore, categories of structures are determined based on their characteristics such as: construction material, lateral load resisting system, presence of irregularities and other characteristics that affect structure response. Several studies exist of building classifications such as classification by HAZUS.
- 3- **Intensity of Earthquakes:** the ground motion excitation measure selected for vulnerability assessment may be peak ground acceleration or spectral acceleration or other measures. Due to the lack of recording stations and to be able to quantify the ground motion at each structure, prediction equations have been used.

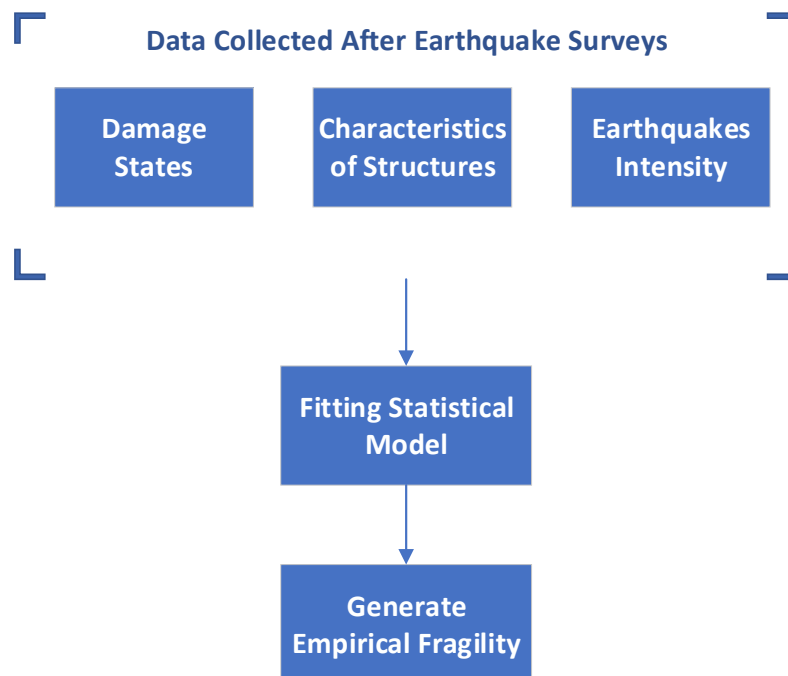


**Figure 2-10 The general framework for constructing empirical fragilities**

After collecting these data, statistical models are applied to evaluate the empirical fragility functions. The reliability and accuracy of the empirical fragility curves depend on the quality and quantity of the observed database. This is considered the main drawback of this method.

#### **2.2.2.3. Experimental Fragility**

Experimental data can be utilized to derive fragility curves utilizing the same approach used for empirical fragility curves but this requires to conduct huge number of tests making this approach very expensive and hence not feasible.



#### 2.2.2.4. Analytical Fragility

The most commonly used method to generate seismic fragility curves is the analytical method as it deals with most of the issue experienced in the other methods. Fig. 2-11 show the framework for deriving analytical fragility curves (Erberik M.A. 2015). Steps of the framework will be presented in detail.

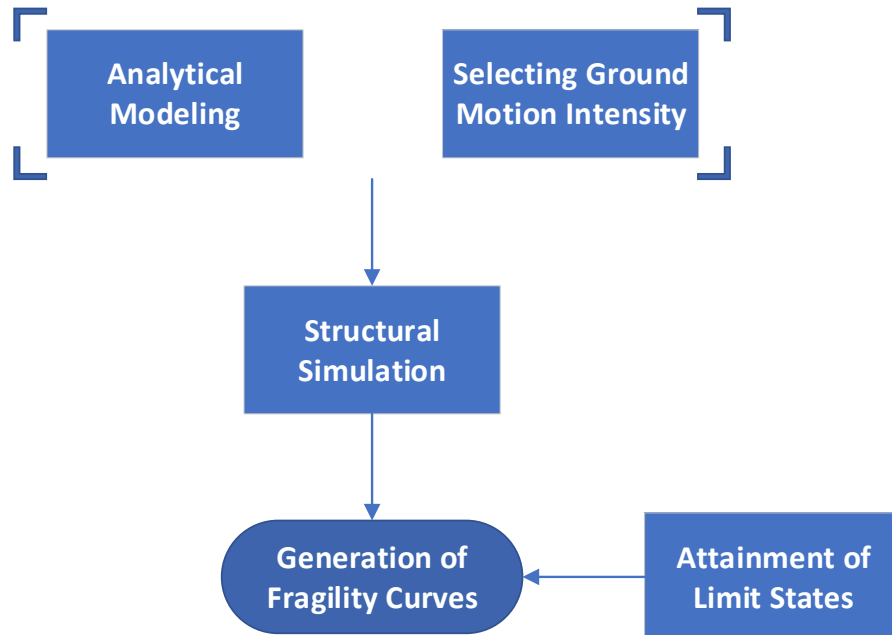


**Figure 2-11 Framework for deriving analytical fragility curves**

##### 2.2.2.4.1. Analytical modeling

The first step of developing fragility curves based on analytical approach is the development of an analytical model and conducting the simulations required to collect the response statistics needed for the derivation of the fragility curves.

Wide range of analytical models can be used to simulate the response of the structures, ranging from lumped mass single or multiple degree of freedom system to 3D detailed finite element meshes as depicted in Fig. 2-12. Since huge number of simulations are required, the single degree of freedom system seems to have the advantage of low computational cost, however the results may deviate from the actual response of the structure and yield fragility curve with low reliability. On the other hand, utilizing finite element meshes model will impose very high effort and computational cost and sometimes it turns to be impractical or even impossible. Therefore, analytical fragility always possesses a trade-off between accuracy and computational efforts.

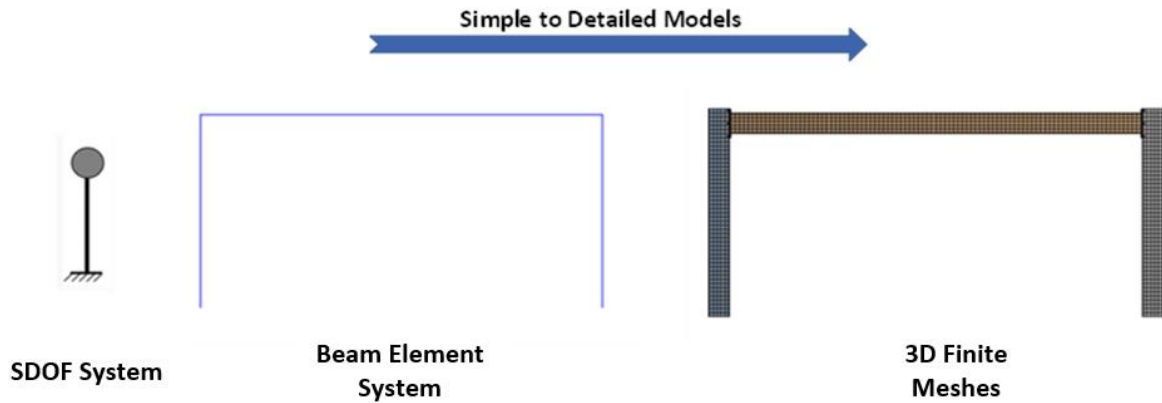


**Figure 2-12 Different detail levels of the analytical model of the same structure**

After selecting the appropriate analytical model type for collecting response statistics, the appropriate analysis type is selected. Different number of analysis types have been used in the structural analysis to be used in generating fragility curves. These types can be broadly classified into nonlinear dynamic-based and nonlinear static-based procedures. Nonlinear dynamic based analysis yields the most accurate results but require high computational efforts. Nonlinear static based analysis yields less accuracy than dynamic based type but is considered efficient from computational cost point of view. Therefore, the analysis type also imposes a trade-off between computational efforts and accuracy. The nonlinear dynamic based analysis types will be presented in some detail in following sections.

#### 2.2.2.4.2. Attainment of limit states

Specifying different damage limit states affects the resulting fragility curves. Limit states are usually defined based on the building category under consideration. However special structural systems require derivation of new limit states. In such case, two different approaches can be used, the first is from data collected from site and experimental observations. Due to lack of this data, analytical procedure is carried out. Pushover nonlinear static analysis is a good approach for this task.

Different codes and guidelines provide values for limit states of damage. For example, HAZUS-MH MR5 [HAZUS 2001], ATC-58-2 [ATC, 2003] and Eurocode-8 [CEN 2004].

In case of attaining limit states analytically the definition of damage states is used from guidelines to be able to define limit state from the analytical simulation. Generally, four damage states are defined slight, moderate, extensive and complete damage. Fig. 2-13 depicts each damage state [D'Ayala, D., et al. 2015].

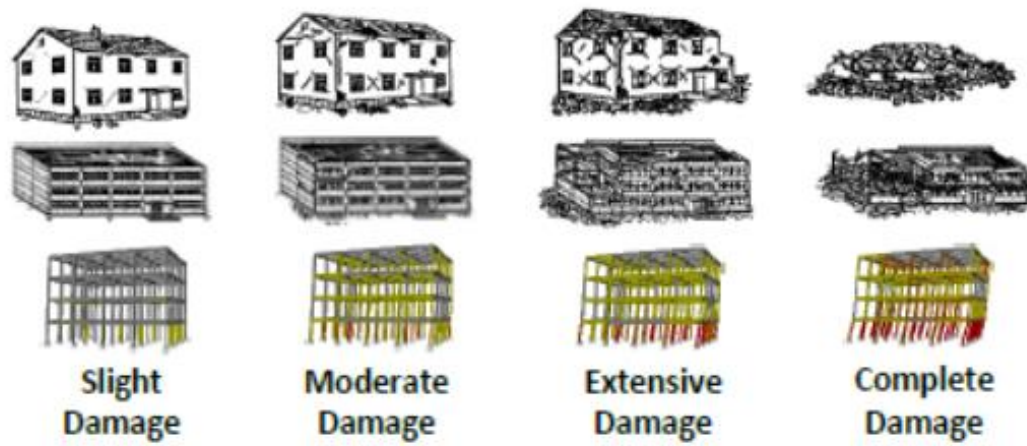


**Figure 2-13 Definition of the Considered Four Damage States [D'Ayala, D., et al. 2015].**

The tables 2-2, 2-3 & 2-4 from several guidelines provide damage state definition and inter-story drift associated with each state.

**Table 2-2 Example of Definition of Damage States According to multiple Guidelines [D’Ayala, D., et al. 2015].**

Performance Level		Slight Damage		Moderate Damage		Extensive Damage		Complete Damage
ASCE/SEI 41-06 (ASCE 2007); ATC-58-2 (ATC 2003), FEMA-356 (ASCE 2000)	Concrete Frames	Primary	Minor hairline cracking; limited yielding possible at a few locations; no crushing (strains below 0.003)	Life Safety (LS)	Extensive damage to beams; spalling of cover and shear cracking (<1/8" width) for ductile columns; minor spalling in non-ductile columns; joint cracks < 1/8" wide.	Collapse Prevention (CP)	Extensive cracking and hinge formation in ductile elements; limited cracking and/or splice failure in some non-ductile columns; severe damage in short columns.	
		Secondary	Minor spalling in a few places in ductile columns and beams; flexural cracking in beams and columns; shear cracking in joints < 1/16" width.	Extensive cracking and hinge formation in ductile elements; limited cracking and/or splice failure in some non-ductile columns; severe damage in short columns.	Extensive spalling in columns (limited shortening) and beams; severe joint damage; some reinforcing buckled.			
	Unreinforced Masonry Infill Walls	Primary	Minor (<1/8" width) cracking of masonry infills and veneers; minor spalling in veneers at a few corner openings.	Extensive cracking and some crushing but wall remains in place; no falling units. Extensive crushing and spalling of veneers at corners of openings.	Extensive cracking and crushing; portions of face course shed.			
		Secondary	Same as primary.	Same as primary.	Extensive crushing and shattering; some walls dislodge.			
Performance Level		Operational		Life Safe		Near Collapse		Collapse
ATC-58-2 (ATC 2003), Vision 2000 (SEAOC 1995)	Primary RC Elements	Minor hairline cracking (0.02"); limited yielding possible at a few locations; no crushing (strains below 0.003)		Extensive damage to beams; spalling of cover and shear cracking (<1/8") for ductile columns; minor spalling in non-ductile columns; joints cracked < 1/8" width.		Extensive cracking and hinge formation in ductile elements; limited cracking and/or splice failure in some non-ductile columns; severe damage in short columns.		partial or total failure/cracking of columns and beams
	Secondary RC Elements	Same as primary		Extensive cracking and hinge formation in ductile elements; limited cracking and/or splice failure in some non-ductile columns; severe damage in short columns		Extensive spalling in columns (possible shortening) and beams; severe joint damage; some reinforcing buckled		Partial or total failure/cracking of infill panels and other secondary elements
Performance level		Damage Limitation (DL)		Significant Damage (SD)		Near Collapse (NC)		
Eurocode-8 (CEN 2004)	Observed damage	Building is considered as slightly damaged. Sustain minimal or no damage to their structural elements and only minor damage to their non-structural components.		Building is considered as significantly damaged. Extensive damage to structural and non-structural components.		Building is considered as heavily damaged. Experience a significant hazard to life safety resulting from failure of non-structural components.		

Table 2-3 Example of Definition of Damage States According to multiple Guidelines (continued) [D'Ayala, D., et al. 2015].

Performance Level	Slight Damage	Moderate Damage	Extensive Damage	Complete Damage
Observed damage	Damage Limitation (DL) For the case of infilled frames: limit state is attained at the deformation when the last infill in a storey starts to degrade. For the case of bare frames: this limit state is attained at the yield displacement of the idealized pushover curve.	Significant Damage (SD) The most critical column controls the state of the structure: the limit state is attained when the rotation at one hinge of any column exceeds 75% of the ultimate rotation	Near Collapse (NC) The most critical column controls the state of the structure: the limit state is attained when the rotation at one hinge of any column exceeds 100% of the ultimate rotation	
Performance level				Collapse
ATC-58 (FEMA P-58, 2012)				Several definitions of collapse failure have been proposed

Table 2-4 Examples of Inter-Story Drift Damage Associated with Damage States According to multiple Guidelines [D'Ayala, D., et al. 2015].

Damage State	Slight Damage		Moderate Damage		Extensive Damage		Complete Damage	
	Overall Building Damage	Interstorey Drift (ID)	Transient	Permanent	Moderate	Severe	Complete	Complete
Vision 2000 (SEAOC 1995); ATC-58-2 (ATC 2003)	Damage State	Interstorey Drift (ID)	Transient	Permanent	Moderate	Severe	Complete	Complete
FEMA-356 (ASCE 2000); ASCE/SEI 41-06 (ASCE 2007); ATC-58-2 (ATC 2003)	Concrete Frame Elements	Interstorey Drift (ID)	Transient	Permanent	Moderate	Severe	Complete	Complete
FEMA-356 (ASCE 2000); ASCE/SEI 41-06 (ASCE 2007); ATC-58-2 (ATC 2003)	Unreinforced Masonry Infill Wall Elements	Interstorey Drift (ID)	Transient	Permanent	Moderate	Severe	Complete	Complete

#### 2.2.2.4.3. Ground Motion Records selection and scaling

A suit of ground motion records has to be selected to cover the full range of structure response. Record-to-record variability must be considered to avoid event bias [FEMA-P695]. After selecting the records, scaling of each record in the set is applied to represent the same hazard level. The method used for selecting and scaling the records have substantial effect on the developed fragility curves as shown by Gehl et al. [2014].

Scaling of earthquakes can be applied to match different objectives as shown in Fig. 2-14 [D'Ayala, D., et al. 2015] such as:

- 1- Matching based on peak ground acceleration (PGA).
- 2- Matching based on spectral acceleration ( $S_a$ ).
- 3- Matching based on minimizing the error on range of periods.

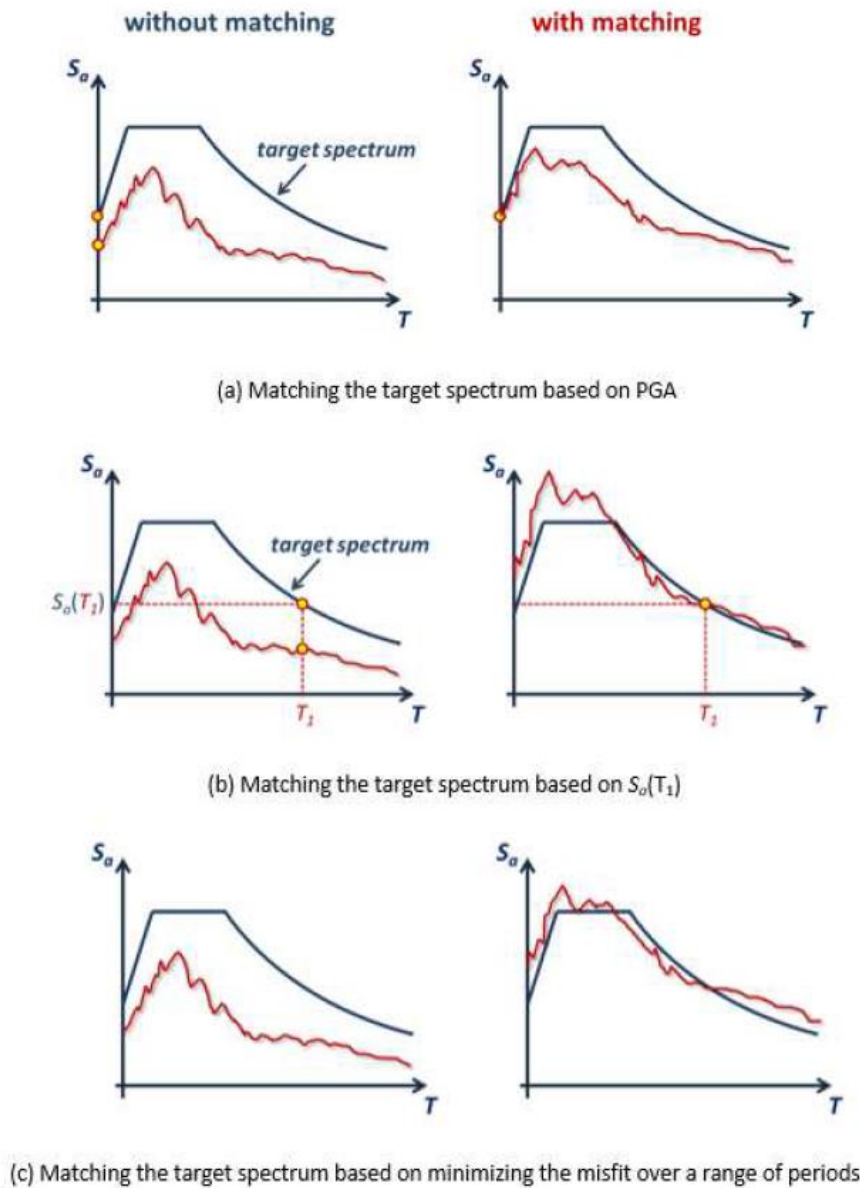


**Figure 2-14 Example of Spectral Matching (Scaling Techniques) [D'Ayala, D., et al. 2015].**



FEMA-P695 provides two sets of ground motions for the evaluation of nonlinear response of buildings namely, Near-field set and Far-field set. Near-field set includes 28 pairs of records from sites located at distance less than 10 km from fault location. Far-Field Set include 22 pairs of records from sites located at distance more than 10 km from fault location. Although the two sets are available, only the Far-field set is used for collapse evaluation. The records in FEMA P695 were collected from strong earthquakes events in the Pacific Earthquake Engineering Center (PEER). To consider variability in records no more than two records were selected from one earthquake. FEMA P695 requires the ground motions to be scaled such that  $S_a$  of all records match at the fundamental period.

### **2.2.3. Nonlinear Dynamic Analysis**

After selecting the suitable model type, analysis will be conducted to determine the response statistics necessary for deriving fragility curves. Analysis can be nonlinear dynamic based or nonlinear static based. The section focuses on nonlinear dynamic based approach is presented. Several nonlinear dynamic based approaches exist in literature such as, the single strip analysis, the cloud analysis, The incremental dynamic analysis (IDA), the multiple stripes analysis (MSA) and cloud to IDA [Jalayer, F. 2015, Di-Sarno, L., & Elnashai, A. S. 2021]. The single strip analysis and the cloud analysis only work for narrow range spectral accelerations and therefore have limited applications and will not be part of this discussion.

#### **2.2.3.1. Incremental Dynamic Analysis (IDA)**

The incremental dynamic analysis (IDA) is one of the common procedures to acquire structural response data for fragility analysis (Vamvatsikos and Cornell 2002; Federal Emergency Management Agency 2009). In this method a suit of ground motions records is applied with increasing intensity until reaching collapse. Collapse may be characterized by inter-story drift limit or any other limit state. This process is done for each record in the set. Fig. 2-15 shows the IDA procedure for one earthquake.

Conducting IDA for each earthquake yield a number of discrete points representing the maximum inter-story drift for the scaled intensity. Interpolation techniques are then applied to generate smooth IDA curve as shown in Fig. 2-16 where it depicts three steps of the response, elastic until yielding, softening and then collapse [D'Ayala, D., et al. 2015].

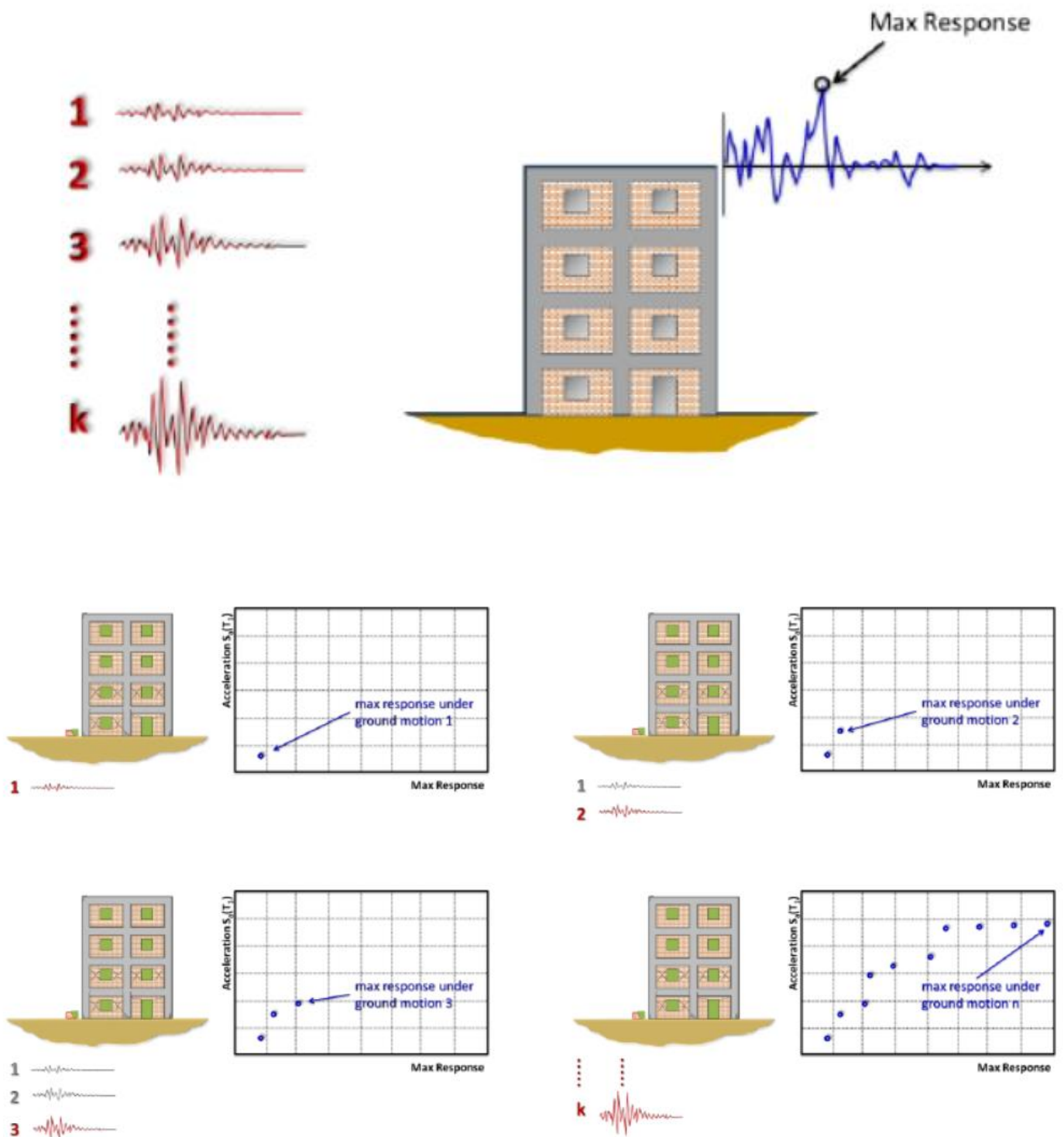
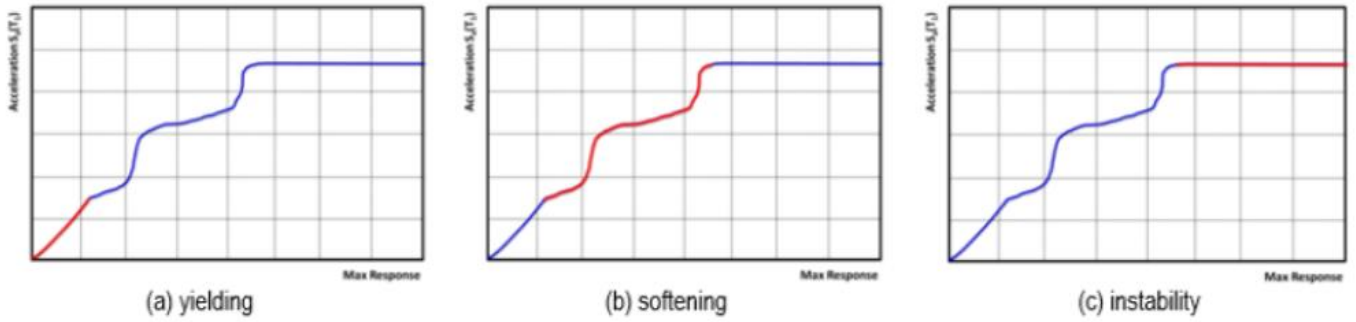


Figure 2-15 The Procedure of Generating One IDA Curve [D'Ayala, D., et al. 2015]





**Figure 2-16 Example of IDA curve with three step response [D'Ayala, D., et al. 2015]**

The process of constructing one IDA curve is then repeated for the entire set of earthquake records. After completing the IDA curves, a set of intensity measure values (IM) (for example  $S_a$ ) associated with start of collapse or exceeding certain limit state are available. The probability of exceeding that limit state at certain value of IM can be calculated as a fraction of the earthquakes where the limit state is violated [Baker 2015]. These probabilities are called empirical cumulative distribution function. Fig. 2-17 shows example of the process.

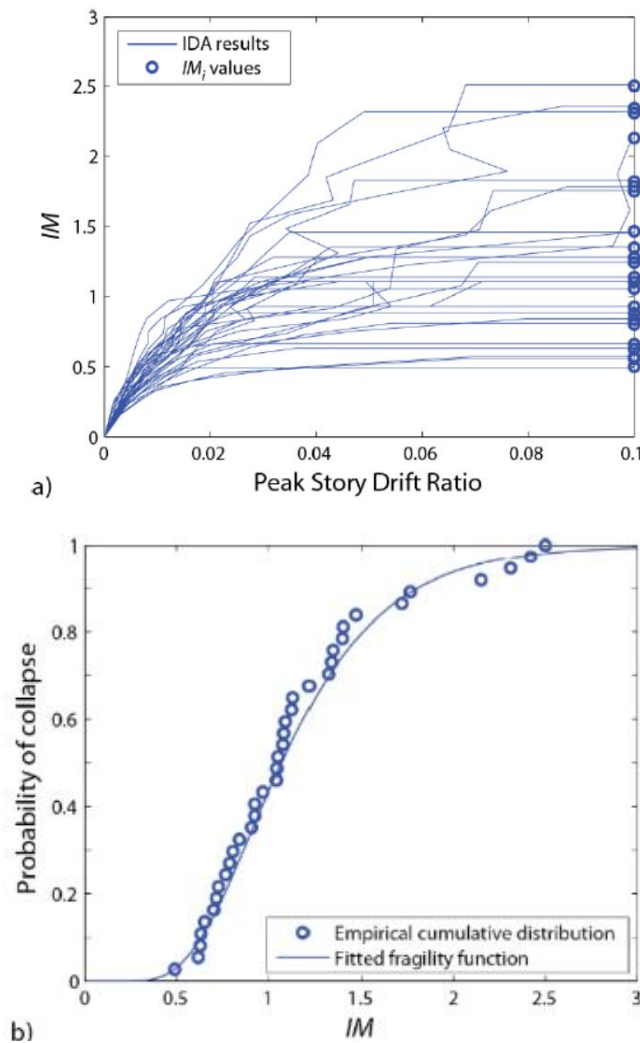


**Figure 2-17 a) Example of IDAs and b) The associated empirical and fitted fragility [Baker 2015]**

As mentioned before fragility function is often expressed as lognormal cumulative distribution function as shown in the following equations:

$$P[C/IM = x] = \Phi\left(\frac{\ln\left(\frac{x}{\theta}\right)}{\beta}\right) \quad (2-5)$$

One method for fitting fragility curves and calculating fragility parameters, called Method A by [Porter et al. 2007], is to take logarithms of the IM values and calculate the mean and standard deviation where,  $\ln\theta$  and  $\beta$  are the mean and standard deviation of the lognormal distribution of the value of  $\ln IM$ .

$$\ln(\theta) = \frac{1}{n} \sum_{i=0}^n (\ln IM_i) \quad (2-6)$$

$$\beta = \sqrt{\frac{1}{n-1} \sum_{i=0}^n (\ln (IM_i/\theta))^2} \quad (2-7)$$

This method is computationally very demanding, especially if the number of ground motion records is large, which will require IDA curves to be constructed for all records. Han, S. W. et al. (2006) investigated the use of modal pushover analysis, nonlinear static based approach, to generate the demand due to each record and they concluded that the method is efficient and provided the results at a useful degree of accuracy. Azarbakht, A. et al. (2011) proposed an approach called progressive IDA. The first step of this approach is to identify a priority list of ground motion records. This is done through constructing a simple model representing the behavior of the original model (ex. SDOF model) then generate the IDA curves for all records based on the simplified model. And then apply optimization algorithm to identify the priority list that minimizes the difference between the original and approximate summarizing (16th, 50th, and 84th fractiles) IDA curves where the original is calculated based on all IDA curves while approximate are calculated based on the first group of the priority list. The second step is to calculate the IDA curve for the first group of records in the priority list and once the accepted tolerance in determining the summarizing IDA curves is reached, the analysis can be halt. This method resulted in reduction of computational cost.

### 2.2.3.2. Multiple Stripes analysis

In IDA all earthquakes need to be scaled with increasing intensity until collapse is reached, this requires large number of analyses. Alternatively, multiple stripes analysis can be used where response to each record is evaluated at specific values of IM (Jalayer 2003) where it is not required to reach collapse from all ground motion records.

The output is in the form of discrete values of response at specific IM from all ground motion records. Therefore, the fitting technique used for IDA is not applicable here since value of IM at onset of collapse are not available. Instead, we can calculate the portion of ground motion records causing collapse at each value of IM. In order to convert this data to fragility curves a different fitting technique will be used. The suitable method of fitting this type of data is the maximum likelihood [Baker et al. 2005]. Fig. 2-18 shows the output of multiple stripes analysis and the conversion to fragility curves [Baker 2015].

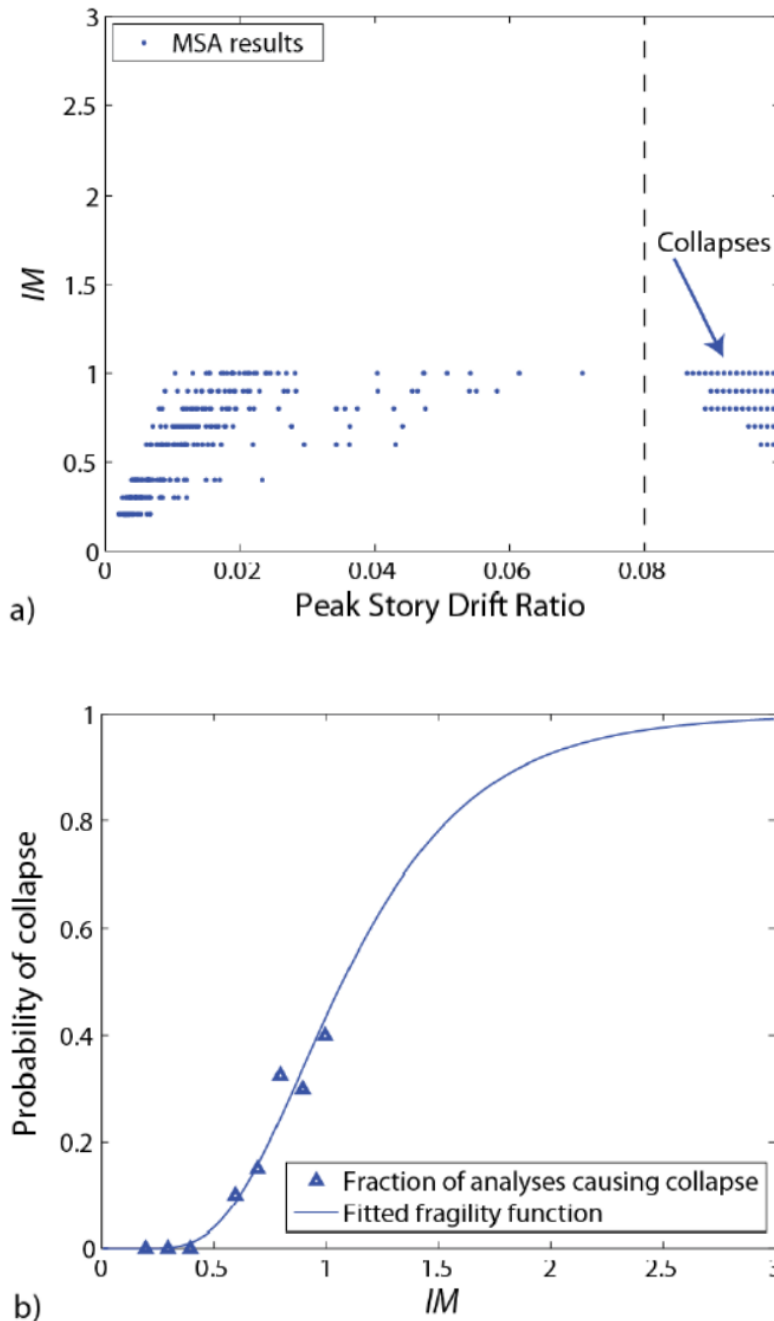


**Figure 2-18 a) the output of multiple stripes analysis and b) the conversion to fragility curves [Baker 2015].**

Miano et al. studied extensively the IDA, MSA and cloud methods and introduces a new approach, called cloud-to-IDA, that aim to achieve the same accuracy with less amount of analysis [Miano et al. 2018]. the key of this method lies in determining the spectral accelerations associated with the onset of exceeding the limit state considered. This is done by conducting a cloud analysis where linear regression is applied to responses from un-scaled records. The spectral acceleration near those corresponding to exceeding the limit state are determined and the records are scaled accordingly.

#### **2.2.4. Nonlinear Static Based Approach for Fragility**

This type of methods for deriving fragility curves represents a simplified alternative to dynamic based procedure. These methods proved to yield fragility curves with less computational cost and good accuracy [Pinho, R. 2009].

Some of these methods are:

- 1- Capacity Spectrum Method (CSM) proposed by Freeman et al. (1975)
- 2- N2 method, proposed by Fajfar et al. (1988)
- 3- Modal Pushover Analysis, proposed by Chopra (2001)
- 4- Adaptive Capacity Spectrum Method, proposed by Casarotti, C. et al.

These methods are out of scope of this research since the dynamic based procedure produce the highest accuracy and therefore will be used in this work.



## Chapter 3 Methodology

In this chapter the methodology adopted to develop the framework, briefly shown in Fig. 3-1, is presented starting with the modeling of the structure and FEMC procedure to finally deriving fragility curves. The methodology can be outlines with the following steps:

- 1- the simplification applied to the detailed FE model
- 2- the method of choosing the updating parameters
- 3- the applied FEMC technique
- 4- the chosen objective function for FEMC
- 5- how the algorithm was implemented
- 6- Derivation of fragility Curves

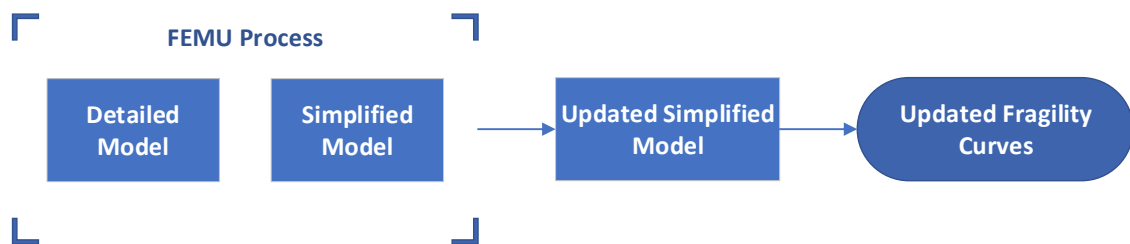


**Figure 3-1 Flowchart of the implemented framework**

### 3.1. Model Updating Stage

In this section the technique used in the FEMC stage is presented. Before getting to the FEMC stage two analytical models are to be formulated and ensured they can be correlated to each other by the comparison and correlation techniques mentioned before. The detailed model whose results are regarded as the correct results will be developed in ANSYS WORKBENCH. While the simplified model will be developed in ANSYS APDL since it supports the formulation of parametric models hence, the automation of the process can be done.

#### 3.1.1. Detailed versus Simplified models

Simplifications are applied to the detailed model to formulate a simplified model whose analysis does not encounter the high computational cost associated with the detailed model and in the same time their response can be correlated together. The simplification includes the following:

- 1- Use of beam elements instead of 3D finite meshes
- 2- Use of fully rigid or hinged connection instead of modeling the exact connection
- 3- Using simplified material models
- 4- Neglecting the soil structure interaction

The first two examples are shown in the Fig. 3-2

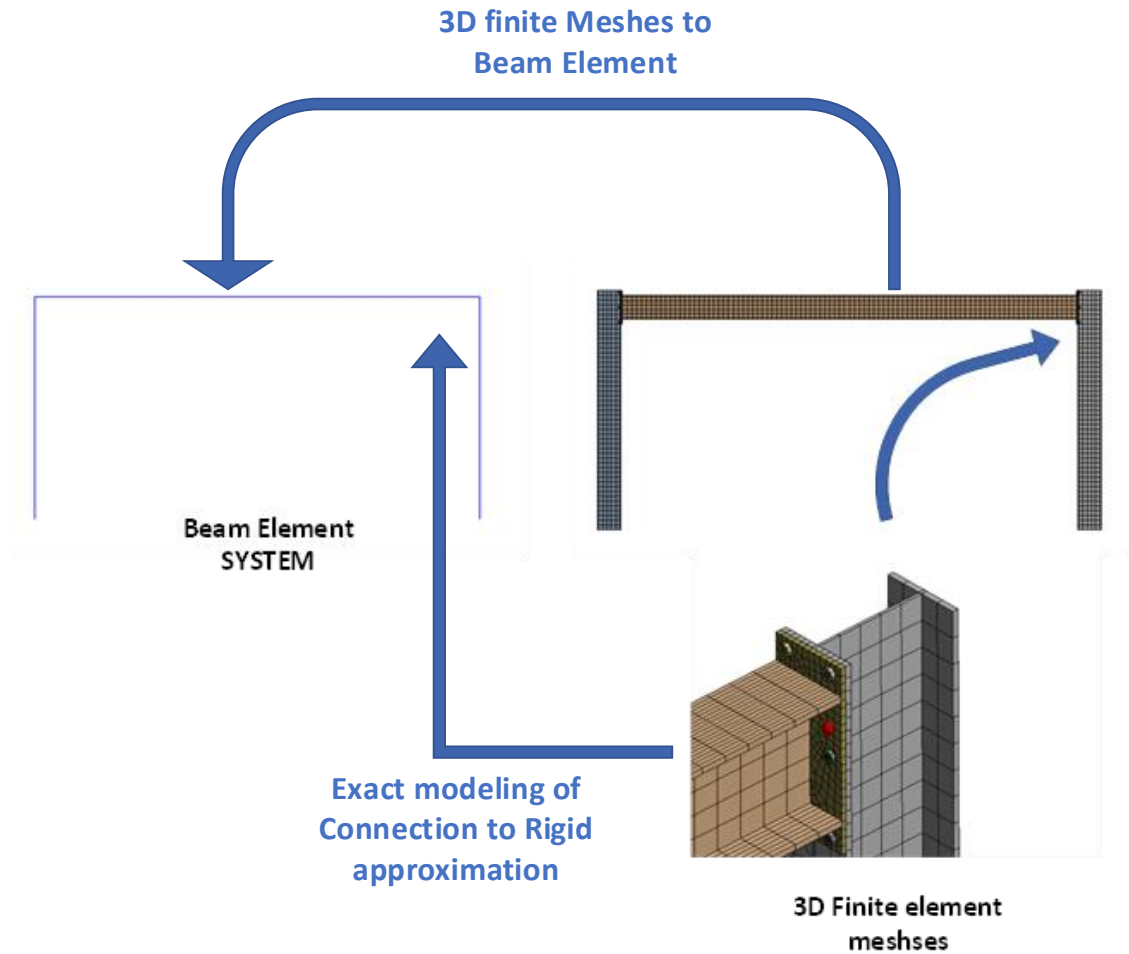


**Figure 3-2 Examples of simplifications applied to the detailed model**

### **3.1.2. Updating Parameters**

The updating parameters will be chosen based on sensitivity analysis in order to identify the parameters that amplify the error between the detailed model and simplified model. For example, a modal analysis can be conducted to investigate the effect of the beam-column connection on the natural frequencies by running FE models with several approaches of modeling the connection.

### **3.1.3. FEMC Technique**

A Genetic Algorithm (GA) was chosen for conducting the FEMC process as it proved to be able to reach the global minimum of the optimization problem. Also, the use of gradient-based methods may be difficult or impossible since the objective function may not be smooth [Marwala, Tshilidzi 2010]. The main drawback is the high computational cost of the method making it not suitable for large scale problems.

### **3.1.4. Objective function**

The objective function of the GA will include the difference of response between the detailed and simplified model. The response may be the difference in the modal characteristics such as the combined error in natural frequencies and mode shapes. But this objective function neglects the nonlinear response characteristics of the structure. Therefore, another objective function will be chosen in order to include the difference in nonlinear behavior in the updating process. The chosen objective function will be the RMS error between the capacity curves obtained from pushover analysis of the two models. This function includes both the linear and nonlinear behavior of the structure instead of only the linear part when choosing the modal parameters as the objective function.

### **3.1.5. Implementation of the Framework**

The FEMC process was implemented through the integration of MATLAB and ANSYS as shown in the following flowchart in Fig. 3-3. The process is implemented as follows:

- 1- MATLAB assigns values of parameters to the first generation
- 2- The values then will be written in text file that will be retrieved by ANSYS when running the analysis
- 3- After running the analysis, the required results which are the points of the capacity curve will be written in a text file that will be retrieved by MATLAB
- 4- After reading the results in MATLAB, the objective function is evaluated to determine the parents of the next generation based on their fitness value
- 5- The parents are then used to determine the population of the next generation through the mutation and crossover processes
- 6- Then the steps from 2-5 will be repeated until the solution is reached



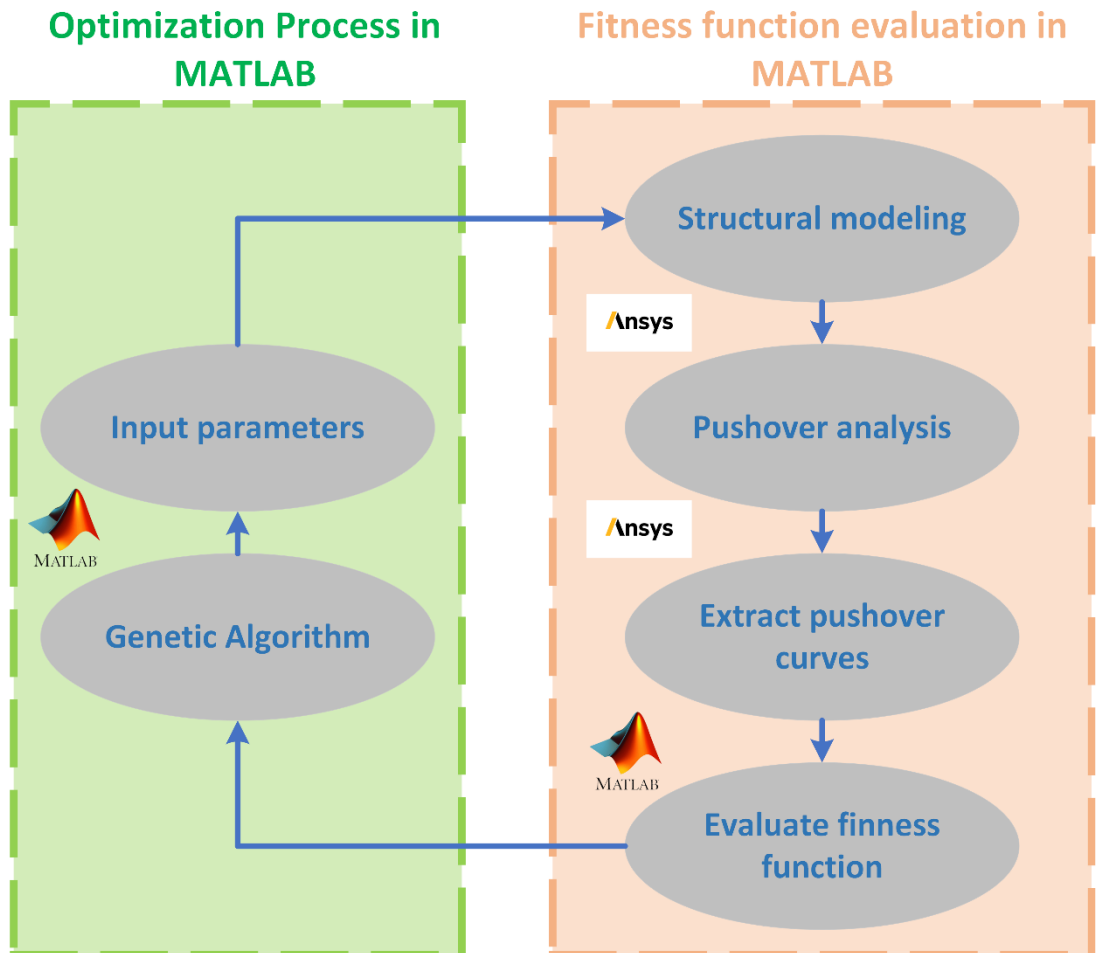


**Figure 3-3 Flowchart of the FEMC process**

The process of FEMC will finally yields the updated model that can be used to derive the fragility curves without the high computational costs associated with the detailed model.

## 3.2. Derivation of Fragility Curves

Ground motion records obtained from FEMA-P695 will be used for generating response statistics for use in derivation of fragility curves. The fragility function generator FFG developed by university of TOLEDO will be used [Gandage, S. et al. 2019]. The input for the FFG are as shown in Fig. 3-4

- 1- Total number of intensities analyzed and their values
- 2- Number of analysis at each intensity
- 3- Number of limit states and their values
- 4- Table of the output value of each analysis

1. Total Number of Load Intensities Analyzed	
2. Intensity Label	
3. Intensity Unit	
[4] Create Data Table	
5. Number of Analysis Performed in Each Intensity	
6. Engineering Demand Parameter (EDP) Considered	
7. EDP Unit	
8. Total Number of Performance Levels Considered	
[9] Create Performance Level Table	
10. Minimum Intensity in the Fragility Function	
11. Maximum Intensity in the Fragility Function	
[12] Create Input Table	

**Figure 3-4 Input of the FFG [Gandage, S. et al. 2019]**

The methodology presented in this chapter will be applied to a case study as will be shown in the following chapters



## Chapter 4 Numerical Modeling

### 4.1. Introduction

In this chapter a case study is presented to evaluate the proposed model calibration procedure. ANSYS Workbench will be used in the modeling of the detailed model and ANSYS APDL will be utilized in the modeling of the simplified model. Since, in ANSYS APDL it is easier to develop a parametric model which will be utilized in the updating process [ANSYS, Inc.]. The model developed by Emad and Hussam 2017, to study modeling resolution effects, will be adopted for the case study [Hassan, E. M et al. 2017].

### 4.2. Case Study Description

The building is a six-story hospital located in Memphis, Tennessee. The hospital was part of a study developed by the National Earthquake Hazard Reduction Program (NEHRP) to investigate cost and benefit of earthquake-resistant construction in Memphis, Tennessee [NIST GCR, 14-917-1]. Full design drawings are available in another document by NIST [NIST GCR, 14-917-2].

The building total dimensions is about 45.72 m by 54.86 m with constant bay spacing of 9.14 m in the two directions. Floor height is 4.27 m except for the first floor which is 6.1 m. The gravity load resisting system consist of composite steel framing. The flooring consists of 3.25 in light weight concrete topping a 3 in slab over a 20-gauge steel deck supported by means of secondary beams. Lateral load resisting system in each direction consist of four bays of buckling restrained braced frames.

The building was designed based on seismic loads according to ASCE/SEI 7-10, Minimum Design Loads for Buildings and Other Structures (ASCE, 2010). The building. The following figures depict the system of the building [NIST GCR, 14-917-2]. Fig. 4-1 shows a typical plan view. Fig. 4-2 shows a typical elevation of the buckling restrained bracing bay.

The derivation of seismic fragilities mainly depends on the lateral load resisting system. Therefore, in this study 2D analysis of the braced bay only was considered. Furthermore, in order to simplify the application of the proposed framework. four stories are only considered.

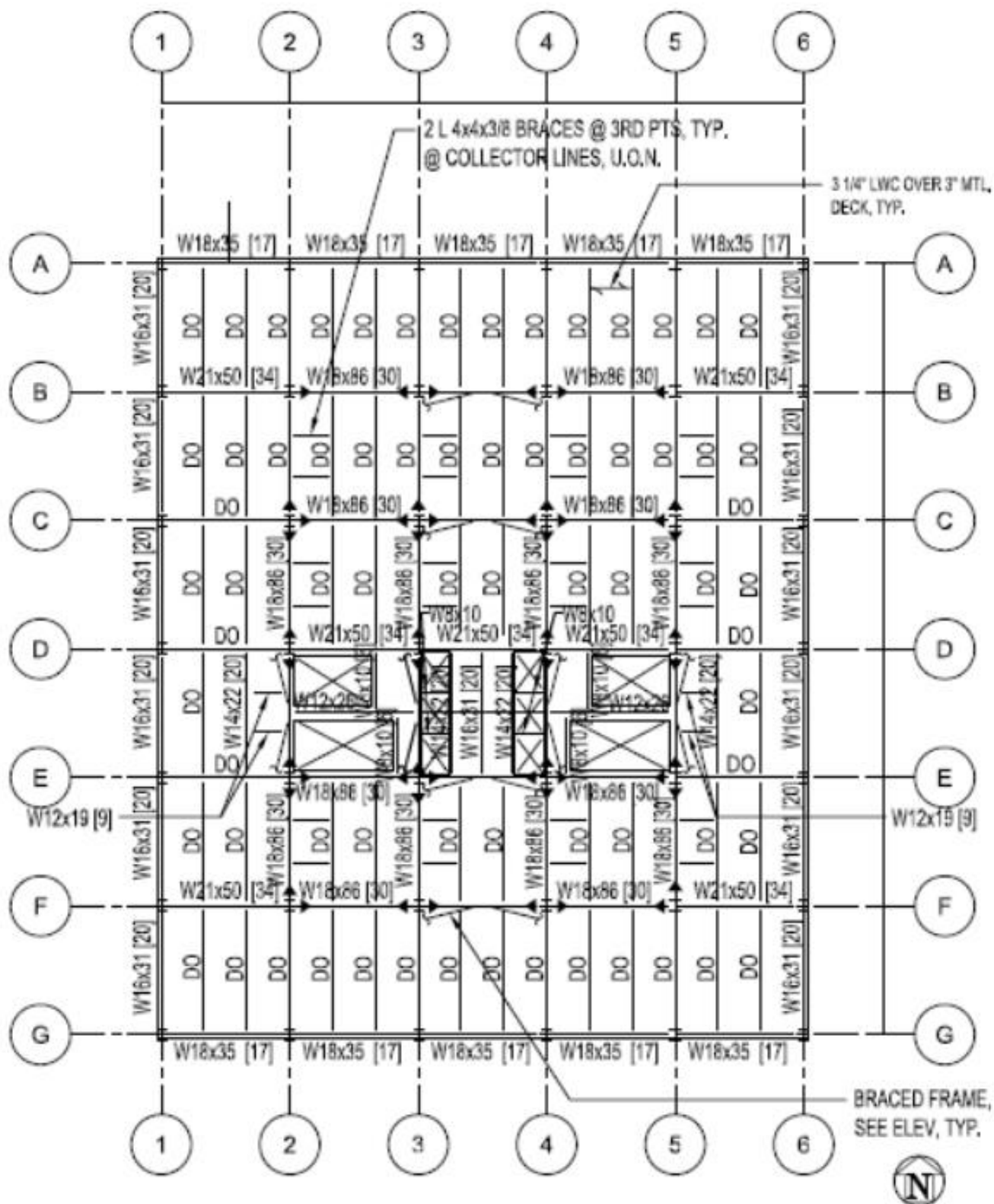


Figure 4-1 Typical Plan of the Hospital [NIST GCR, 14-917-2]

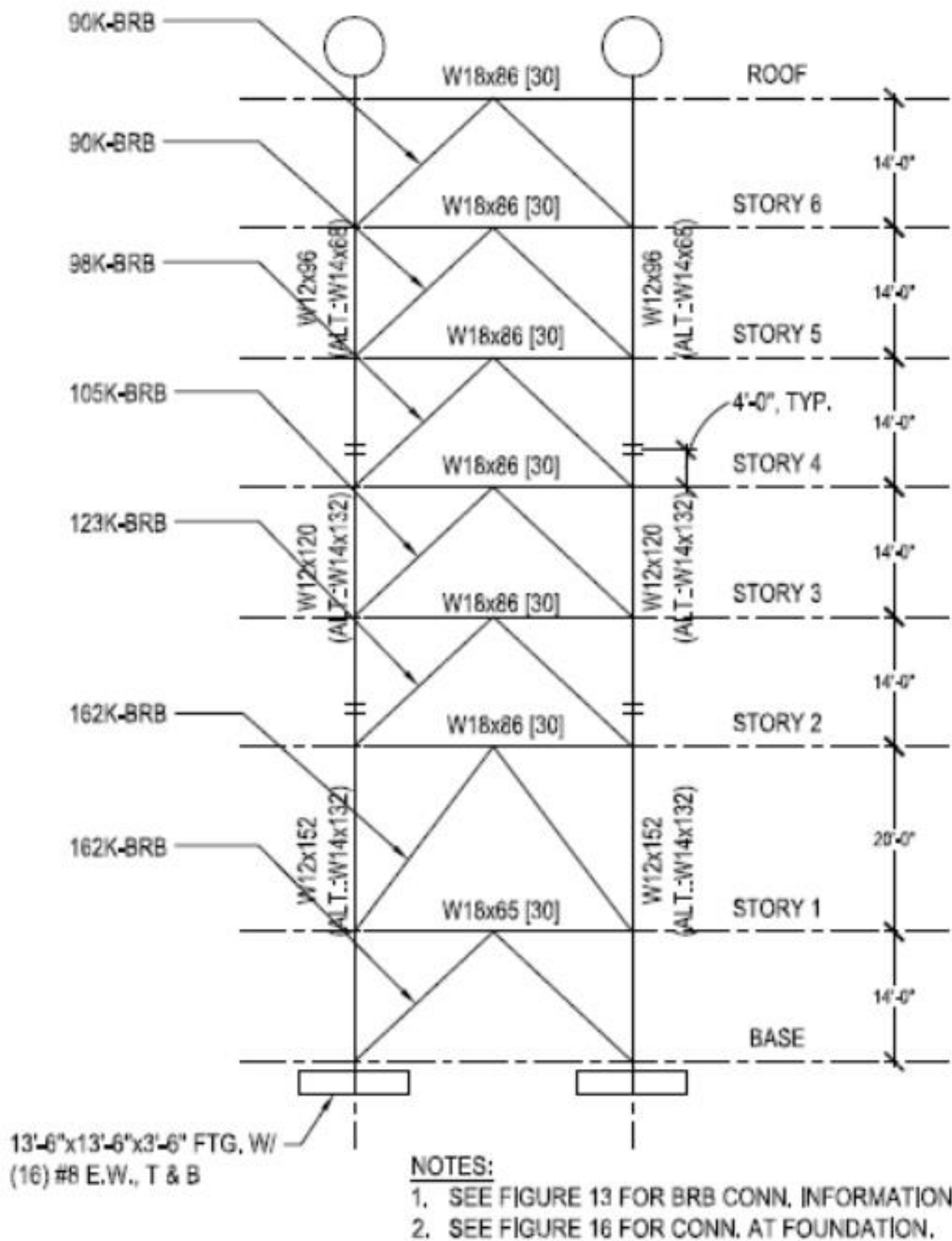


Figure 4-2 Typical Elevation of the Braced Bay [NIST GCR, 14-917-2].

### 4.3. Detailed Simulation Model

In this section all aspects of modeling the detailed simulation model will be presented.

#### 4.3.1. Model General Description

The following figures depict the considered model geometry.

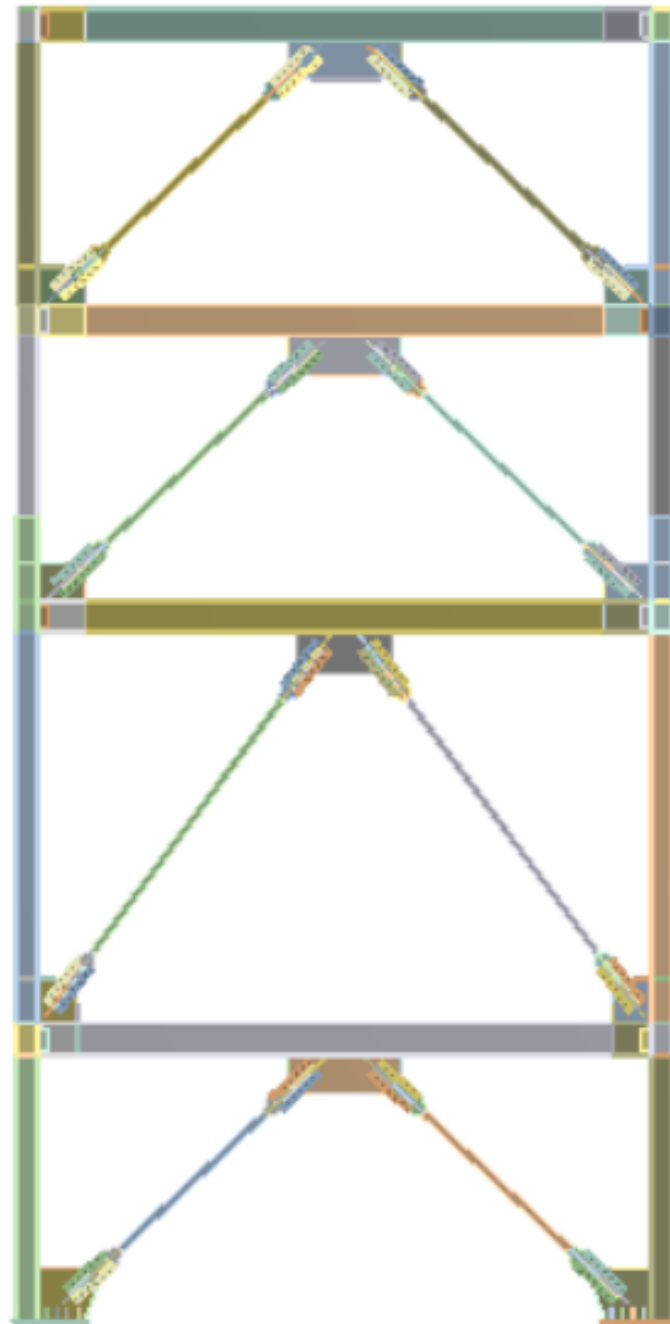


**Figure 4-3 Elevation of the Full Structure in Study**

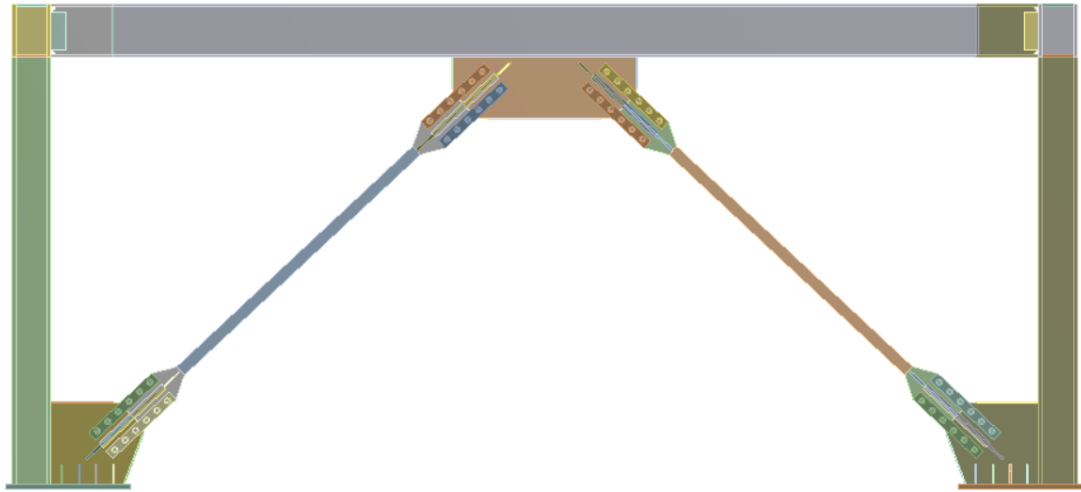


**Figure 4-4 Elevation of the First Floor**

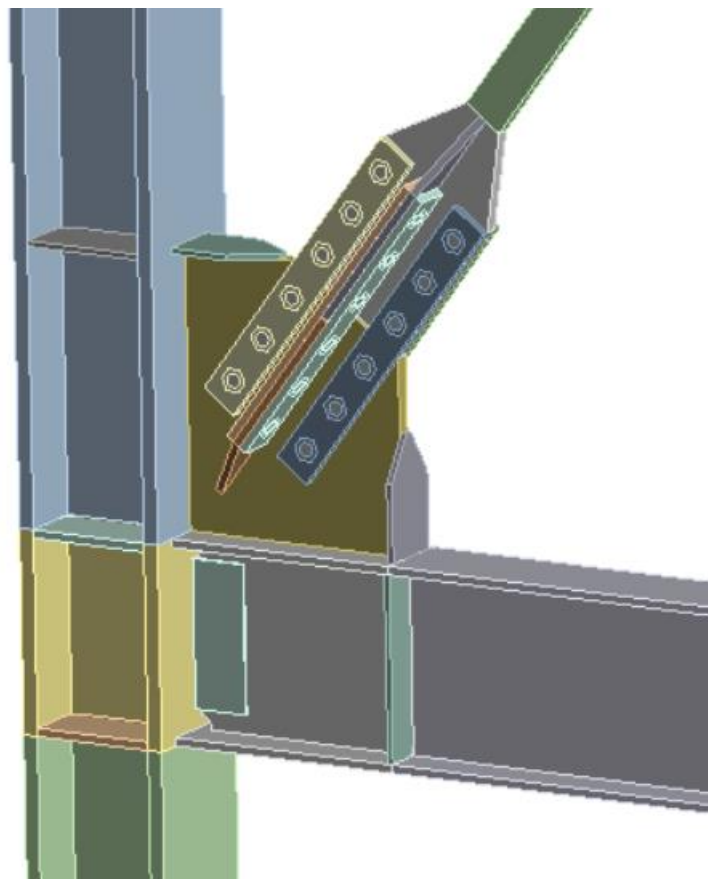


**Figure 4-5 Connection of BRB to Column Beam Joint**



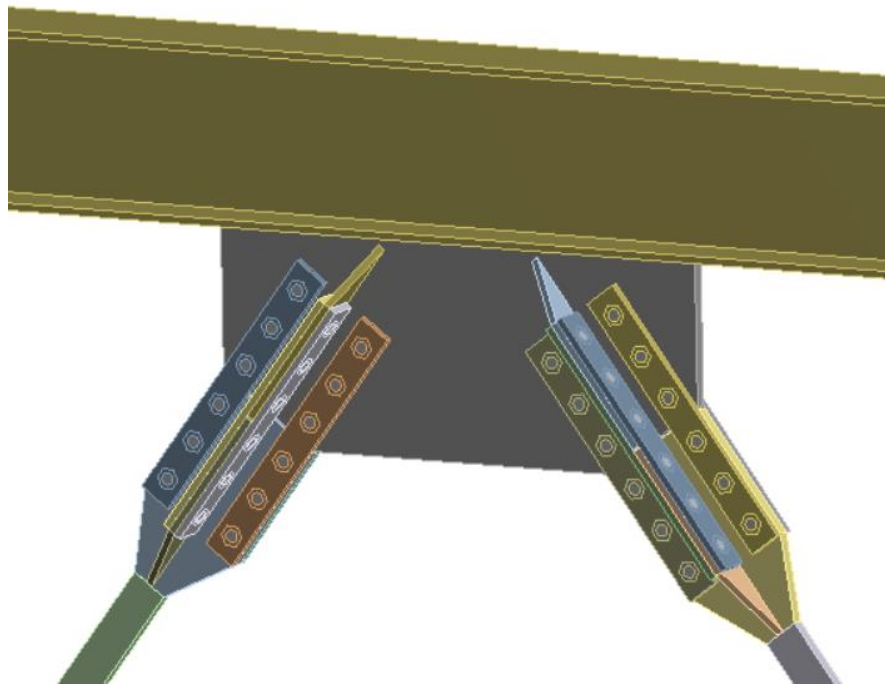


**Figure 4-6 Inverted-V Connection of BRB to Beam**

### 4.3.2. Material Modeling

The structure was modeled using ASTM A992 steel with yield stress of 344.7MPa, ultimate strength of 448.2 MPa, Young's modulus of 200,000 MPa and Poisson's ratio of 0.3. The stress strain curve used is a bilinear behavior with a strain hardening of 3% as shown in Fig. 4-7.

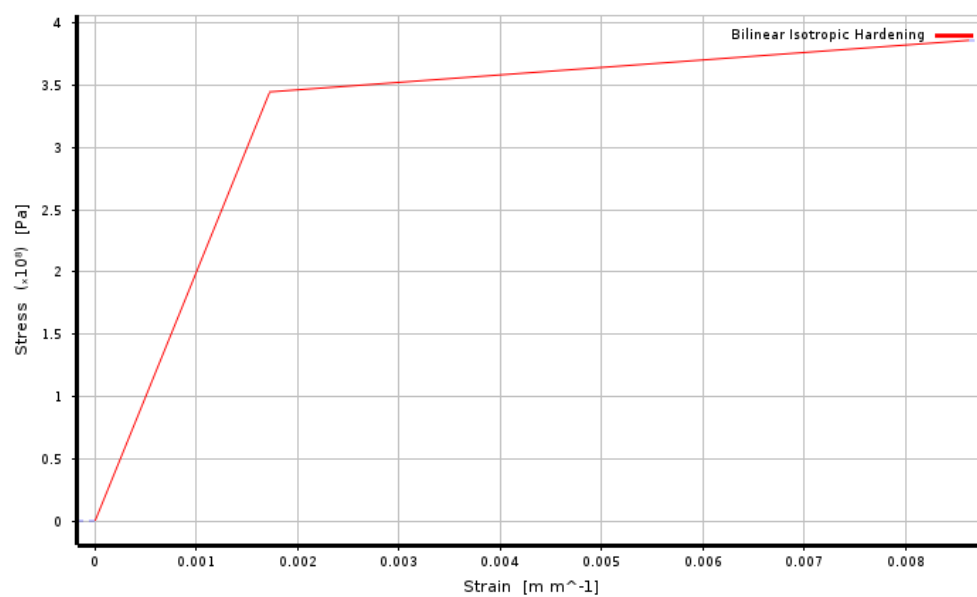


**Figure 4-7 Idealized Stress-Strain Curve With 3% Isotropic Hardening**

### 4.3.3. Type of Elements

3D Solid element was used in developing the detailed simulation model. Workbench use element SOLID186 for meshing of 3D solid body. SOLID186 is a 20 node second order structural solid element which is hexahedral in shape but can convert to tetrahedron, triangle prism or quadrilateral pyramid as shown in Fig. 4-8. Therefore, this element type is suitable for complex structural shapes. Each node has three degrees of freedom: translation in x,y and z. In meshing, Workbench allows neglecting the intermediate node reducing the element to first order element but this is not advisable since studies show that first order elements have poor convergence capabilities [Huei-Huang Lee. 2017]. Detailed information is available in [ANSYS Element Reference Manual].

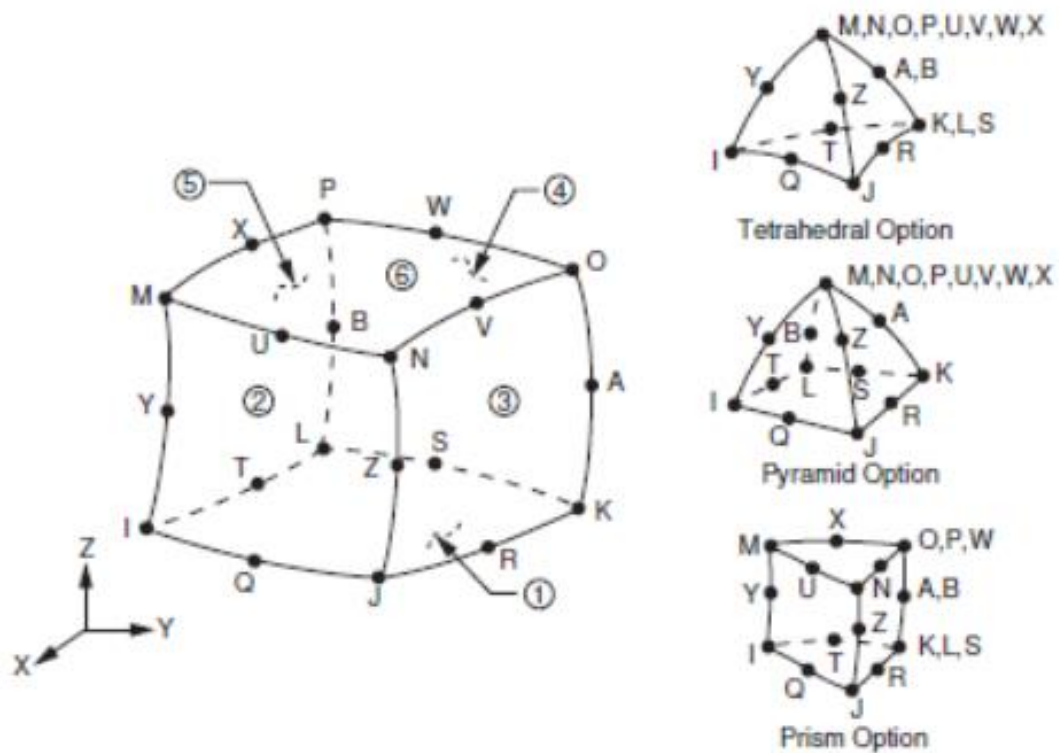
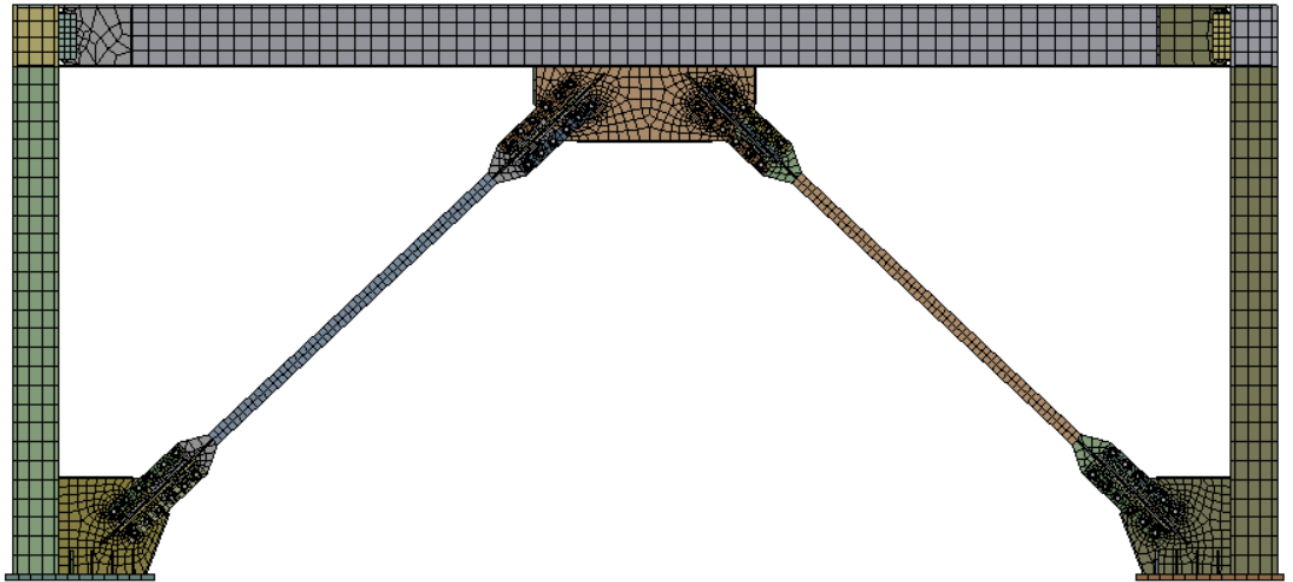


Figure 4-8 SOLID186 Structural Element Geometry [ANSYS Element Reference Manual]

### 4.3.4. Meshing of Elements

In finite element analysis, the use of fine mesh often imposes high computational cost but yield accurate. Whereas the use of relatively course mesh yields a less accurate results and may encounter convergence problems but have the benefit of being computationally efficient. Analysts often conduct a mesh size sensitivity analysis in order to reach a size which achieve the targeted accuracy with affordable computational cost.

Mesh size sensitivity analysis was conducted and resulted in an average mesh size of 130 mm is applied for the beams and columns, while for plates and stiffeners 50 mm is used. Additionally, edge sizing of 15 mm was applied to holes of bolts to introduce refinement at bolts locations. The meshing process results in about 70,000 elements and 500,000 nodes. Figures 4-9, 4-10 & 4-11 show the resulted mesh.



**Figure 4-9 Meshing of the First Floor**

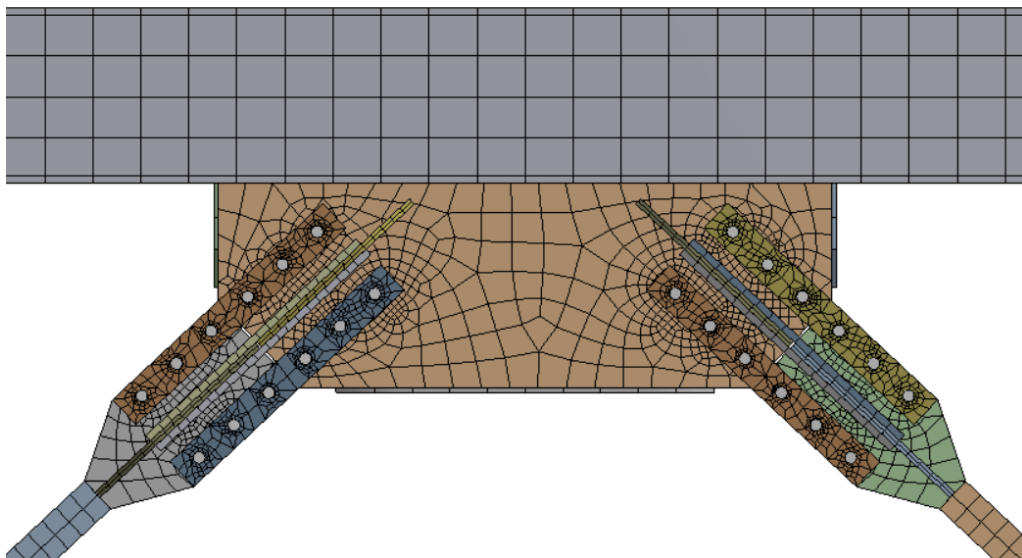


**Figure 4-10 Meshing of the Inverted-V BRB Connection to Beam**

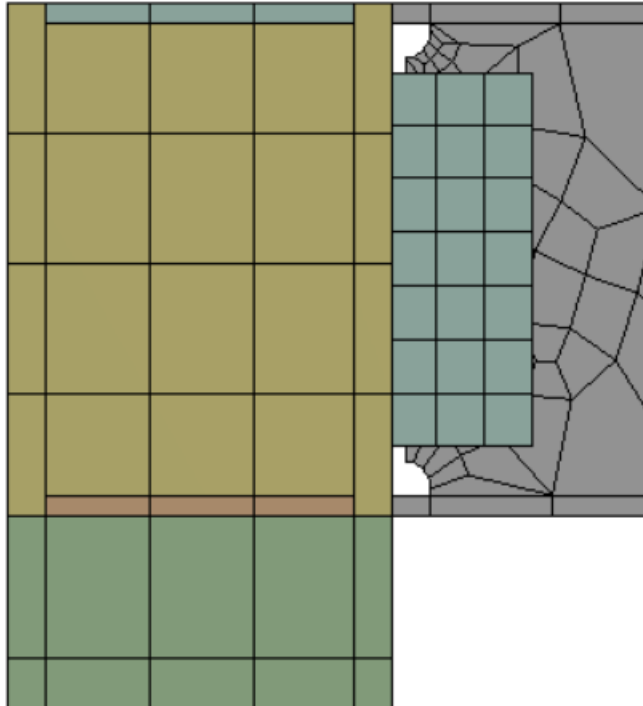


**Figure 4-11 Meshing of the Beam to Column Connection**

#### **4.3.5. Contact Between Elements**

Contact elements were utilized to simulate the interaction between different elements in the model. Two types of contact were used: bonded contact that simulates the behavior of welded plates and frictional contact between plates in bolted connection. In contact regions. Elements do not penetrate each other. Therefore, Workbench must ensure that no penetration will happen, this is known as enforcing contact compatibility. Workbench offers multiple formulation to enforce contact compatibility such as multiple point constrain (MPC), pure penalty, normal Lagrange, augmented Lagrange.

MPC adds constrain equation to ensure equal displacement on the contact surfaces. MPC is recommended for linear type contact: bonded and no separation contact. But sometimes produce over constrain in model. In this case one can use pure penalty contact. In this type of formulation if the contact surface is penetrating the target surface by amount (x) the contact surface is then subjected to a force equal ( $k \cdot x$ ) where k represents the contact stiffness which is numerical value that doesn't have physical meaning. The higher the value of k the less penetration will happen which mean more accurate results but convergence problems may arise. Workbench include the feature of automatically adjusting the value of k that is to reduce its value when encountering convergence problems.

Another formulation is the normal Lagrange multiplier, which uses an additional degree of freedom which is the contact pressure. This method ensures zero penetration therefore convergence problems may arise. To overcome this difficulty, Lagrange method was coupled with the pure penalty method to form the augmented Lagrange method. Augmented Lagrange method is advised to use in frictional and frictionless contact problems.

#### 4.3.5.1. Bonded contact

In bonded contact, the two elements are coupled in both tangential and normal directions. No non-linearity is introduced in this contact. Example of using bonded contact is shown in the following figure where it's used to represent the welded connection between column and base plate. Behavior of contact is set to symmetric that is Workbench doesn't differentiate between contact and target surface and check that each point on one surface doesn't penetrate the other surface. For this example, as well as other bonded connection, pure penalty formulation is used as MPC formulation caused over constrain in model.

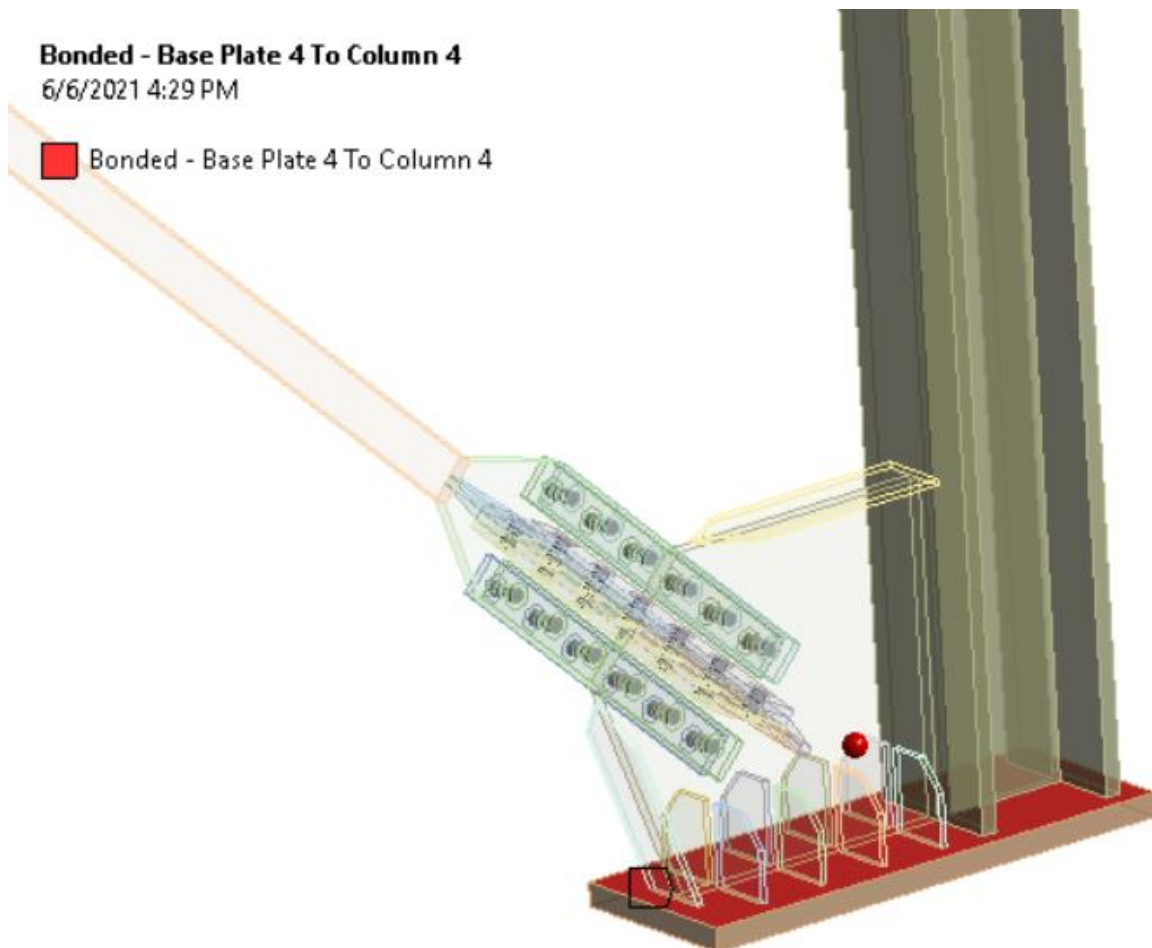
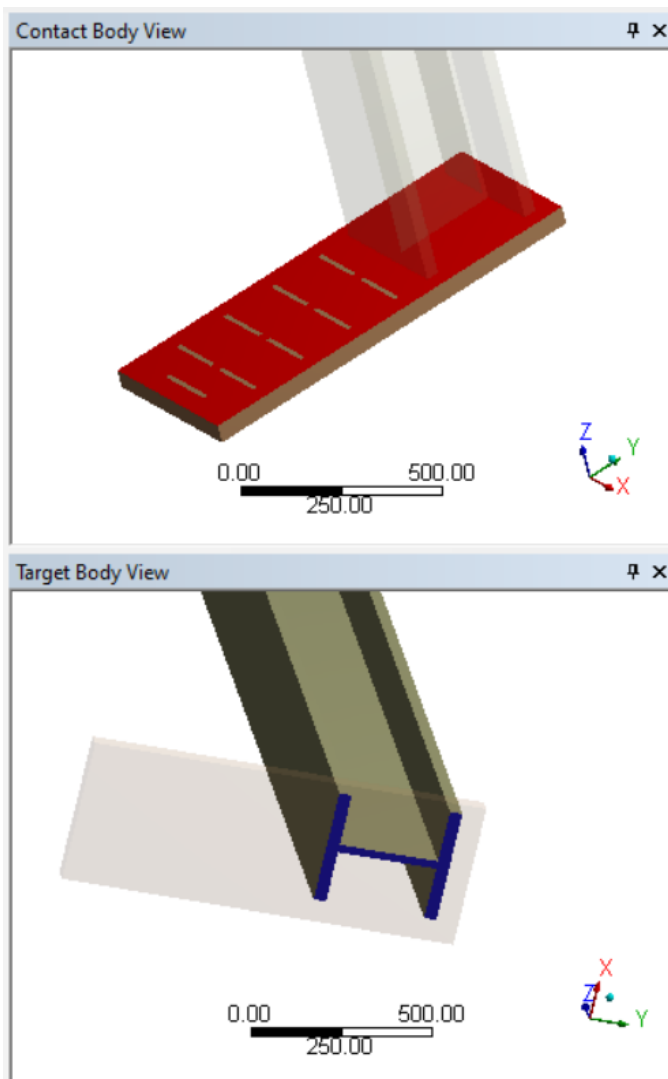


**Figure 4-12 Bonded Contact between Column and Base Plate**



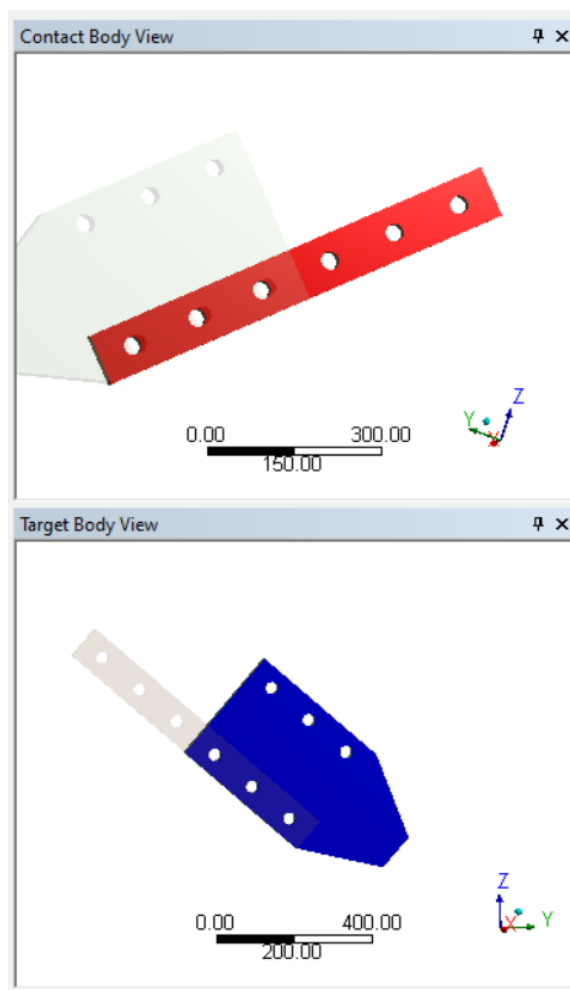
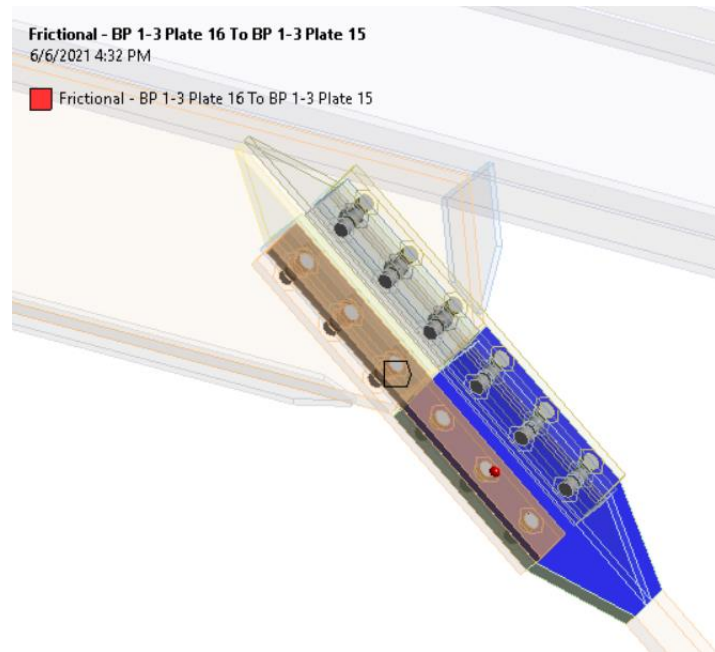
Details of "Bonded - Base Plate 4 To Column 4"	
[-] Scope	
Scoping Method	Geometry Selection
Contact	2 Faces
Target	1 Face
Contact Bodies	Base Plate 4
Target Bodies	Column 4
Protected	No
[-] Definition	
Type	Bonded
Scope Mode	Automatic
Behavior	Symmetric
Trim Contact	Program Controlled
Trim Tolerance	10. mm
Suppressed	No
[-] Advanced	
Formulation	Pure Penalty
Small Sliding	Program Controlled
Detection Method	Program Controlled
Penetration Tolerance	Program Controlled
Elastic Slip Tolerance	Program Controlled
Normal Stiffness	Program Controlled
Update Stiffness	Program Controlled
Pinball Region	Program Controlled
[-] Geometric Modification	
Contact Geometry Correction	None
Target Geometry Correction	None

**Figure 4-13 Bonded Contact between Column and Base Plate (Continued)**

#### 4.3.5.2. Frictional Contact

This type of contact introduces contact status nonlinearity since the stiffness change when contact status change from touched to separate. Similar to bonded contacts, behavior was set to symmetric hence, the need to determine the target element is eliminated. The augmented Lagrange formulation was chosen as it's recommended for frictional type contacts.

This type of contact was used to simulate the interaction between plates in bolted connections with a friction coefficient of 0.3. An example is shown in Fig. 4-14



Details of "Frictional - BP 1-3 Plate 16 To BP 1-3 Plate 15"	
<b>Scope</b>	
Scoping Method	Geometry Selection
Contact	1 Face
Target	1 Face
Contact Bodies	BP 1-3 Plate 16
Target Bodies	BP 1-3 Plate 15
Protected	No
<b>Definition</b>	
Type	Frictional
Friction Coefficient	0.3
Scope Mode	Automatic
Behavior	Symmetric
Trim Contact	Program Controlled
Trim Tolerance	10. mm
Suppressed	No
<b>Advanced</b>	
Formulation	Augmented Lagrange
Small Sliding	Program Controlled
Detection Method	Program Controlled
Penetration Tolerance	Program Controlled
Elastic Slip Tolerance	Program Controlled
Normal Stiffness	Program Controlled
Update Stiffness	Program Controlled
Stabilization Damping Factor	0.
Pinball Region	Program Controlled
Time Step Controls	None
<b>Geometric Modification</b>	
Interface Treatment	Add Offset, No Ramping
Offset	0. mm
Contact Geometry Correction	None
Target Geometry Correction	None

Figure 4-14 Example of Contact between Two Bolted Plates



### 4.3.6. Modeling of Bolts

Several methods of modeling the effect of bolts can be utilized in finite element analysis. In this section an overview of these methods will be presented.

#### 4.3.6.1. Use bonded regions

The bonded regions method is considered the simplest one in which bolts and nuts geometry are suppressed from the model then a bonded region around each bolt is taken with a diameter equal the diameter of the washer. This method doesn't provide high accuracy but it's efficient from computational efforts point of view. An example of this method is shown in Fig. 4-15 [ENDEAVOS Innovations Inc.]

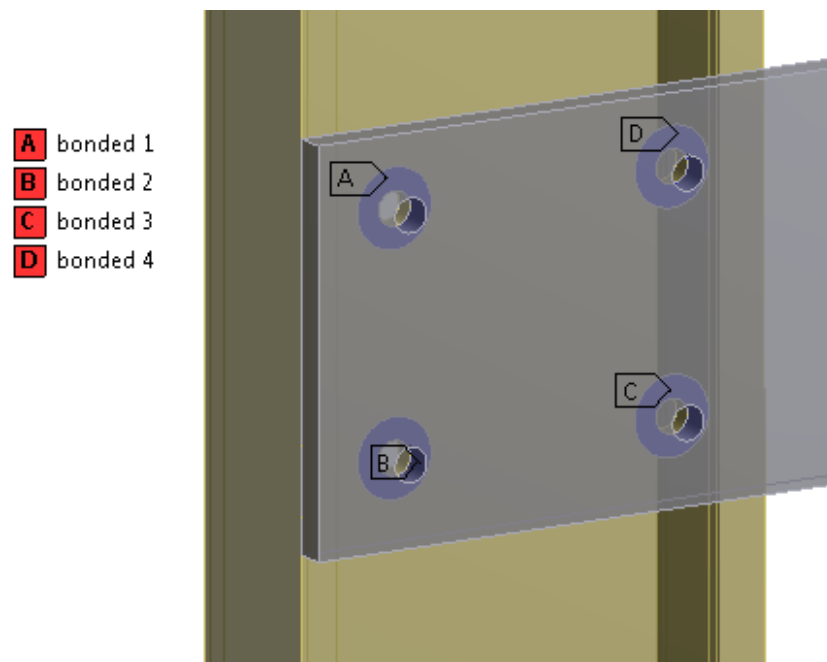


**Figure 4-15 Example of Bolted Connection Using Bonded Regions**  
[ENDEAVOS Innovations Inc.]

#### 4.3.6.2. Beam Bolts

In this method, bolt head and nut surfaces are imprinted on the faces of the connected plates then, both bolt and nut geometry are suppressed, and a beam line element is utilized to connect the imprinted surfaces. The beam element may be set to have rigid or deformable behavior. Although, this method can't capture the true behavior of the bolt it proved to have high accuracy. An example is shown in Fig 4-16 [ENDEAVOS Innovations Inc.]

#### 4.3.6.3. 3D Solid Bolts

3D Solid Bolts method is considered to be the most accurate method for modeling bolted connection, in which the geometry of both bolt and nut are fully presented in the



model. The main drawback of this method is the high computational cost. Therefore, it's not suitable for assembly with high number of bolts. In this method several contact elements are applied between different parts as shown in Fig. 4-17. A frictional or bonded contact is applied between bolt head and top plate and between nut and lower plate. Frictional contact is applied between the two connected plates.

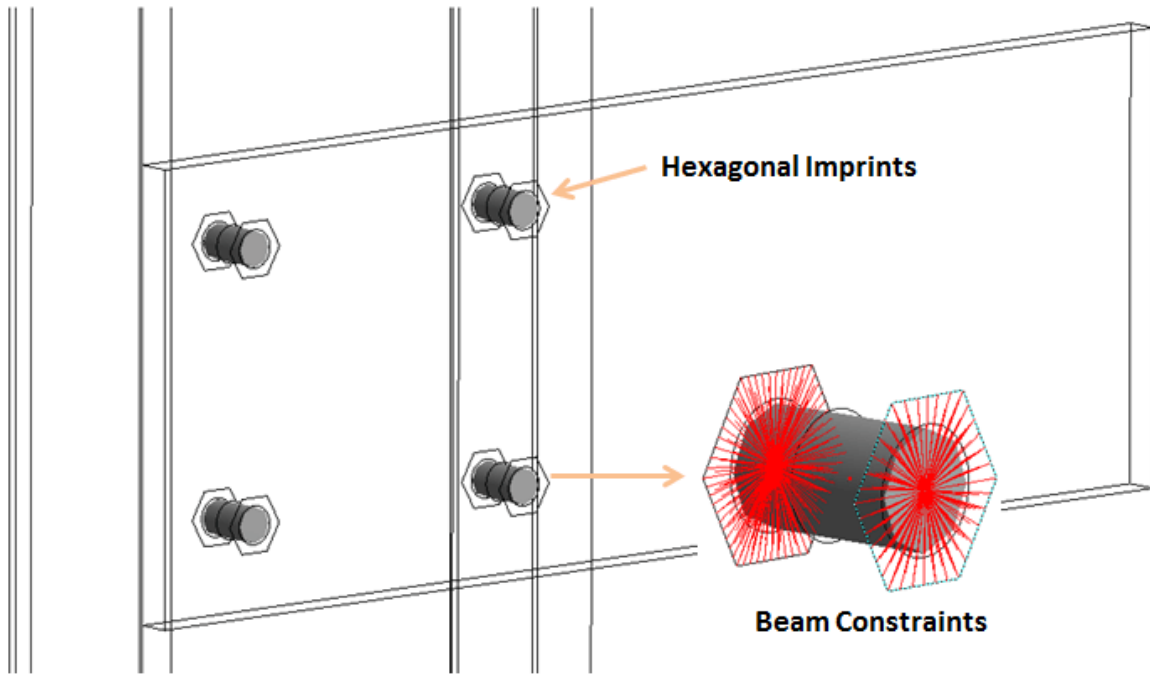


**Figure 4-16 Example of Beam Bolts [ENDEAVOS Innovations Inc.]**

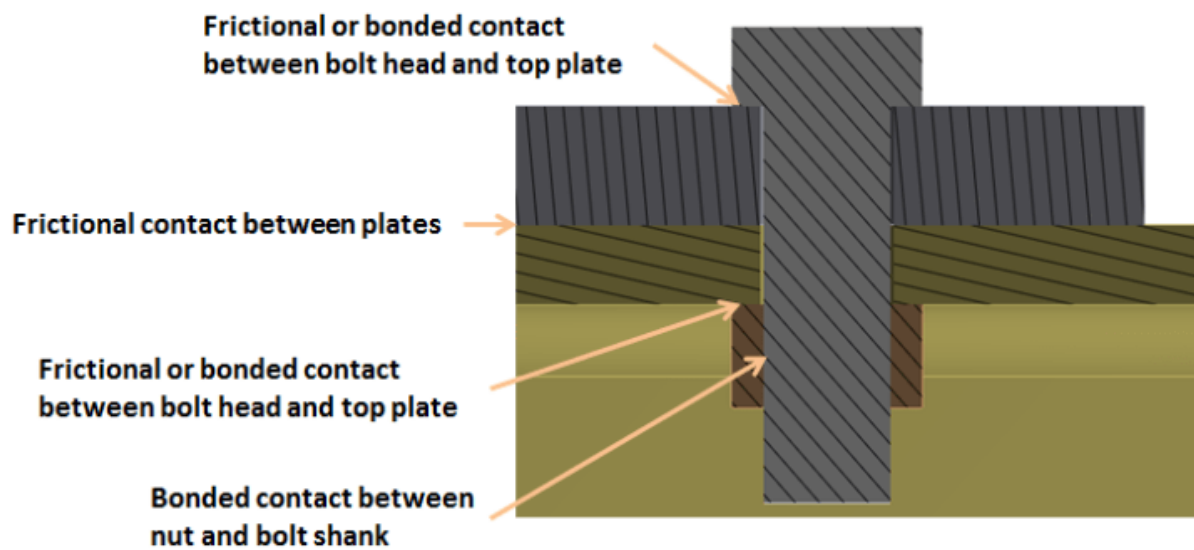


**Figure 4-17 Contact in 3D Solid Bolted Connection [ENDEAVOS Innovations Inc.]**

#### 4.3.6.4. Used Method in Study

The method of beam bolts is used in the current study since it provides high accuracy with suitable computational time. First a verification is conducted against 3D bolts as shown in the following figures. In this verification a cantilever plate is bolted to channel column with fixed base. The model is solved twice, one time with 3D solid bolts and another with beam bolts. The results showed 94% accuracy when investigating the maximum deflection of the plate when subjected to a force at the end side of the plate as shown in Fig. 4-18

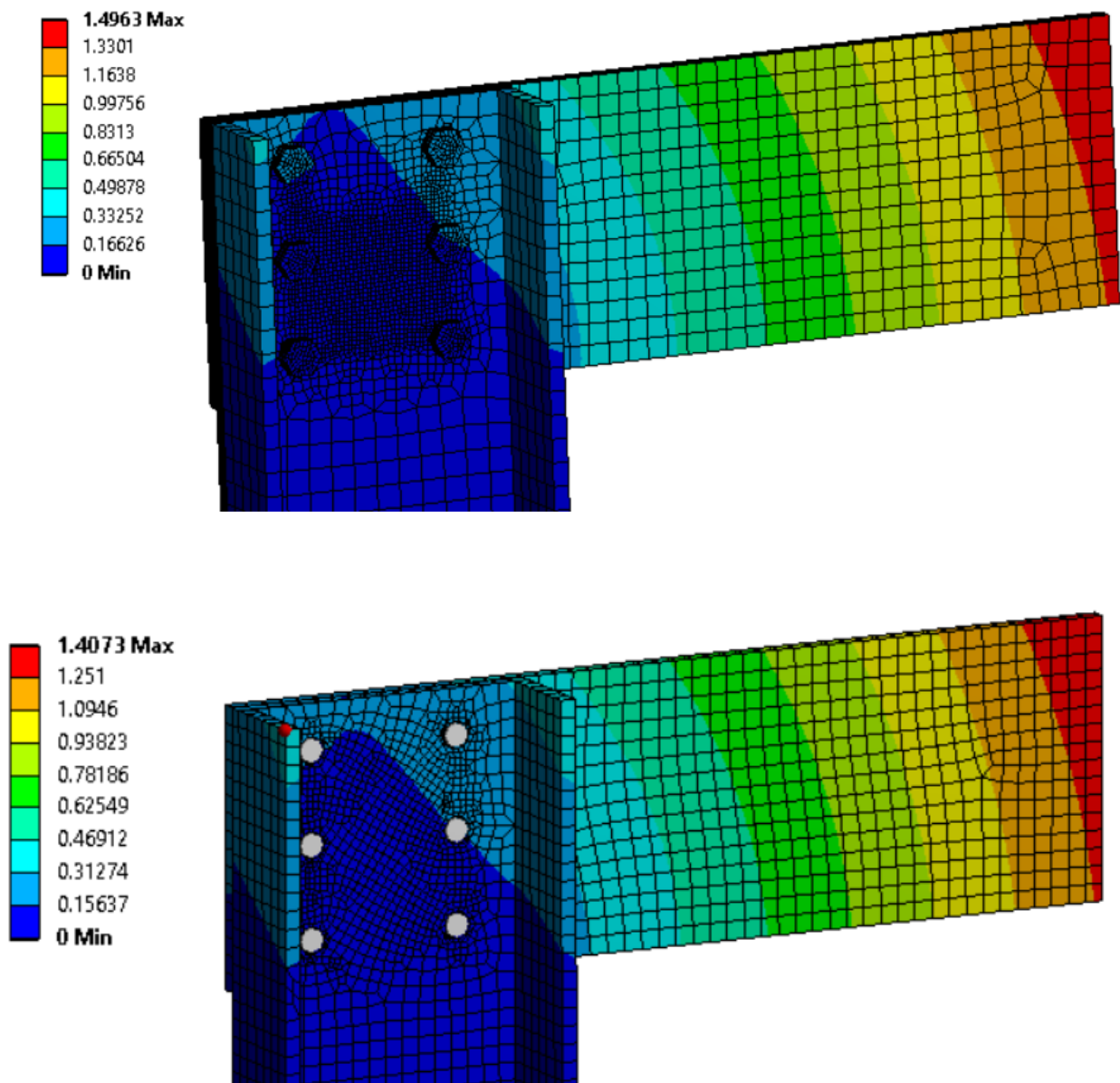


Figure 4-18 Verification Study on the Use of Beam Bolts Instead of 3D Solid Bolts

#### **4.3.7. Modeling of Buckling restrained bracing**

Buckling restrained brace (BRB) consist of several parts, the steel core which provide all the axial stiffness, and concrete and steel tube casing which provide restrain to buckling therefore the brace can reach the yield strength in tension and compression.

In modeling of BRB, the core is the only element modeled since it is the only element that add to the stiffness of the structure. Buckling of the steel core is guaranteed not to occur in both types of analysis conducted on the model as follows

- 1- In modal analysis, conducted to perform the comparison and correlation step in FEMC, linear elastic analysis is conducted which takes into account only the initial un-deformed stiffness and since the casing does not contribute to this stiffness, it is not mandatory to be modeled.
- 2- In nonlinear static pushover analysis, conducted to obtain the pushover curves, geometric nonlinearity is neglected for sake of simplification hence no stress stiffening effect will be considered and no buckling will occur. Geometric nonlinearity was tested in nonlinear transient analysis and proved to have little effect on results and hence it was neglected.

## 4.4. Simplified Model

The simplified model was developed in ANSYS APDL in order to create a parametric model that enables iterations in the FEMC process to reach the best value of the chosen parameters that minimize the fitness function. In the following sections all aspects of modeling of the simplified model will be presented. Regarding the material model, the same model presented before will be used here.

### 4.4.1. Model General Description

Figure 4-19 shows an extruded view of the developed simplified model.

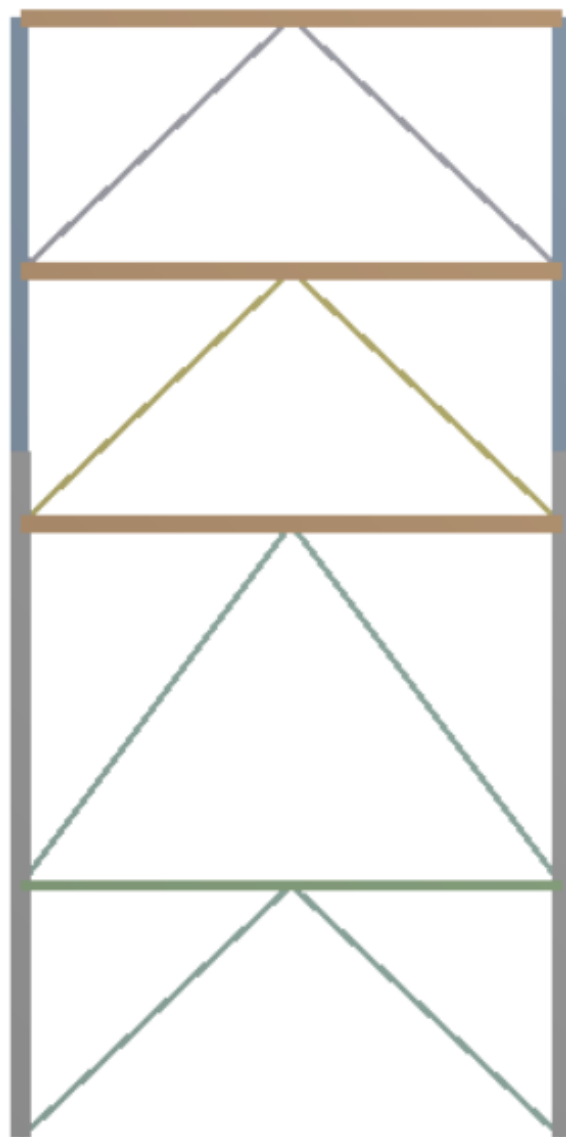


**Figure 4-19 Extruded View of the Simplified Model**

#### 4.4.2. Type of elements

Two types of elements are used in this FE model, BEAM188 element for modeling beams and columns and LINK180 for modeling of BRB elements [ANSYS Element Reference Manual]. These elements are explained in the following section

##### 4.4.2.1. BEAM188 Element

This element is based on Timoshenko theory which include shear deformations. This element is a 2-node element that has six degrees of freedom at each end, three directions and three rotations, and can have another additional degree of freedom, namely warping but it's optional to include or not. Fig. 4-20 shows the geometry of BEAM188.

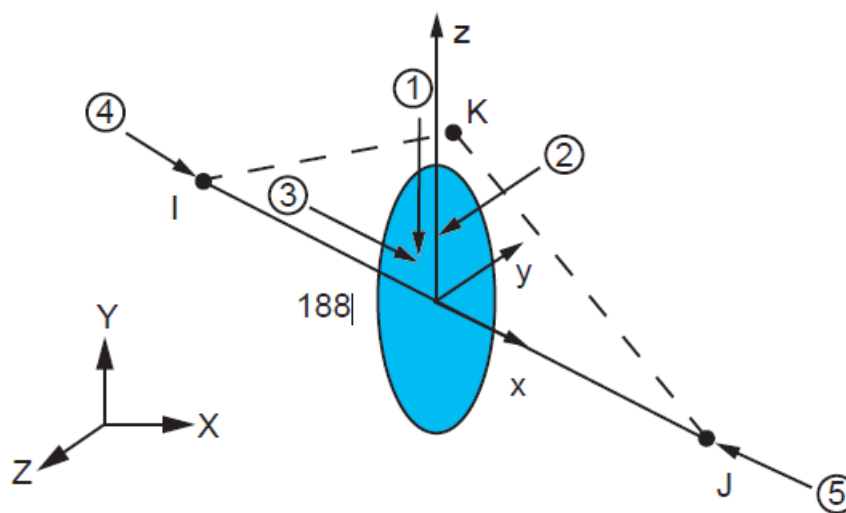


**Figure 4-20 BEAM188 Structural Element Geometry [ANSYS Element Reference Manual]**

##### 4.4.2.2. LINK180 element

The element is a uniaxial tension-compression 2 node element that has three degrees of freedom at each node which are the translations in all directions. This element is suitable in many applications such as pinned joints where bending stiffness has no effect. Fig. 4-21 shows the geometry of the element

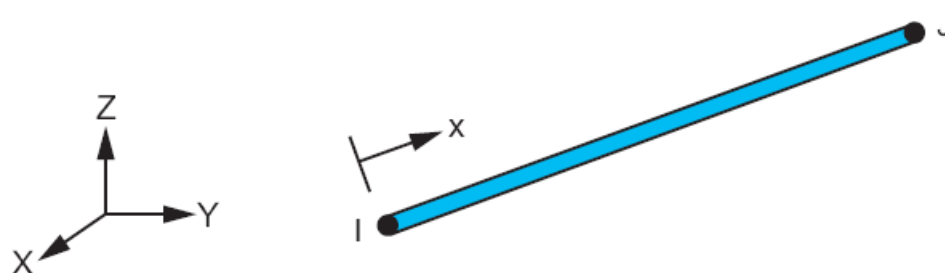


**Figure 4-21 Link180 Structural Element Geometry [ANSYS Element Reference Manual]**

#### 4.4.3. Meshing of elements

In order to increase analysis accuracy, beams and columns were meshed with approximately 100 elements for each of them and only one element for the BRB link elements since no internal result is required so modeling with one element reduce the run time. Fig 4-22 shows the meshing.

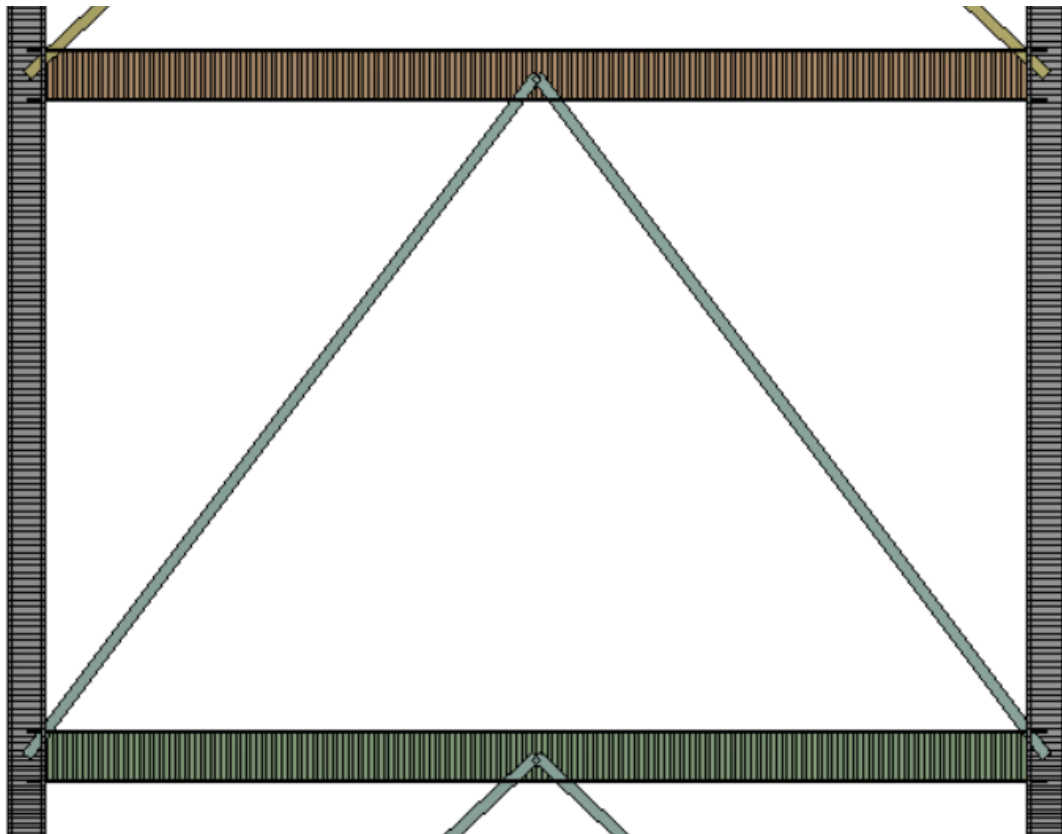


**Figure 4-22 Meshed View of Portion of the Model**

#### 4.4.4. Connections

Connection between BRB to Beam and BRB to beam-column joint is considered a pin end connection that is bending stiffness of BRB is not considered.

Rigid connection between beam and column is assumed i.e., no rotational spring is applied between joint of column and joint of beam.



## Chapter 5 FEMC Process

As mentioned before, the FEMC process will be conducted in order to approximate the results of the simplified model to the detailed simulation model to derive accurate fragility curves without very high computational cost. The steps of FEMC will be represented in detail in this chapter

### 5.1. Comparison and Correlation Results

The results of the detailed simulation model are compared with the results of the simplified model to determine whether the results possess any correlation or new FE model shall be formulated.

Several comparison techniques are presented later in this section. Modal data consisting of the main two horizontally vibrating modes and the main two vertically vibrating modes are used in that process.

#### 5.1.1. Comparison of Natural Frequencies

In the following table a comparison of natural frequencies is conducted which shows a maximum error of 20%. This is considered a good correlation between the FE models.

**Table 5-1 Shows Comparison between Detailed and Initial FE Models**

Mode Number	Detailed Model	Simplified Model	Percentage error
1	1.3549	1.1186	17 %
2	4.1993	3.3780	20%
3	4.4803	3.9465	12%
4	5.4603	4.5701	16%

#### 5.1.2. Visual Comparison of Mode Shapes

A visual comparison is conducted to compare the mode shapes considered as shown in the Figs. 5-1 to 5-4.

#### 5.1.3. MAC Correlation

The modal assurance criteria MAC is utilized to test the relation between the mode shapes. The results shown in Fig. 5-5 show excellent correlation as the diagonal values are almost 1 and off-diagonals are almost zeros.



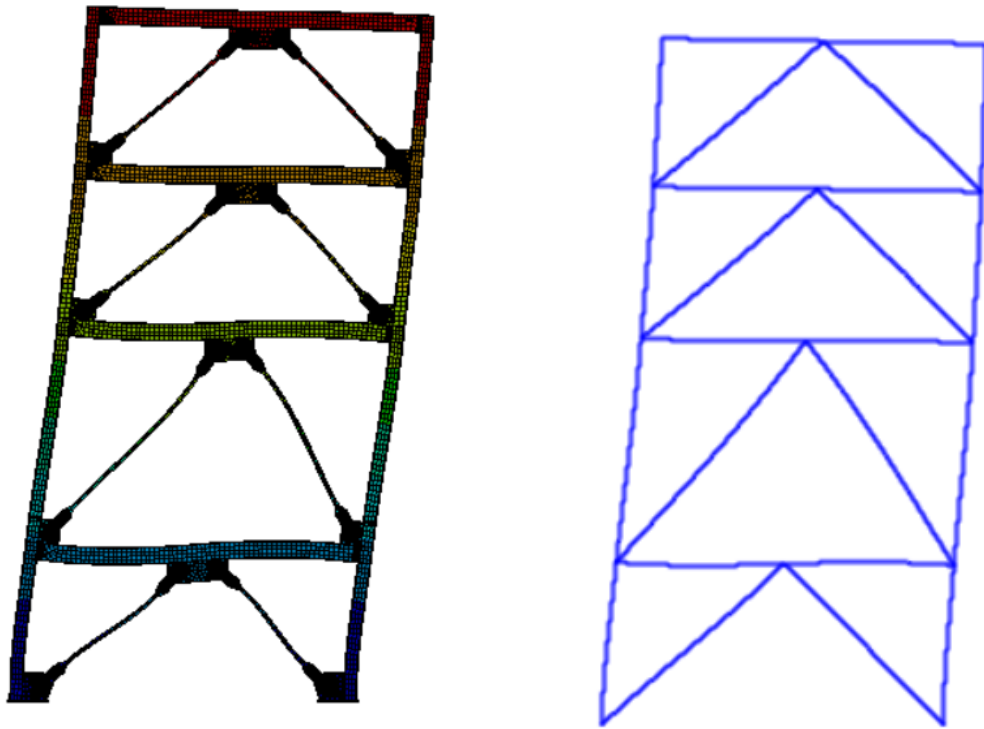


**Figure 5-1 Comparison of Mode 1**

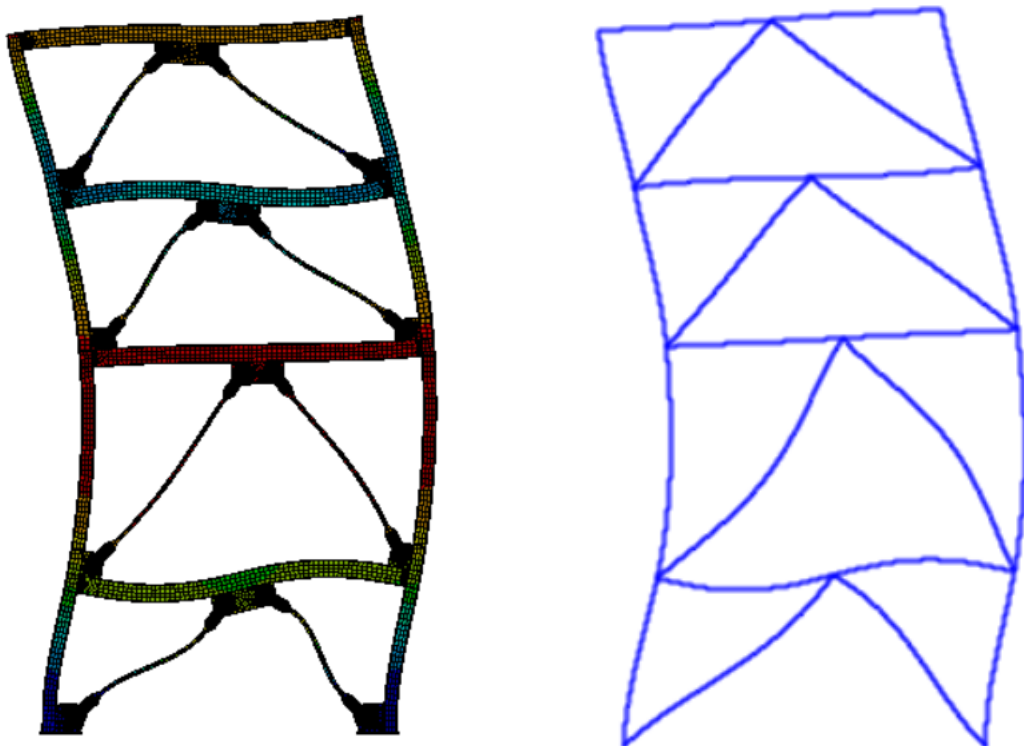


**Figure 5-2 Comparison of Mode 2**

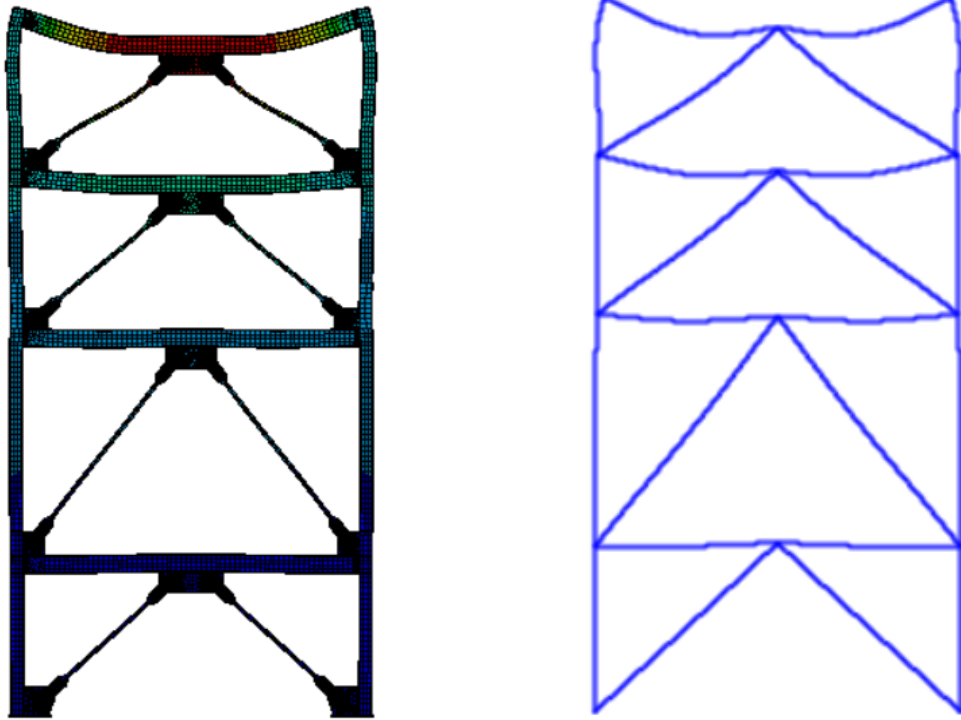


**Figure 5-3 Comparison of Mode 3**

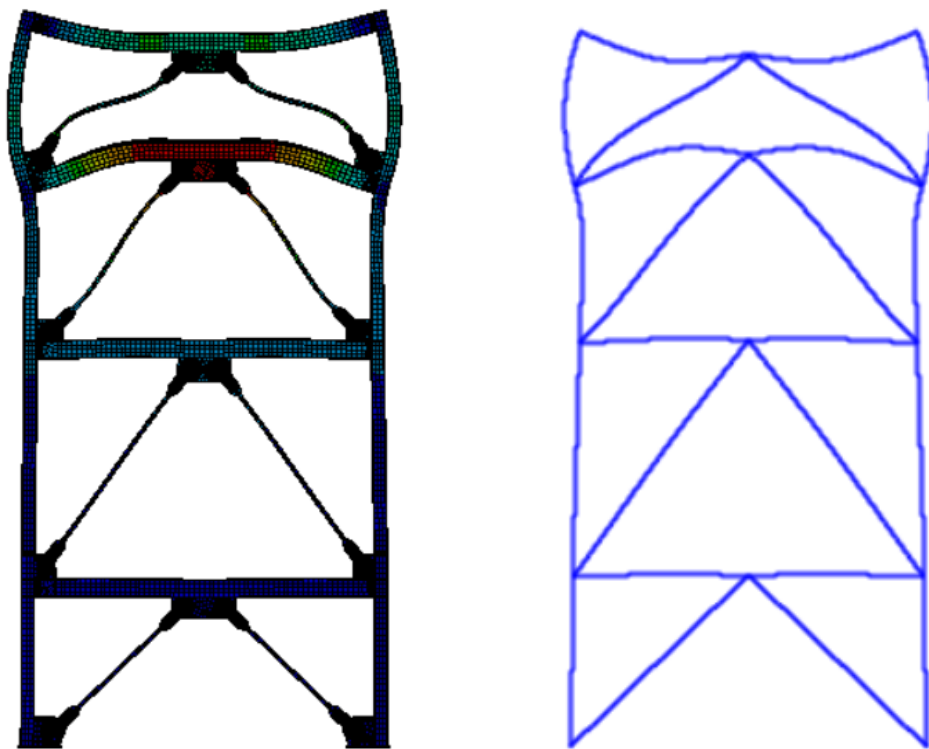


**Figure 5-4 Comparison of Mode 4**

0.9989	0.0007	0.0007	0.0007
0.0007	0.9800	0.0000	0.0039
0.0007	0.0000	0.9932	0.0000
0.0007	0.0039	0.0000	0.9941

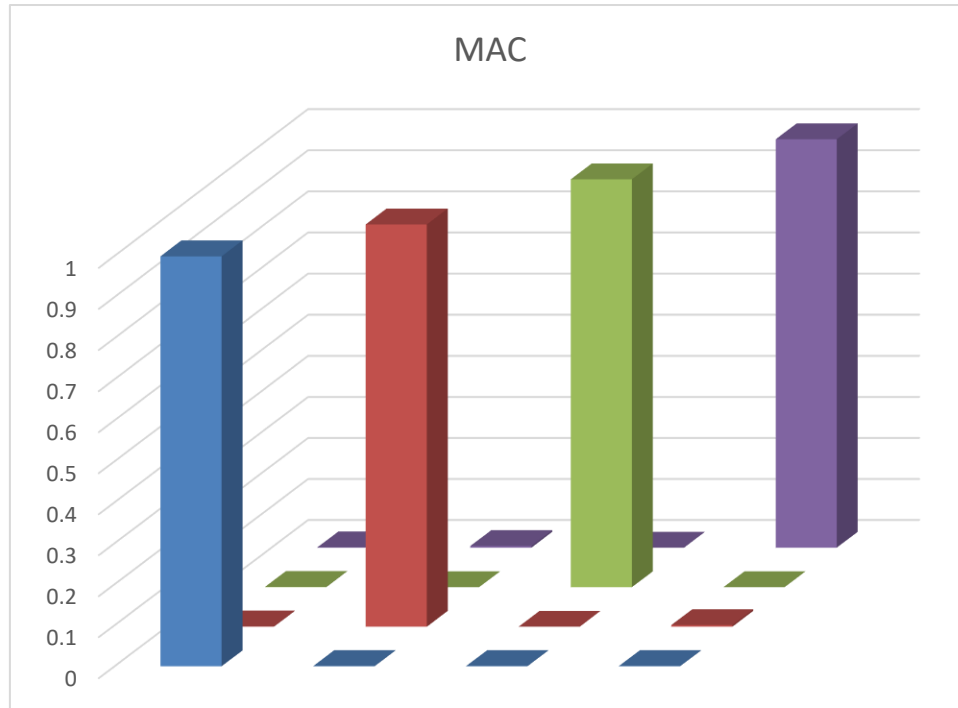


**Figure 5-5 Calculation of MAC Values**

## 5.2. Step Size Compatibility

Reduction technique was applied where only 20 DOF were selected for comparison. The 20 DOFs were selected so that they can depict mode shapes with those 20 DOFs only. Those DOFs were selected upon investigating all mode shapes. The selected degrees of freedom are as follow:

- 1- 4 horizontal DOF located at the corner of the 4 floors
- 2- 4 vertical DOF located at the corner of the 4 floors
- 3- 4 vertical DOF located at 1/8 distance of the beam length as shown in Fig. 5-6.
- 4- 4 vertical DOF located at 1/4 distance of the beam length as shown in Fig. 5-7.
- 5- 4 vertical DOF located at 1/2 distance of the beam length.

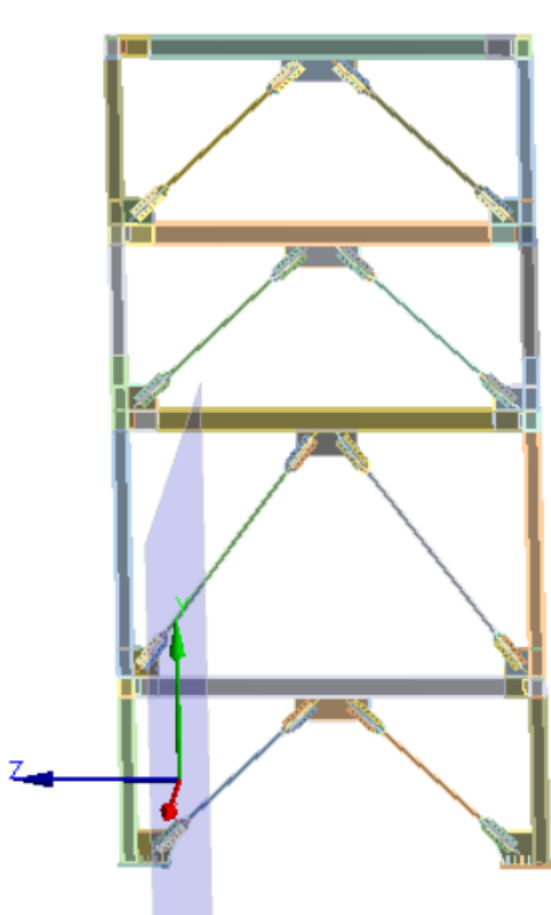


**Figure 5-7 Four Vertical DOF Located at 1/8 Distance of the Beam Length**

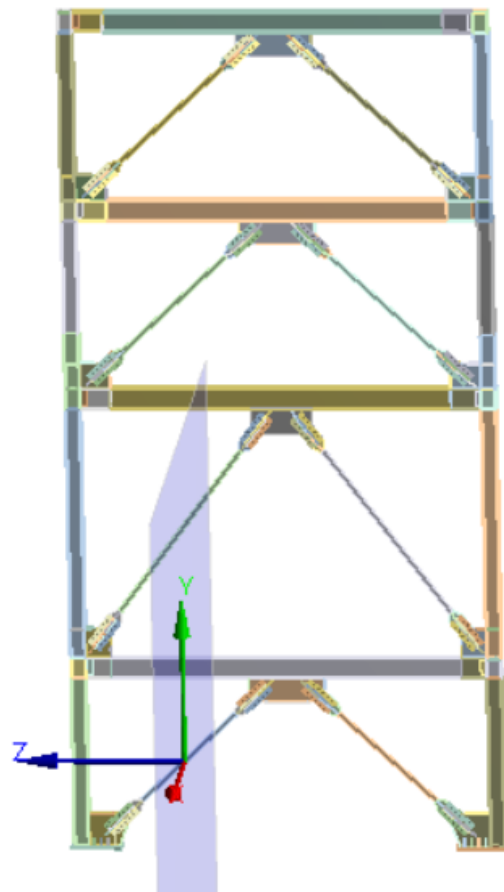


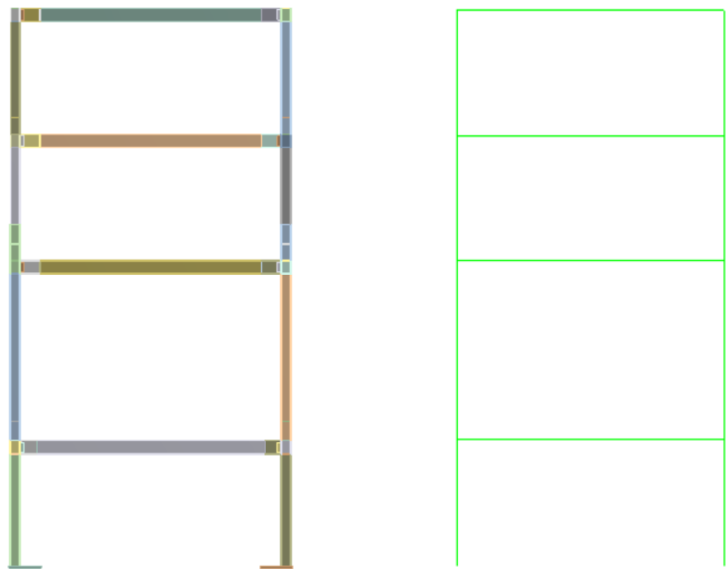
**Figure 5-6 Four Vertical DOF Located at 1/4 Distance of the Beam Length**

### 5.3. Updating Parameters

FE model results may be thought of as function of several parameters that formulate the system matrices. Change in results can be more susceptible to change in specific parameters. Choosing these parameters cannot always be justified by engineers [Mottershead, J. E., et al. 2000]. Several methods are available in the literature regarding parameter selection. Choosing updating parameters is a critical step in FEMC as the chosen parameters can affect the physical interpretation of results.

In this study, two categories of parameters were investigated namely, the axial stiffness of the BRB elements characterized by the thickness of BRB core member and the rotational stiffness of the beam-column moment connection. A sensitivity analysis was conducted to determine the effect of each category. At first the BRB members were suppressed to study the influence of the beam-column moment connection alone as shown in Fig 5-8. And showed the maximum error in natural frequency dropped to 3% from 20% in the case of existence of BRB members. Therefore, the main discrepancies arise from the members of BRB which mainly contribute to the axial stiffness. Reaching this conclusion, the thickness of the BRB elements was chosen to be updating parameter

and the error due to assuming the beam-column moment connection to be rigid is to be compensated for in the chosen parameters. The four updating parameters representing the thickness of BRB members of each floor are shown in Fig. 5-9.



MODE NUMBER	Detailed Model	Simplified Model	% Error
1	0.307	0.308	0.33%
2	1.185	1.193	0.68%
3	2.026	2.089	3.11%
4	2.160	2.139	0.97%

**Figure 5-8 Model with the BRB Members and the Error in Natural Frequencies**

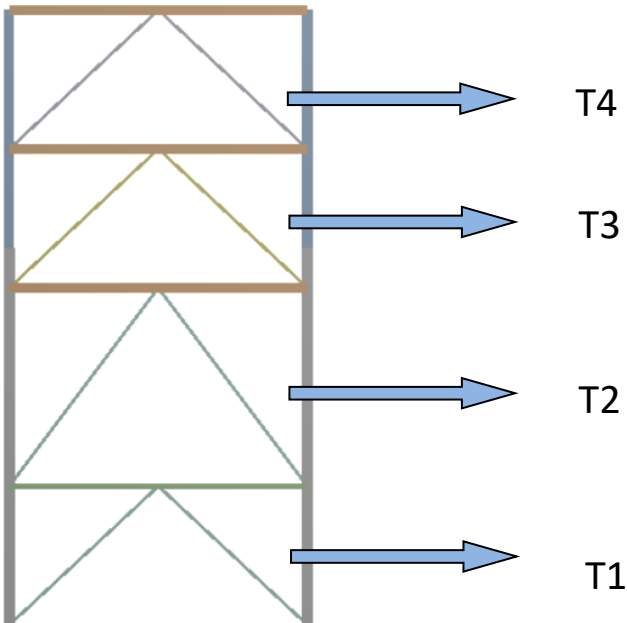


**Figure 5-9 The Four Updating Parameters**

## 5.4. FEMC Method

The genetic algorithm was chosen as The FEMC method since it is capable of dealing with highly non-linear problems and can reach the global minimum without getting stuck in local ones. In FEMC process MATLAB is coupled with ANSYS APDL to be able to change the values of parameters and calculate the corresponding response.

The objective function can be a combination of difference in natural frequencies and mode shapes but since the objective of the current study is deriving accurate fragility curves another objective function that includes non-linear behavior was chosen. As stated before, pushover curves can be utilized to derive non-linear static based fragility curve instead of the high computational cost non-linear dynamic based fragility curves. Therefore, the objective now to approximate the capacity curve of each of the detailed model and simplified model hence, the root mean square error (RMS Error) between the two curves was used as an objective function.

In pushover analysis, since the structure being studied is a BRB structure, the main elements resisting the lateral loads are the BRB members hence, the material nonlinearity was limited to BRB members to limit the computational time to a reasonable limit since the analysis will be run for huge number of times in order for the updating process to be completed. The initial RMS error between the two pushover curves is 21.2. Fig. 5-10 shows the two curves. The curves show a residual stiffness representing two components, the first is the beam-column moment connection stiffness since no nonlinearity is considered in beams and columns. The second component is the 3% plastic stiffness of the BRB braces.

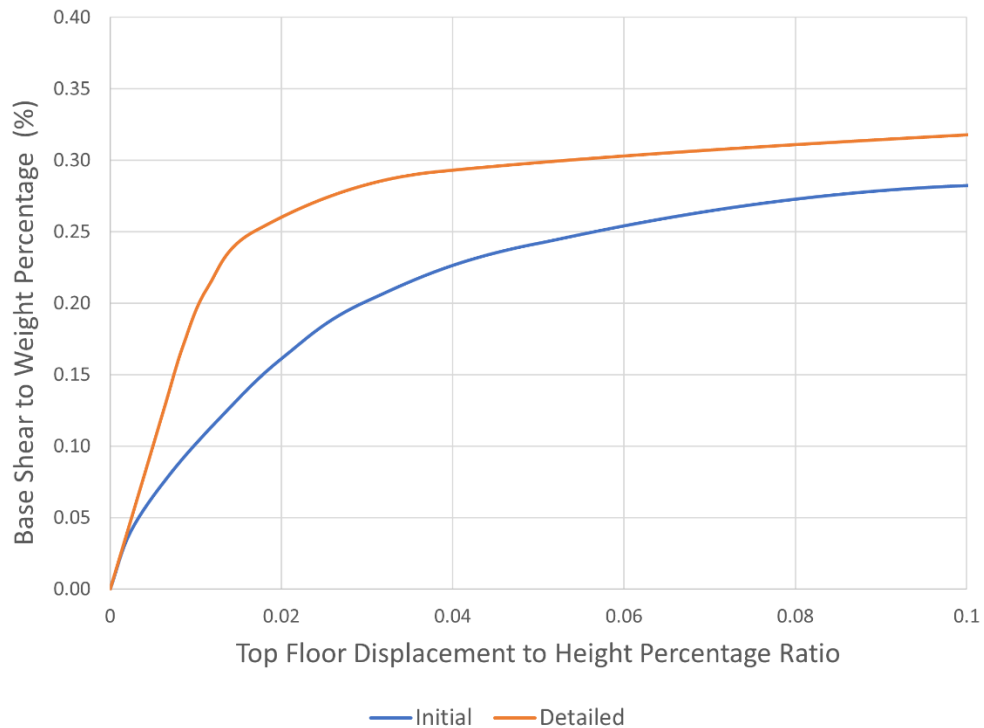


**Figure 5-10 The Pushover Curves of the Initial and Detailed Models**

The flowchart shown in Fig. 3-3 shows the process of FEMC in which the genetic algorithm assigns value of the parameters to a population of a predefined size. The objective function, the error between the two pushover curves, is then calculated for population points to determine the parents of the next generation. This process continues until a predefined maximum number of generations is achieved or the error tolerance is achieved.

In the first part of the flowchart the GA assumes values of the parameters for the all the population of the first generation. Each generation has a population size of 100. The number of generations was limited to 70 to limit the computational cost. After evaluating the fitness function of the population of the first generation, the parents of the next generation are selected based on fitness value then, using mutation and crossover techniques the children of selected parents are produced which are considered the population of the next generation. This process is repeated until certain error is achieved or until the maximum number of generations is reached. The code for setting the GA options is shown here:

- `function optimization2`
- `options= gaoptimset('PopInitRange',[1.5 1 .4`  
`.4;4.5 4 1.7`  
`1.7],'Generations',70,'PopulationSize',100);`
- `lb=[1.5 1 .4 .4];`
- `ub=[4.5 4 1.7 1.7];`
- `[x,fval,exitflag]=ga(@fitnessfunction,4,[],[],[],`  
`[],lb,ub,[],options);`
- `x`
- `fval`
- `exitflag`

The flowchart second part shows evaluation of fitness function, where input parameters from GA are written in text file which is run in ANSYS APDL and the pushover analysis is conducted and results are written in a text file which is then retrieved by Matlab to evaluate the RMS error between. Following is the Matlab Code utilized in this part is shown:

- `function salud=fitnessfunction(T)`
- `T1=abs(T(1));`
- `T2=abs(T(2));`
- `T3=abs(T(3));`
- `T4=abs(T(4));`
- `fid=fopen('parameters.inp','w+');`
- `fprintf(fid,'T1=%f\n',T1);`
- `fprintf(fid,'T2=%f\n',T2);`
- `fprintf(fid,'T3=%f\n',T3);`
- `fprintf(fid,'T4=%f\n',T4);`

- `fclose(fid);`
- `system('SET KMP_STACKSIZE=4096k & "C:\Program Files\ANSYS Inc\v192\ANSYS\bin\winx64\ANSYS192.exe" -b -i frame.txt -o feaout.txt" ')`
- `fid=fopen("Pushover.txt",'r');`
- `Pushovercalc=fscanf(fid,'%f');`
- `fclose(fid);`
- `Pushovermeasured=[0.8087138679 2.782988961 5.082542239 8.567513293 13.64348284 19.00899812 24.44582721 30.32485361 36.20361568 42.08166408 47.95879214 53.8349446 59.71017432 65.58449092 71.45787517 77.33038474 83.20181779 89.07218873 94.94124285 100.8092204]'; %replace here with detailed pushover curve`
- `ER=Pushovercalc-Pushovermeasured;`
- `RMSD=sqrt(sum(ER.^2)/20);`
- `salud=RMSD;`



## 5.5. Results of FEMC

The FEMC process resulted in error reduction of about 85%. Fig. 5-11 shows the updated parameters along with the final RMS error.

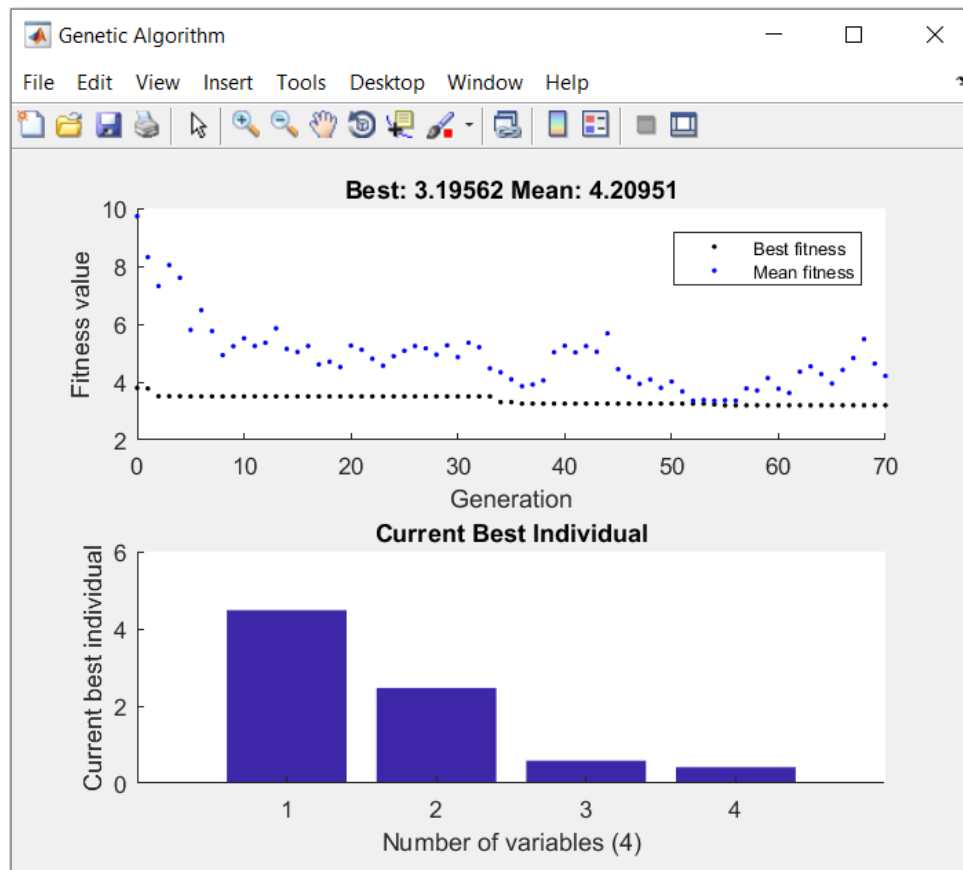


**Figure 5-11 Final Updated Parameters and the Value of the Fitness Function at each Generation**

The values of initial vs updated parameters are shown in Table 5-2.

**Table 5-2 Initial and Updated Values of Selected Parameters**

Parameters	Initial Value	Updated Value
T1	1.25	4.482
T2	1.25	2.471
T3	.9375	0.587
T4	.8125	0.415

Fig. 5-12 depicts the comparison of pushover curves between detailed models, initial simplified model, updated simplified model.

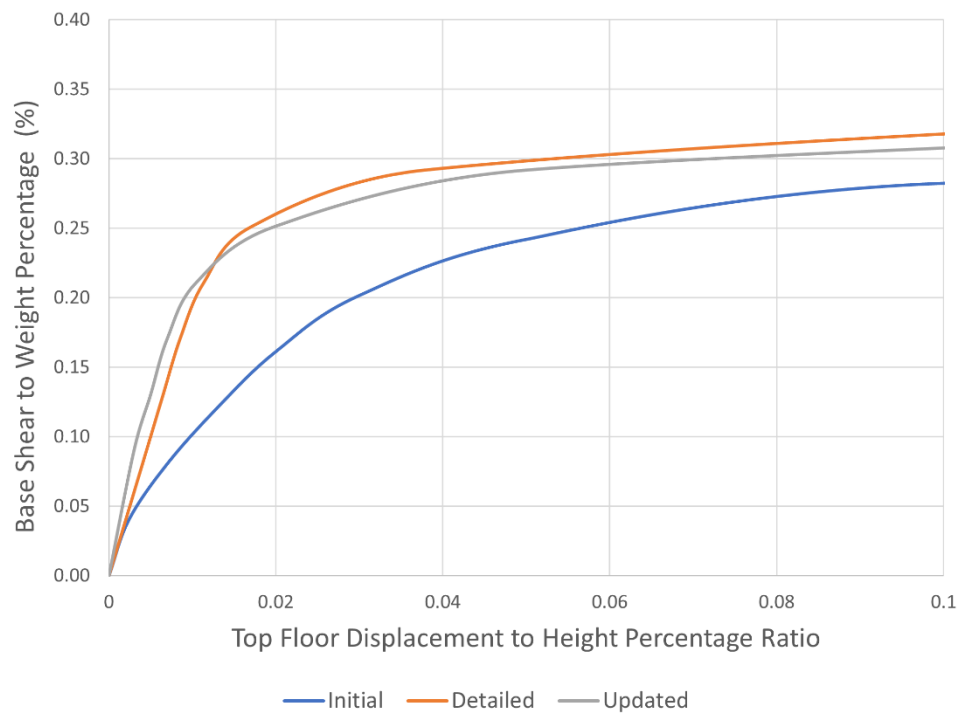


**Figure 5-12 Pushover Curves of the Detailed, Initial and Updated Models**

The results showed that FEMC succeeded in approximating the nonlinear response of the simplified model to the detailed model and hence the updated simplified model is ready to be utilized in deriving accurate fragility curves as will be shown next.



## Chapter 6 Fragility analysis

The second phase of the proposed two-stage framework is presented here which is the derivation of fragilities of both initial and updated models in order to see the effect of using FEMC on fragility curves. The selected ground motions, limit states, and method of deriving fragilities are introduced.

### 6.1. Selection of Ground Motions

As stated before, FEMA-P695 provides the Far-Field set which include 22 pairs of ground motion records for collapse assessment. In this study only 10 pairs were used in deriving fragility curves as Cimellaro et al. (2011) showed that for the structure in their case study the minimum number of records when using spectral acceleration as intensity measure is 20 records and they stated that this conclusion can be used for buildings which are first mode predominant.

**Table 6-1 Summary of the data of far-field record set [FEMA-P695]**

ID No.	Earthquake			Recording Station	
	M	Year	Name	Name	Owner
1	6.7	1994	Northridge	Beverly Hills - Mulhol	USC
2	6.7	1994	Northridge	Canyon Country-WLC	USC
3	7.1	1999	Duzce, Turkey	Bolu	ERD
4	7.1	1999	Hector Mine	Hector	SCSN
5	6.5	1979	Imperial Valley	Delta	UNAMUCSD
6	6.5	1979	Imperial Valley	El Centro Array #11	USGS
7	6.9	1995	Kobe, Japan	Nishi-Akashi	CUE
8	6.9	1995	Kobe, Japan	Shin-Osaka	CUE
9	7.5	1999	Kocaeli, Turkey	Duzce	ERD
10	7.5	1999	Kocaeli, Turkey	Arcelik	KOERI
11	7.3	1992	Landers	Yermo Fire Station	CDMG
12	7.3	1992	Landers	Coolwater	SCE
13	6.9	1989	Loma Prieta	Capitola	CDMG
14	6.9	1989	Loma Prieta	Gilroy Array #3	CDMG
15	7.4	1990	Manjil, Iran	Abbar	BHRC
16	6.5	1987	Superstition Hills	El Centro Imp. Co.	CDMG
17	6.5	1987	Superstition Hills	Poe Road (temp)	USGS
18	7.0	1992	Cape Mendocino	Rio Dell Overpass	CDMG
19	7.6	1999	Chi-Chi, Taiwan	CHY101	CWB
20	7.6	1999	Chi-Chi, Taiwan	TCU045	CWB
21	6.6	1971	San Fernando	LA - Hollywood Stor	CDMG
22	6.5	1976	Friuli, Italy	Tolmezzo	--

**Table 6-2 Summary of Site and Source Data for the Far-Field Record [FEMA-P695]**

ID No.	Site Data		Source (Fault Type)	Site-Source Distance (km)			
	NEHRP Class	Vs_30 (m/sec)		Epicentral	Closest to Plane	Campbell	Joyner-Boore
1	D	356	Thrust	13.3	17.2	17.2	9.4
2	D	309	Thrust	26.5	12.4	12.4	11.4
3	D	326	Strike-slip	41.3	12	12.4	12
4	C	685	Strike-slip	26.5	11.7	12	10.4
5	D	275	Strike-slip	33.7	22	22.5	22
6	D	196	Strike-slip	29.4	12.5	13.5	12.5
7	C	609	Strike-slip	8.7	7.1	25.2	7.1
8	D	256	Strike-slip	46	19.2	28.5	19.1
9	D	276	Strike-slip	98.2	15.4	15.4	13.6
10	C	523	Strike-slip	53.7	13.5	13.5	10.6
11	D	354	Strike-slip	86	23.6	23.8	23.6
12	D	271	Strike-slip	82.1	19.7	20	19.7
13	D	289	Strike-slip	9.8	15.2	35.5	8.7
14	D	350	Strike-slip	31.4	12.8	12.8	12.2
15	C	724	Strike-slip	40.4	12.6	13	12.6
16	D	192	Strike-slip	35.8	18.2	18.5	18.2
17	D	208	Strike-slip	11.2	11.2	11.7	11.2
18	D	312	Thrust	22.7	14.3	14.3	7.9
19	D	259	Thrust	32	10	15.5	10
20	C	705	Thrust	77.5	26	26.8	26
21	D	316	Thrust	39.5	22.8	25.9	22.8
22	C	425	Thrust	20.2	15.8	15.8	15

## 6.2. Scaling Records of Ground Motion

The records of the Far-Field set were scaled, or anchored, so that the spectral acceleration of the structure in consideration is equal to 1g. This was done by converting the record history into a response spectrum, determine the value of the spectral acceleration and divide all the record history by this value.

### 6.3. Limit states for Deriving Fragilities

The building under consideration can be classified as a mid-rise building. Therefore, four damage limit state can be obtained from HAZUS based on inter-story drift ratio as follows:

1. Slight damage, identified by inter-story drift ratio of 1/300
2. Moderate damage, identified by inter-story drift ratio of 1/150
3. Extensive damage, identified by inter-story drift ratio of 1/50
4. Complete damage, identified by inter-story drift ratio of 4/75

### 6.4. Fragility Curves

Figures 6-1 to 6-6 show the resulted Fragility Curves of Both Initial and Updated Models. The comparison between the two sets of fragility curves shows a difference of more than 20% is reached at some spectral acceleration and that difference increase at relatively high value of spectral acceleration. This can be attributed to the lack of accuracy of the simplified model in predicting the nonlinear behavior. However, the simplified model could predict the linear behavior at higher accuracy as can be seen in the comparison at lower levels of  $S_a$ . and then both curves converge to 100% probability of failure at extreme values of spectral acceleration.

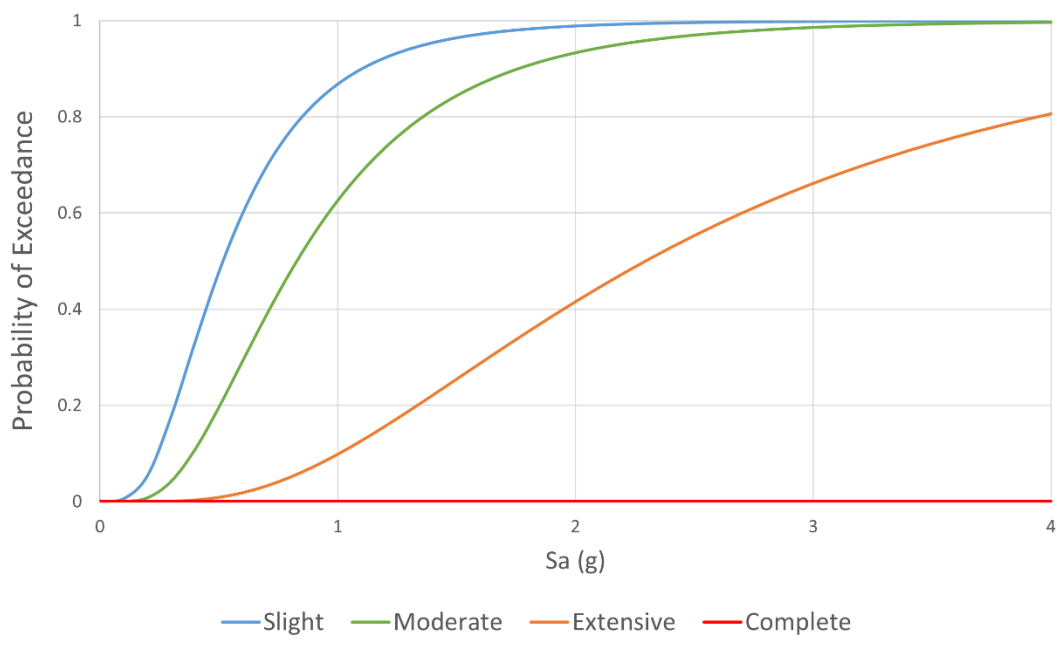


**Figure 6-1 Fragility curves of initial model at different damage limit states**

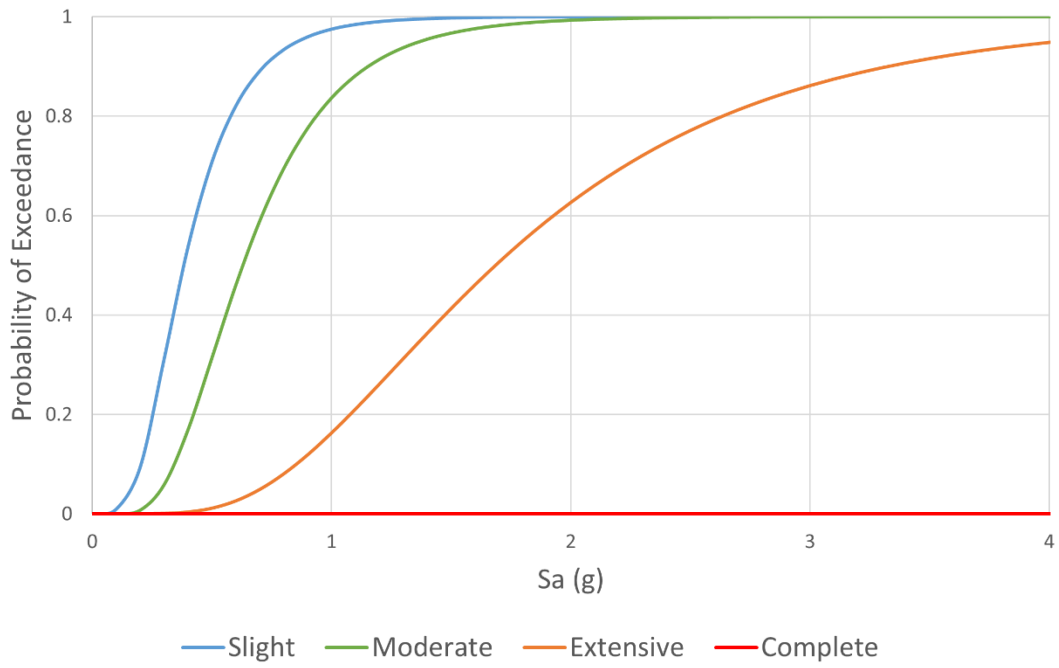


**Figure 6-2 Fragility curves of updated model at different damage limit states**

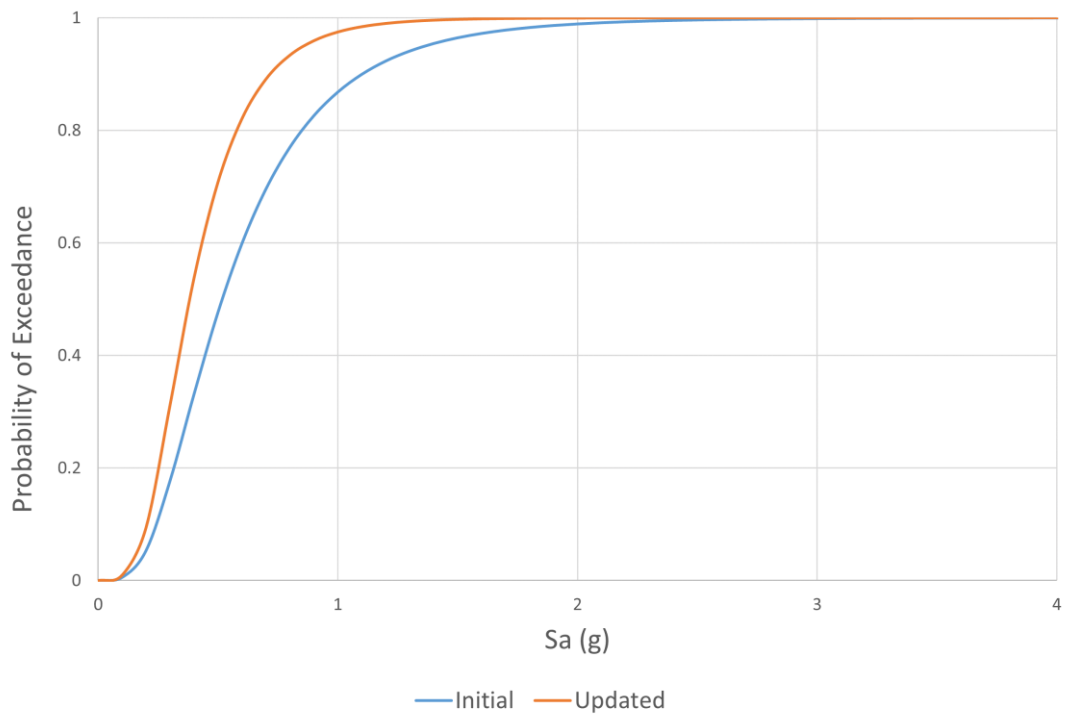


**Figure 6-3 Fragility curves of initial and updated model at slight damage limit state**

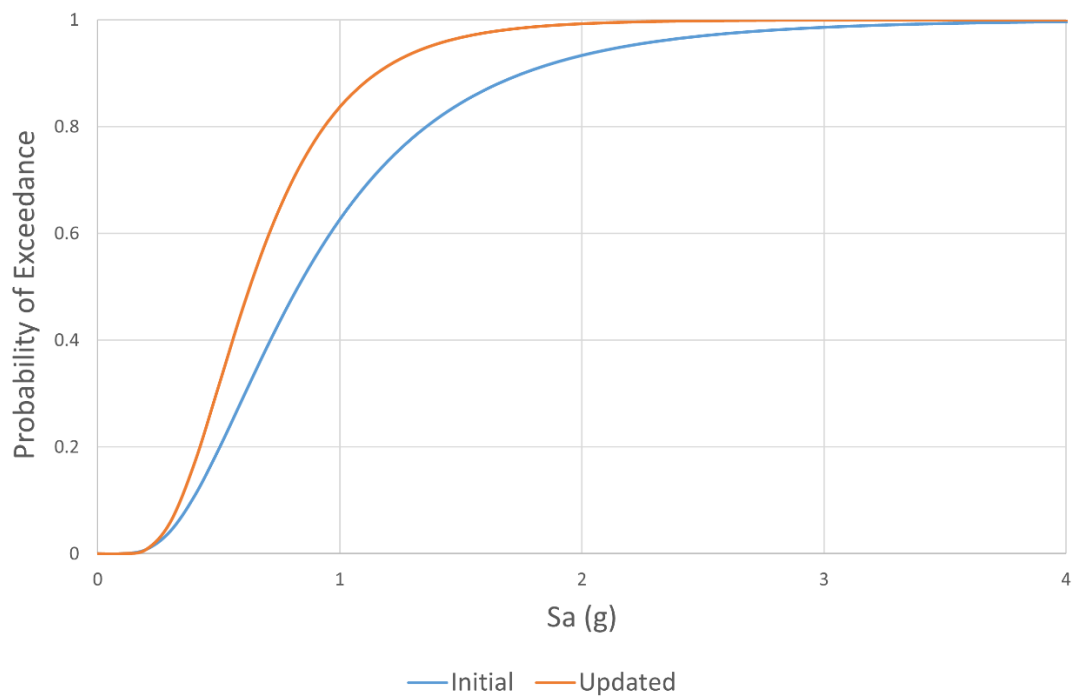


**Figure 6-4 Fragility curves of initial and updated model at moderate damage limit state**

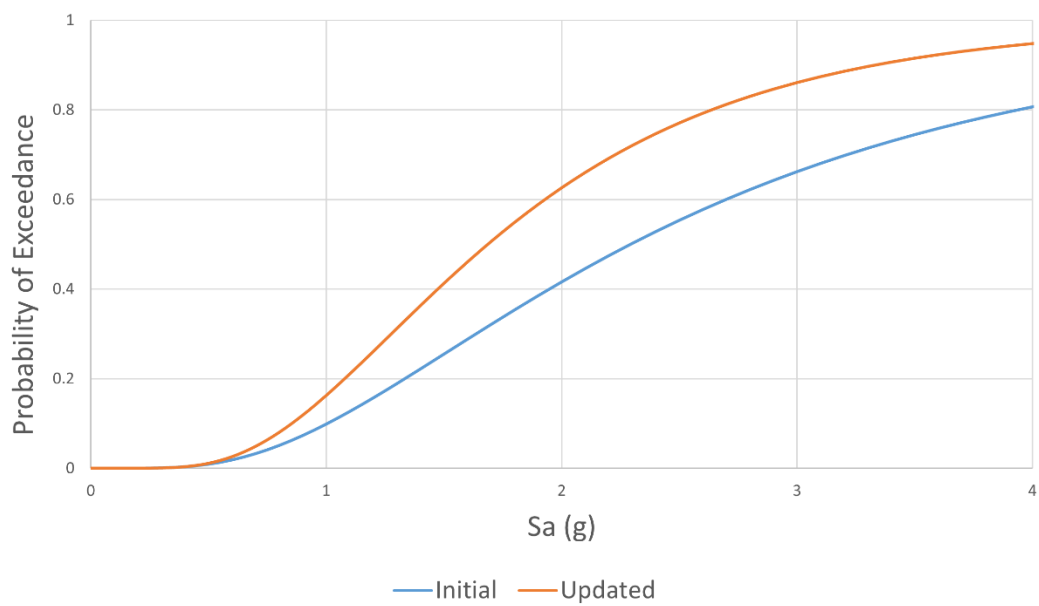


**Figure 6-5 Fragility curves of initial and updated model at extensive damage limit state**



## Chapter 7 Discussion and Conclusions

In this research a two-stage approach is proposed to develop high-accuracy fragility curves while limiting the computational cost. The most common method used for developing fragility curves is the analytical simulation of the structures, which generates the statistics of response under wide range of ground motion records. However, this method is challenging due to high computational efforts and due to the ability to model the structure in reliable manner. Derivation of fragility curves can take substantial amount of effort and time especially when it's necessary to run dynamic analysis for hundreds of times hence it's necessary to introduce simplifications to the analytical model to make the efforts and time reasonable. However, the response may deviate from the actual response. Therefore, fragility curves imply a trade-off between accuracy and computational efforts. Another simplification approach is to utilize nonlinear static and linear dynamic analysis, which will impact the accuracy of the results compared to nonlinear dynamic analysis. In the proposed approach two analytical models are developed. The first is a detailed 3D solid mesh FE Model developed in ANSYS WORKBENCH. The second is a beam element FE model developed in ANSYS APDL to be able to develop parametric model. Upon comparing the results of modal analysis, difference was found between the two models and hence to be able to use the simplified model to derive fragility curves, calibration must be applied first to the simplified model. The process of calibration is finite element model calibration (FEMC). Several techniques exist in literature for conducting FEMC. The chosen method is an optimization-based namely genetic algorithm (GA) since it's able to reach a global minimum without getting stuck in local ones. The objective of the optimization process was to minimize the difference in the pushover curves of the initial and detailed model. The objective function was inspired by the nonlinear static-based approaches for developing nonlinear fragility curves which are based on pushover curves. This objective also incorporates both linear and nonlinear behavior of the structure unlike an objective function that consists of difference in modal parameters which includes only the linear portion of behavior. The process was done by coupling ANSYS APDL with MATLAB environment where the GA is processed. In this process MATLAB assign values to updating parameters in the initial population. Then run ANSYS APDL to evaluate results and retrieve them back to MATLAB where a fitness function is evaluated. After evaluating the fitness function of all candidates of the initial population, parents are selected to produce children by means of mutation and crossover techniques. The children are considered the population of the second generation. The same process continues until the optimum result is achieved. After the process is completed, an updated model is now available for deriving accurate fragility curves. The multiple stripes analysis was utilized in deriving fragility curves using fragility function generator FFG developed by university of TOLEDO using ground motion records obtained from FEMA-P695.

In order to evaluate the proposed procedure, non-linear dynamic analysis fragility curves are developed for a four-story buckling restrained frame building. The results

showed error reduction of about 85% in the RMS error between the two pushover curves. Then fragility curves were developed for both initial and updated models. The comparison between the two sets of fragility curves shows a difference of more than 20% is reached at some spectral acceleration and that difference increase at relatively high value of spectral acceleration. This can be attributed to the lack of accuracy of the simplified model in predicting the nonlinear behavior. However, the simplified model could predict the linear behavior at higher accuracy as can be seen in the comparison at lower levels of  $S_a$ . and then both curves converge to 100% probability of failure at extreme values of spectral acceleration.

## References

1. Erberik M.A. (2015) Seismic Fragility Analysis. In: Beer M., Kougoumtzoglou I., Patelli E., Au I.K. (eds) Encyclopedia of Earthquake Engineering. Springer, Berlin, Heidelberg. [https://doi.org/10.1007/978-3-642-36197-5\\_387-1](https://doi.org/10.1007/978-3-642-36197-5_387-1)
2. Sadraddin, "Fragility Assessment of High-Rise Reinforced Concrete Buildings" (2015). Master's Theses. 605.
3. Shah, N. N., and S. N. Tande. "Study of the Stiffening Systems For Seismic Loads in Multistoreyed Building." International Journal of Engineering Science and Technology 6.6 (2014): 261.
4. Rojahn, Christopher, and Roland L. Sharpe. Earthquake damage evaluation data for California. Applied technology council, 1985.
5. National Institute of Building Sciences (1999) HAZUS technical manual. Prepared for Federal Emergency Management Agency, Washington, DC
6. AmiriHormozak, E. (2013). Analytical fragility curves for horizontally curved steel girder highway bridges (Doctoral dissertation). University of Nevada, Reno.
7. Whitman, Robert V., John W. Reed, and S. T. Hong. "Earthquake damage probability matrices." Proceedings of the Fifth World conference on earthquake engineering. Vol. 2. Rome, Italy: Palazzo Dei Congressi, 1973.
8. Ioannou I., Rossetto T. (2015) Empirical Fragility. In: Beer M., Kougoumtzoglou I.A., Patelli E., Au S.K. (eds) Encyclopedia of Earthquake Engineering. Springer, Berlin, Heidelberg. [https://doi.org/10.1007/978-3-642-35344-4\\_249](https://doi.org/10.1007/978-3-642-35344-4_249).
9. Hazus-MH MR5, Earthquake Loss Estimation Methodology, 2001.
10. European Committee for Standardization (CEN) (2004), Design of structures for earthquake resistance, Part 1: General rules, seismic actions and rules for buildings, Eurocode-8, ENV 1998-1-1, Brussels, Belgium.
11. Federal Emergency Management Agency (FEMA P-58) (2012), Seismic Performance Assessment of Buildings, ATC-58, Applied Technology Council, Washington, D.C.
12. Federal Emergency Management Agency (FEMA P-695) (2009), Quantification of Building Seismic Performance Factors, ATC-63, Applied Technology Council, Redwood City, CA.
13. D'Ayala, D., Meslem, A., Vamvatsikos, D., Porter, K., & Rossetto, T. (2015). Guidelines for analytical vulnerability assessment: Low/mid-rise, GEM vulnerability and loss modelling. Global Earthquake Model (GEM) Foundation, Pavia.
14. Gehl, P., Douglas, J., Rossetto, T., Macabuag, J., Nassirpour, A., Minas, S., & Duffour, P. (2014). Investigating the use of record-to-record variability in static capacity approaches. In Vulnerability, Uncertainty, and Risk: Quantification, Mitigation, and Management (pp. 1675-1684).
15. Jalayer, F., De Risi, R., & Manfredi, G. (2015). Bayesian Cloud Analysis: efficient structural fragility assessment using linear regression. Bulletin of Earthquake Engineering, 13(4), 1183-1203.

16. Di-Sarno, L., & Elnashai, A. S. (2021). Seismic Fragility Relationships for Structures. In *Advances in Assessment and Modeling of Earthquake Loss* (pp. 189-222). Springer, Cham.
17. Vamvatsikos, Dimitrios, and C. Allin Cornell. "Incremental dynamic analysis." *Earthquake engineering & structural dynamics* 31.3 (2002): 491-514.
18. Jalayer, Fatemeh. *Direct probabilistic seismic analysis: implementing non-linear dynamic assessments*. Diss. Stanford University, 2003.
19. Baker, J. W. (2015). Efficient analytical fragility function fitting using dynamic structural analysis. *Earthquake Spectra*, 31(1), 579-599.
20. Porter, K., Kennedy, R., and Bachman, R. (2007). "Creating Fragility Functions for Performance-Based Earthquake Engineering." *Earthquake Spectra*, 23(2), 471–489.
21. Han, S. W., & Chopra, A. K. (2006). Approximate incremental dynamic analysis using the modal pushover analysis procedure. *Earthquake Engineering & Structural Dynamics*, 35(15), 1853-1873.
22. Azarbakht, A., & Dolšek, M. (2011). Progressive incremental dynamic analysis for first-mode dominated structures. *Journal of Structural Engineering*, 137(3), 445-455.
23. J. W., and Cornell, C. A. (2005). Vector-valued ground motion intensity measures for probabilistic seismic demand analysis. Report No. 150, John A. Blume Earthquake Engineering Center, Stanford, CA, 321p.
24. Miano, A., Jalayer, F., Ebrahimian, H., & Prota, A. (2018). Cloud to IDA: Efficient fragility assessment with limited scaling. *Earthquake Engineering & Structural Dynamics*, 47(5), 1124-1147.
25. Pinho, R., Monteiro, R., Casarotti, C., & Delgado, R. (2009). Assessment of continuous span bridges through nonlinear static procedures. *Earthquake Spectra*, 25(1), 143-159.
26. Freeman, S. A. (1998, September). The capacity spectrum method. In *Proceedings of the 11th European conference on earthquake engineering*, Paris (pp. 6-11).
27. Fajfar, P., & Fischinger, M. (1988, August). N2-A method for non-linear seismic analysis of regular buildings. In *Proceedings of the ninth world conference in earthquake engineering* (Vol. 5, pp. 111-116).
28. Chopra, A. K., & Goel, R. K. (2001). A modal pushover analysis procedure to estimate seismic demands for buildings: theory and preliminary evaluation. *PEER* 2001/03.
29. Casarotti, C., & Pinho, R. (2007). An adaptive capacity spectrum method for assessment of bridges subjected to earthquake action. *Bulletin of Earthquake Engineering*, 5(3), 377-390.
30. Ewins, D.J. 1984. *Modal Testing: Theory and Practice*. Research Studies Press, Letchworth.
31. Sehgal, S., & Kumar, H. (2016). Structural dynamic model updating techniques: a state of the art review. *Archives of Computational Methods in Engineering*, 23(3), 515-533.
32. Ewins, D. J. (2009). *Modal testing: theory, practice and application*. John Wiley & Sons.

33. R. J. Allemang and D. L. Brown, "A Correlation Coefficient for Modal Vector Analysis," Proceedings of the 1st International Modal Analysis Conference, Orlando, 8-10 November 1982, pp. 110-116.
34. Kidder, R. L. (1973). Reduction of structural frequency equations. AIAA journal, 11(6), 892-892.
35. Baruch, M., & Bar Itzhack, I. Y. (1978). Optimal weighted orthogonalization of measured modes. AIAA journal, 16(4), 346-351.
36. Berman, A., & Nagy, E. J. (1983). Improvement of a large analytical model using test data. AIAA journal, 21(8), 1168-1173.
37. Chen, J. C., Kuo, C. P., & Garba, J. (1983, January). Direct structural parameter identification by modal test results. In 24th Structures, Structural Dynamics and Materials Conference (p. 812).jian
38. Caesar, B. (1986, January). Update and identification of dynamic mathematical models. PROCEEDING OF INTERNATIONAL MODAL ANALYSIS CONFERENCE.
39. Hu, S. L. J., Li, H., & Wang, S. (2007). Cross-model cross-mode method for model updating. Mechanical Systems and Signal Processing, 21(4), 1690-1703.
40. Fang, H., Wang, T. J., & Chen, X. (2011). Model updating of lattice structures: A substructure energy approach. Mechanical systems and signal processing, 25(5), 1469-1484.
41. Jacquelin, E., Adhikari, S., & Friswell, M. I. (2012). A second-moment approach for direct probabilistic model updating in structural dynamics. Mechanical Systems and Signal Processing, 29, 262-283.
42. Jiang, J., Dai, H., & Yuan, Y. (2013). A symmetric generalized inverse eigenvalue problem in structural dynamics model updating. Linear Algebra and its Applications, 439(5), 1350-1363.
43. Wang, Q., & Qin, S. (2021, June). Direct Calculation of Updating Parameters Based on Kriging Model for Bridge Finite Element Model Updating. In IOP Conference Series: Earth and Environmental Science (Vol. 787, No. 1, p. 012188). IOP Publishing.
44. Collins, J. D., Hart, G. C., Hasselman, T. K., & Kennedy, B. (1974). Statistical identification of structures. AIAA journal, 12(2), 185-190.
45. Lin RM, Ewins DJ (1990) Model updating using FRF data. Proceedings of 15th international modal analysis seminar. KU Leuven, Belgium, pp 141–162
46. Modak, S. V., Kundra, T. K., & Nakra, B. C. (2002). Comparative study of model updating methods using simulated experimental data. Computers & structures, 80(5-6), 437-447.
47. Arora, V., Singh, S. P., & Kundra, T. K. (2009). Finite element model updating with damping identification. Journal of Sound and Vibration, 324(3-5), 1111-1123.
48. Petersen, Ø. W., & Øiseth, O. (2017). Sensitivity-based finite element model updating of a pontoon bridge. Engineering Structures, 150, 573-584.

49. Conde, B., Ramos, L. F., Oliveira, D. V., Riveiro, B., & Solla, M. (2017). Structural assessment of masonry arch bridges by combination of non-destructive testing techniques and three-dimensional numerical modelling: Application to Vilanova bridge. *Engineering Structures*, 148, 621-638.
50. Tian, W., Weng, S., Xia, Q., & Xia, Y. (2021). Dynamic condensation approach for response-based finite element model updating of large-scale structures. *Journal of Sound and Vibration*, 506, 116176.
51. Alkayem, N. F., Cao, M., Zhang, Y., Bayat, M., & Su, Z. (2018). Structural damage detection using finite element model updating with evolutionary algorithms: a survey. *Neural Computing and Applications*, 30(2), 389-411.
52. Atalla, M. J., & Inman, D. J. (1998). On model updating using neural networks. *Mechanical Systems and Signal Processing*, 12(1), 135-161.
53. Tran-Ngoc, H., Khatir, S., De Roeck, G., Bui-Tien, T., & Wahab, M. A. (2019). An efficient artificial neural network for damage detection in bridges and beam-like structures by improving training parameters using cuckoo search algorithm. *Engineering Structures*, 199, 109637.
54. Zhang, Z., & Sun, C. (2021). Structural damage identification via physics-guided machine learning: a methodology integrating pattern recognition with finite element model updating. *Structural Health Monitoring*, 20(4), 1675-1688.
55. Guo Q, Zhang L (2004) Finite element model updating based on response surface methodology
56. Ren, W. X., & Chen, H. B. (2010). Finite element model updating in structural dynamics by using the response surface method. *Engineering structures*, 32(8), 2455-2465.
57. Chakraborty, S., & Sen, A. (2014). Adaptive response surface based efficient finite element model updating. *Finite Elements in Analysis and Design*, 80, 33-40.
58. Alpaslan, E., & Karaca, Z. (2021). Response surface-based model updating to detect damage on reduced-scale masonry arch bridge. *Structural Engineering and Mechanics*, 79(1), 9-22.
59. Levin, R. I., & Lieven, N. A. J. (1998). Dynamic finite element model updating using simulated annealing and genetic algorithms. *Mechanical systems and signal processing*, 12(1), 91-120.
60. Marwala, T. (2010). Finite-element-model updating using computational intelligence techniques: Applications to structural dynamics.
61. He, R. S., & Hwang, S. F. (2006). Damage detection by an adaptive real-parameter simulated annealing genetic algorithm. *Computers & Structures*, 84(31-32), 2231-2243.
62. Tran-Ngoc, H., Khatir, S., De Roeck, G., Bui-Tien, T., Nguyen-Ngoc, L., & Abdel Wahab, M. (2018). Model updating for Nam O bridge using particle swarm optimization algorithm and genetic algorithm. *Sensors*, 18(12), 4131.
63. Kang, F., Li, J. J., & Xu, Q. (2012). Damage detection based on improved particle swarm optimization using vibration data. *Applied Soft Computing*, 12(8), 2329-2335.

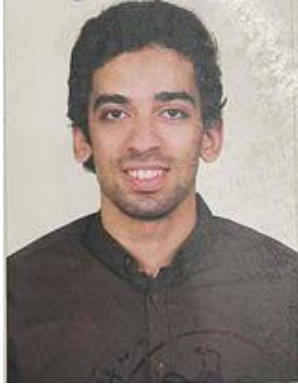
64. Otsuki, Y., Li, D., Dey, S. S., Kurata, M., & Wang, Y. (2021). Finite element model updating of an 18-story structure using branch-and-bound algorithm with epsilon-constraint. *Journal of Civil Structural Health Monitoring*, 11(3), 575-592.
65. Zapico, J. L., González-Buelga, A., Gonzalez, M. P., & Alonso, R. (2008). Finite element model updating of a small steel frame using neural networks. *Smart Materials and Structures*, 17(4), 045016.
66. Jaishi, B., & Ren, W. X. (2006). Damage detection by finite element model updating using modal flexibility residual. *Journal of sound and vibration*, 290(1-2), 369-387.
67. Elanwar, Hazem H., and Amr S. Elnashai. "Framework for online model updating in earthquake hybrid simulations." *Journal of Earthquake Engineering* 20.1 (2016): 80-100.
68. Marwala, Tshilidzi. "Finite-element-model updating using computational intelligence techniques: Applications to structural dynamics." (2010): 978-1.
69. Gandage, S., Salgado, R., and Guner, S. (2019), "Fragility Function Generator," Macro-Enabled Spreadsheet. The University of Toledo, OH, USA. Available at: [http://www.utoledo.edu/engineering/faculty/serhanguner/data1/3S\\_FragilityFuncGenerator\\_V1.0.zip](http://www.utoledo.edu/engineering/faculty/serhanguner/data1/3S_FragilityFuncGenerator_V1.0.zip)
70. DeSalvo, G. J., Kohnke, P. C., & Swanson, J. A. (1985). ANSYS engineering analysis system. Swanson Analysis Systems.
71. Hassan, E. M., & Mahmoud, H. (2017). Modeling resolution effects on the seismic response of a hospital steel building. *Journal of Constructional Steel Research*, 139, 254-271.
72. Venture, N. C. J. (2013). Cost analyses and benefit studies for earthquake-resistant construction in Memphis, Tennessee. NIST GCR, 14-917.
73. Venture, N. C. J. (2013). Cost analyses and benefit studies for construction in Memphis, Tennessee (design drawings). Gaithersburg, MD.
74. ASCE/SEI 7-10, Minimum Design Loads for Buildings and Other Structures, 2010.
75. Huei-Huang Lee. 2017. Finite Element Simulations with ANSYS Workbench 17. SDC Publications.
76. ANSYS Documentation\\Mechanical APDL\\Element Reference.
77. ENDEAVOS Innovations Inc. Bolted Connections in ANSYS Workbench: Part 1. <https://www.endeavos.com/bolted-connections-ansys-workbench-part-1/>
78. Mottershead, J. E., Mares, C., Friswell, M. I., & James, S. (2000). Selection and updating of parameters for an aluminium space-frame model. *Mechanical Systems and Signal Processing*, 14(6), 923-944.
79. Cimellaro, G. P., Reinhorn, A. M., D'Ambrisi, A., & De Stefano, M. (2011). Fragility analysis and seismic record selection. *Journal of structural engineering*, 137(3), 379-390.

## الملخص

أتاح تحسين أدوات التحليل واستخدام الحواسيب القوية إجراء تحليل دقيق باستخدام طريقة العناصر المحدودة للمباني والهياكل الأساسية. ومع ذلك، قد يعوق الوقت الحسابي المفرط التمثيل الدقيق لبعض المنشآت باستخدام طريقة العناصر المحدودة. خاصة عندما يكون من الضروري إجراء نفس التحليل لعدة مرات. واحدة من هذه الحالات هي عندما يكون مطلوباً إيجاد منحنيات الهشاشة حيث يتم استخدام التحليل الديناميكي غير الخطي عدة مرات. يستخدم تحليل الهشاشة في العديد من مجالات تقييم أداء البناء والبنية التحتية. يمكن اشتقاق منحنيات الهشاشة لأنواع عديدة من المخاطر حيث تمثل احتمال الانهيار أو احتمال انتهاك شرط محدد مسبقاً. تحليل الهشاشة غالباً ما يكون مكلفاً حسابياً وبالتالي قد يتم إدخال بعض التبسيطات للمنشأ. ويمكن إدخال التبسيط بطريقتين. الأول هو استخدام نوع آخر من التحليل بدلاً من التحليل الديناميكي غير الخطي مثل التحليل الاستاتيكي غير الخطي ولكن بعد ذلك تكون منحنيات الهشاشة المشتقة أقل دقة. النهج الثاني هو من خلال إدخال التبسيطات إلى النموذج المستخدم للتحليل ولكن بعد ذلك سوف تنحرف الاستجابة عن الاستجابة الفعلية و تنتج منحنيات هشاشة أقل دقة. وبناء على ذلك، نقترح في هذه الدراسة إطاراً من مرحلتين لتقييم منحنيات الهشاشة الدقيقة باستخدام التحليل الديناميكي غير الخطي دون التكلفة الحسابية العالية المرتبطة بتحليل النموذج المفصل. في البداية يتم تطوير نموذجين ، الأول هو نموذج مفصل تعتبر استجابته الاستجابة الفعلية بينما يتم تبسيط النموذج الثاني لتقليل وقت المعالجة. يمكن تطبيق هذا التبسيط على العديد من العوامل ، مثل كثافة العناصر المحدودة ، وتمثيل الوصلات ، وما إلى ذلك. بعد ذلك ، يتم تقليل الاختلافات بين النموذج المفصل والنموذج المبسط من أجل تقليل النفقات الحسابية قدر الإمكان مع تقريب نتائج النموذج المبسط إلى النموذج التفصيلي. في هذه المرحلة نستخدم تقنية معايرة تسمى تحديث نموذج العنصر المحدود. حيث يتم تشكيل دالة تضم الخطأ بين النموذج المفصل والنموذج المبسط ويتم استخدام تقنية تكرارية حيث تغير العوامل المختارة كل مرة حتى يتم تحقيق أفضل قيمة للدالة وتسمى العوامل المقابلة العوامل المحدثة. في المرحلة الثانية، نقوم بحساب منحنيات الهشاشة باستخدام تحليل ديناميكي غير خطي دون وقت تشغيل مرهق. ومن ثم فإن الإطار المقترح يحقق منحنيات هشاشة عالية الدقة دون نفقات حسابية عالية جداً.



ثم يتم تطبيق الإطار المقترح على مبنى مكون من شكاالات من أربعة طوابق لتقييم جدواه. يتم تطوير النموذج التفصيلي في برنامج ANSYS WORKBENCH باستخدام شبكات صلبة ثلاثية الأبعاد بينما يتم تطوير النموذج المبسط في ANSYS APDL باستخدام عناصر احادية البعد. ثم يتم تطبيق تحديث نموذج العنصر المحدود باستخدام طريقة التحسين الخوارزمية الوراثة لمعرفة المعلمات المحدثة. وأخيرا، يستخدم النموذج المحدث لتطوير منحنيات الهشاشة باستخدام تحليل ديناميكي غير خطي.



مهندس: عمر خالد وهبة متولي  
تاريخ الميلاد: ١٩٩٦/٠٢/١٩  
الجنسية: مصري  
تاريخ التسجيل: ٢٠١٨/١٠/١  
تاريخ المنح: ٢٠٢٢/١٠/١٠  
القسم: الهندسة الانشائية  
الدرجة: ماجستير العلوم  
المشرفون:

أ.د شريف احمد مراد  
د حازم حسام الانور  
د حسام محمود

#### الممتحنون:

أ.د شريف احمد مراد (المشرف الرئيسي)  
د. حسام محمود (المشرف)  
جامعة كولورادو  
أ.د اشرف محمود عثمان (الممتحن الداخلي)  
أ.د شريف م ابراهيم (الممتحن الخارجي)  
هندسة عين شمس

#### عنوان الرسالة:

استخدام تقنية معايرة النموذج لاشتقاق منحنيات هشاشة دقيقة

#### الكلمات الدالة:

تحليل الهشاشة ، تحليل المشارب المتعددة ، تحديث النموذج ، نمذجة العناصر المحدودة ،  
شكالات مضادة للالتواء

#### ملخص الرسالة:

يستخدم تحليل الهشاشة في تقييم الأداء الزلزالي للمباني والبنية التحتية. ولذلك، فإن هناك حاجة متزايدة إلى منحنيات هشاشة دقيقة. في هذا البحث نقتراح إطار مرحلتين لتقييم منحنيات الهشاشة الدقيقة باستخدام التحليل الديناميكي غير الخطي دون التكلفة الحسابية المكلفة. أولاً نقوم بتقليل الاختلافات بين نموذج مفصل ونموذج مبسط من أجل تقليل النفقات الحسابية قدر الإمكان. ثم نقوم بحساب منحنيات الهشاشة باستخدام تحليل ديناميكي غير خطي دون وقت تشغيل مرهق. ثم يتم تطبيق عمل الإطار على مبنى إطار مقيد من أربعة طوابق لتقييم جدواه.

## استخدام تقنية معايرة النموذج لاشتقاق منحنيات هشاشة دقيقة

اعداد  
عمر خالد وهبة متولي

رسالة مقدمة إلى كلية الهندسة – جامعة القاهرة  
كجزء من متطلبات الحصول على درجة ماجستير العلوم  
في  
الهندسة الانشائية

يعتمد من لجنة الممتحنين:  
الاستاذ الدكتور: شريف احمد مراد      المشرف الرئيسى

الدكتور: حسام محمود      المشرف  
جامعة كولورادو

الاستاذ الدكتور: اشرف محمود عثمان      الممتحن الداخلى

الاستاذ الدكتور: شريف محمد ابراهيم      الممتحن الخارجى  
هندسة عين شمس

كلية الهندسة - جامعة القاهرة  
الجيزة - جمهورية مصر العربية  
2022

# استخدام تقنية معايرة النموذج لاشتقاق منحنيات هشاشة دقيقة

اعداد  
عمر خالد وهبة متولي

رسالة مقدمة إلى كلية الهندسة – جامعة القاهرة  
كجزء من متطلبات الحصول على درجة ماجستير العلوم  
في  
الهندسة الانشائية

تحت اشراف

أ.د. شريف أحمد مراد	د. حازم حسام الأنور
أستاذ الكباري و المنشآت المعدنية	مدرس الكباري و المنشآت المعدنية
قسم أنشاءات	قسم أنشاءات
كلية الهندسة جامعة القاهرة	كلية الهندسة جامعة القاهرة

د. حسام محمود  
أستاذ مساعد  
قسم الهندسة المدنية والبيئية  
كلية الهندسة جامعة كولورادو

كلية الهندسة - جامعة القاهرة  
الجيزة - جمهورية مصر العربية

2022



## استخدام تقنية معايرة النموذج لاشتقاق منحنيات هشاشة دقيقة

اعداد  
عمر خالد وهبة متولي

رسالة مقدمة إلى كلية الهندسة – جامعة القاهرة  
كجزء من متطلبات الحصول على درجة ماجستير العلوم  
في  
الهندسة الانشائية

كلية الهندسة - جامعة القاهرة  
الجيزة - جمهورية مصر العربية  
2022